A ^{1}H and ^{13}C Nuclear Magnetic Resonance Study of Renal, Adrenal and Hepatic Metabolism in *Meriones unguiculatus* Infected With *Echinococcus multilocularis*

By

Charis A. Kepron

A Thesis
Submitted to the Faculty of Graduate Studies
in Partial Fulfillment of the Requirements
for the Degree of

Master of Science (M.Sc.)

Department of Human Anatomy and Cell Science
University of Manitoba
Winnipeg, Manitoba

THE UNIVERSITY OF MANITOBA

FACULTY OF GRADUATE STUDIES

*****

COPYRIGHT PERMISSION PAGE

A ^{1}H and ^{13}C Nuclear Magnetic Resonance Study of Renal, Adrenal and Hepatic Metabolism in *Meriones unguiculatus* Infected With *Echinococcus multilocularis*

BY

Charis A. Kepron

A Thesis/Practicum submitted to the Faculty of Graduate Studies of The University of Manitoba in partial fulfillment of the requirements of the degree of

Master of Science

Table of Contents

Abstract

Nuclear magnetic resonance (NMR) spectroscopy was utilized to test the hypothesis that infection with the cestode parasite *Echinococcus multilocularis* will result in metabolic alterations in the kidneys, adrenal glands and liver of the intermediate host *Meriones unguiculatus*. ^{1}H NMR analysis of chloroform/methanol extracts of kidneys and adrenal glands from infected jirds revealed that the lipid profile of these organs changes as a result of infection. Kidneys from infected animals had lower concentrations of phosphatidylcholine (PTC), phosphatidylethanolamine (PTE), total glycerophospholipid (GPL), arachidonic acid (AA) and CH_2 in the unsaturated fatty acid (FA) moiety -CH=CH(CH_2CH=CH)$_n$-. In addition, the ratios of both AA and CH_2 in -CH=CH(CH_2CH=CH)$_n$- to total FA decreased in infected animals. Meanwhile, the adrenal glands from infected jirds had lower concentrations of cholesterol (CTL), PTE, total GPL, total FA, total triacylglycerol, linoleic acid, and the FA moieties -CH_2CH_2COO, -CH_2COO, -(CH_2)$_n$-, -CH=CH-, -CH_2CH=CH- and CH_2 in -CH=CH(CH_2CH=CH)$_n$-. The adrenal concentrations of AA, docosahexaenoic acid (DHA) and CTL esters were unchanged. The ratios of -CH_2CH_2COO, -CH_2COO, CH_2 in -(CH_2)$_n$-, -CH_2CH=CH to total FA all decreased in infected animals, while that of DHA increased and that of CH_2 in -CH=CH(CH_2CH=CH)$_n$- remained the same. The average FA chain length and degree of unsaturation were also lower in adrenals from infected jirds.

Using ^{13}C NMR spectroscopy, perchloric acid (PCA) extracts of livers were

analyzed following portal vein injections of an equimolar mixture of [1,2-$^{13}C_2$]acetate and [3-^{13}C]lactate. Isotopomer analysis using the glutamate resonances showed that the relative contributions of endogenous and exogenous substrates to the acetyl coenzyme A entering the TCA cycle differed significantly between infected and control groups. In uninfected animals, the relative proportion of acetyl-CoA derived from labeled lactate (F_{LL}) was 0.18, that from labeled acetate (F_{LA}) was 0.32 and that from endogenous, unlabeled sources (F_U) was 0.50. The corresponding values from livers of infected animals were 0.27, 0.38 and 0.34, respectively. In addition, the ratio of F_{LA}: F_{LL} was significantly smaller in the infected group, while the percentage of ^{13}C detected at carbon-3 of glutamate was the same in both groups.

The results of both experiments clearly show that hepatic, renal and adrenal metabolism of *M. unguiculatus* is profoundly affected by infection with *E. multilocularis*.

Acknowledgments

If there is one lesson I have learned throughout the course of this project, it is that there are no solo efforts in research. Many people have helped me reach this goal, and they have all earned my gratitude.

First, I would like to say thank you to my advisors, Dr. Marie Novak and Dr. Barry Blackburn. Without their guidance, advice and knowledge, none of this would have been possible. They have taught me a lot about the world of research science, both the good and the not-so-good, and helped me to realize the excitement and satisfaction that comes from learning.

Also, thanks go out to the other members of my advisory committee, Dr. Judy Anderson and Dr. Jim Peeling, for the careful editing of my thesis and all their helpful suggestions.

I received a great deal of financial support throughout the course of my degree, and would like to thank both the Natural Sciences and Engineering Research Council of Canada and the Department of Human Anatomy and Cell Science for all the assistance they provided.

Thank you to Ian Corbin, Jodi Schoen and Rachel Simkoff for teaching me how to do things right, and many thanks to Terry Wolowiec for the excellent technical assistance, and the reminder that life is never so bad that you can't have a good laugh.

Finally, I would like to thank my family and friends. My parents, Jim and Dawne Kepron, for all their love and support of every possible variety, and for allowing me to discuss parasites at the dinner table. My grandmother, Rose Collins, for her support and undying interest, and my grandparents, Michael and Olga Kepron, for always being proud of me, no matter what. My sister, Zoë, and my brother, Chris, for making the attempt to understand what I was doing, and Ogo, for the wonderful lunches. Special thanks to my friends Andrea Sampson, Aidan Topping and Heather Finlay for reassuring me when times were bad, and being there to share with me when times were good. The Collective Brain now has a Masters! A big hug to Ross Baker for pushing me through to the end and reminding me that I am never alone.

In memory of my grandfather, Jim Collins.

List of Abbreviations

AA: arachidonic acid

ABZ: albendazole

Acetyl-CoA: acetyl coenzyme A

ACAT: acyl-coenzyme A - cholesterol acyltransferase

ACP: acyl carrier protein

ACTH: adrenocorticotropin

ADP: adenosine diphosphate

ATP: adenosine triphosphate

α-KG: alpha ketoglutarate

β-HB: β-hydroxybutyrate

cAMP: cyclic adenosine monophosphate

CDP: cytidine diphosphate

CFT: complement fixation test

CNS: central nervous system

COX: cyclooxygenase

CT: computed tomography

CTL: cholesterol

DAG: diacylglycerol

DHA: docosahexaenoic acid

DHAP: dihydroxyacetone phosphate

E. granulosus: *Echinococcus granulosus*

ELISA: enzyme-linked immunosorbent assay

E. multilocularis: *Echinococcus multilocularis*

ER: endoplasmic reticulum

ETC: electron transport chain

FA: fatty acid

FAD^+: flavin adenine dinucleotide (oxidized form)

$FADH+H^+$: flavin adenine dinucleotide (reduced form)

G3P: glycerol-3-phosphate

Glu: glutamate

GPC: glycerophosphocholine

GPL: glycerophospholipid

GTP: guanosine triphosphate

HETE: hydroxyeicosatetraenoic acid

HMG-CoA: β-hydroxy-β-methylglutaryl coenzyme A

IDL: intermediate density lipoprotein

IE: immunoelectrophoresis

IFN: interferon

IHA: indirect hemagglutination

IIF: indirect immunofluorescence

IL-12: interleukin 12

LA: linoleic acid

LDH: lactate dehydrogenase

LDL: low density lipoprotein

LT: leukotriene

LX: lipoxin

MAG: monoacylglycerol

MRI: magnetic resonance imaging

M. vogae: *Mesocestoides vogae*

Na^+: sodium

NAD^+: nicotinamide adenine dinucleotide (oxidized form)

$NADH+H^+$: nicotinamide adenine dinucleotide (reduced form)

NH_4^+: ammonia

NMR: nuclear magnetic resonance

O_2: oxygen

OAA: oxaloacetate

PBMC: peripheral blood mononuclear cell

PC: phosphocholine

PCA: perchloric acid

PCx: pyruvate carboxylase

PDH: pyruvate dehydrogenase

PE: phosphoethanolamine

PEMT: phosphatidylethanolamine methyltransferase

PEP: phosphoenolpyruvate

PG: prostaglandin

PLA_2: phospholipase A_2

PLC: phospholipiase C

PTC: phosphatidylcholine

PTE: phosphatidylethanolamine

PTI: phosphatidylinositol

PTS: phosphatidylserine

TAG: triacylglycerol

TCA cycle: tricarboxylic acid cycle

T. crassiceps: *Taenia crassiceps*

TX: thromboxane

US: ultrasonography

VLDL: very low density lipoprotein

WHO: World Health Organization

List of Figures

List of Tables

Introduction

I. *Echinococcus multilocularis* and Alveolar Hydatidosis

Echinococcus multilocularis is an obligate endoparasite and the causative agent of one of the most lethal parasitic zoonoses known to man. In spite of the fact that the juvenile stage (metacestode) of this cestode was first described by Leuckart in 1863, *E. multilocularis* was not formally recognized as an individual species until 1957 when H. Vogel published his morphological and biological studies that finally proved the specific nature of the tapeworm (Schantz, 1982; Tornieporth and Disko, 1994; Rausch, 1995). Up to that point, it was generally assumed that metacestodes of *E. multilocularis* were a result of the anomalous development of the juvenile stage of *E. granulosus*, the first member of the genus to be characterized, and an organism that has been known to science since the days of Hippocrates (Schantz, 1982; Tornieporth and Disko, 1994). Although the development of the adult stages of these two *Echinococcus* species, as well as the eggs they produce, are very similar, *E. multilocularis* has proven to be highly distinct with respect to its global distribution, some aspects of its life cycle patterns and the development of its metacestode (Thompson, 1995; Amman and Eckert, 1996).

Whereas *E. granulosus* is a cosmopolitan parasite, and has been identified in many regions on each continent save Antarctica (Rausch, 1995; Amman and Eckert, 1996), *E. multilocularis* is endemic to the Northern Hemisphere only. Its geographic distribution includes areas in France, Germany, Austria, Poland, Switzerland, the Czech Republic, Latvia, Russia, China, Japan, Turkey and surrounding regions of the Middle

East (Akinoglu *et al.*, 1991; Petavy *et al.*, 1991; Suzuki *et al.*, 1993; Tornieporth and Disko, 1994; Malczewski *et al.*, 1995; Rausch, 1995; Amman and Eckert, 1996; Kolářová *et al.*, 1996), and also North America, where the parasite was reported in animals in Alaska, North and South Dakota, Minnesota, Wyoming, Montana, Iowa, Nebraska, Wisconsin, Illinois, Indiana, Ohio, Missouri, Alberta, Saskatchewan and Manitoba (Schantz, 1993; Storandt and Kazacos, 1993; Suzuki *et al.*, 1993; Rausch, 1995; Schantz *et al.*, 1995; Amman and Eckert, 1996). Humans are not natural hosts for this parasite and, like other accidental hosts, do not play a biological role in the worm's life cycle (Amman and Eckert, 1996). Although relatively common in endemic regions of Europe and Asia, North American cases of human infection appear to be restricted almost exclusively to Alaska (Wilson and Rausch, 1980; Stehr-Green *et al.*, 1988; Schantz, 1993; Suzuki *et al.*, 1993; Tornieporth and Disko, 1994; Amman and Eckert, 1996) with only two other cases being reported, one from each of Manitoba (James and Boyd, 1937) and Minnesota (Schantz, 1993).

Like all members of the family Taeniidae, *E. multilocularis* requires 2 mammalian hosts for the completion of its life cycle (Figure 1) (Schantz, 1982; Amman and Eckert, 1992). The juvenile stage develops in the viscera of an intermediate host which is normally a small rodent, and forms cysts that contain the primordia of the adult worms, the protoscoleces. The most common intermediate hosts for the worm are voles and lemmings, but many other species may be infected as well, including mice, rats, squirrels and the Mongolian gerbil, *Meriones unguiculatus* (Rausch, 1995). When an infected

Figure 1

Life cycle of *Echinococcus multilocularis*.

This figure demonstrates the complete life cycle of *E. multilocularis*. The juvenile stage or metacestode develops as a multilocular cyst in the viscera of a rodent intermediate host. When the infected animal is eaten by a mammalian carnivore, the protoscoleces are liberated and from each of them an adult will develop. Gravid worms produce eggs which are released into the environment in the feces of the definitive host. The life cycle is complete when a naive rodent host accidentally ingests a viable egg. Although uncommon, humans may also serve as intermediate hosts for the parasite.

Key:

A. Adult worm

B. Egg

C. Juvenile worm (cyst)

a. host tissue

b. laminated layer

c. germinal layer

d. protoscolex

e. matrix

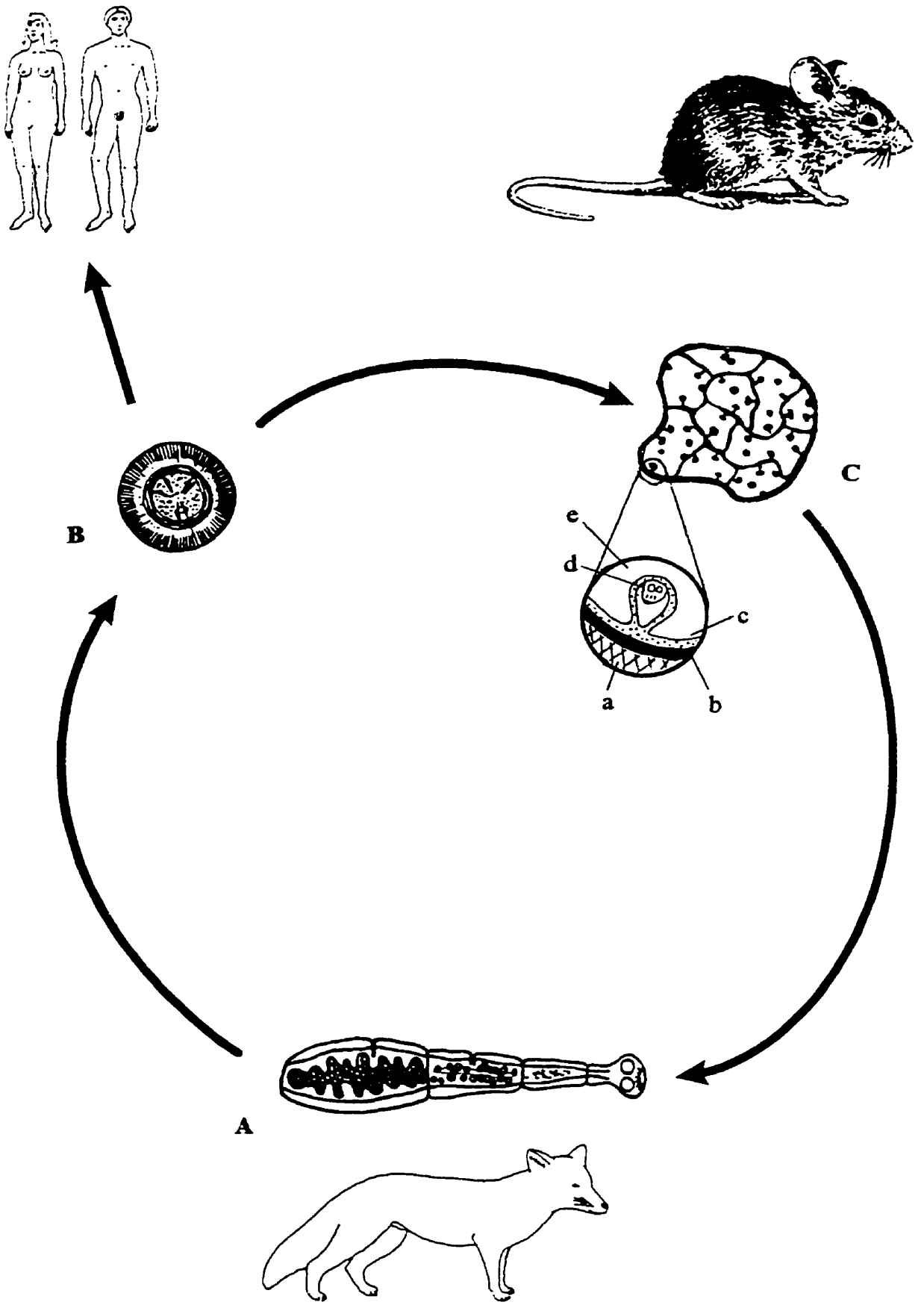
B
C
e
d
c
a
b
A

rodent is eaten by a mammalian carnivore, the protoscoleces are liberated from the surrounding cyst tissue, both by the masticatory actions of the predator and gastric acid and enzymes, especially pepsin (Thompson, 1995). Within the small intestine, each protoscolex will attach with four powerful suckers and two rows of rostellar hooks to the intestinal mucosa, and start to grow the segmented body called a strobila (Schantz, 1982; Schmidt and Roberts, 1989; Gottstein, 1992; Thompson, 1995). The hermaphroditic adults will reach sexual maturity in approximately four weeks (Schantz, 1982; Gottstein, 1992), at which time egg production commences. *E. multilocularis* is the smallest of the taeniid tapeworms, and when fully grown, adults are a mere 1.2-4.5 mm long (Gottstein, 1992). The mature strobila consists of two-five segments called proglottids. The posterior-most proglottid is gravid, containing 100-200 eggs, each of which has a fully developed larva (oncosphere) which is infective to any susceptible intermediate host (Tornieporth and Disko, 1994; Amman and Eckert, 1996). The gravid proglottids are shed by the worm at regular intervals and they, along with the eggs they contain, are released into the environment in the feces of the definitive host (Tornieporth and Disko, 1994). The most common of these carnivorous definitive hosts are foxes, both red and arctic, but adult worms have also been detected in coyotes, wolves and domestic dogs and cats (Storandt and Kazacos, 1993; Malczewski *et al.*, 1995; Rausch, 1995).

When a suitable intermediate host ingests a viable egg, the egg shell and protective layers surrounding the larva are digested by the host's proteolytic enzymes and the oncosphere is released into the stomach or small intestine. Once liberated, the oncospheres become "activated", a process thought to be dependent on the action of bile

salts (Gottstein, 1992; Thompson, 1995). The activated larvae are able to penetrate the gut wall and enter the venous and lymphatic vessels, through which they are carried to the visceral organs (Gottstein, 1992; Thompson, 1995; Amman and Eckert, 1996). There, growth and differentiation continue, leading to the development of the cyst-like metacestode (Thompson, 1995). The favoured location for the formation of the juvenile stage is the liver, although rare cases have demonstrated primary cyst development in organs such as the lungs and brain (Gottstein, 1992; Tornieporth and Disko, 1994; Amman and Eckert, 1996). Because the metacestodes have adapted to growth in short-lived rodent hosts, their development is rapid when compared to that of *E. granulosus* for which larger herbivores such as deer and sheep serve as intermediate hosts (Rausch, 1995; Thompson, 1995). In the natural rodent hosts, the parasite produces infective protoscoleces after only two-six months (Tornieporth and Disko, 1994; Thompson, 1995) compared to *E. granulosus* which requires a minimum of 10 months to reach an equivalent stage of development (Thompson, 1995).

In addition to the rate of growth, the structure of the *E. multilocularis* metacestodes is very different than that of other *Echinococcus* species. Macroscopically, the cyst starts out unilocular, but soon takes on the multilocular appearance characteristic to *E. multilocularis*. The mature metacestode resembles a malignant neoplasm, and is composed of numerous small contiguous vesicles (Schantz, 1982; Tornieporth and Disko, 1994; Amman and Eckert, 1996) filled with a semisolid matrix (Tornieporth and Disko, 1994; Thompson, 1995). Microscopically, the cyst consists of an inner cellular germinal layer surrounded by a non-cellular laminated layer. Unlike *E. granulosus*, metacestodes

of *E. multilocularis* lack an adventitial layer external to the laminated layer. This fibrous tissue layer is of host origin, and acts as a limiting barrier between parasite and host (Thompson, 1995). The absence of this barrier allows *E. multilocularis* to proliferate exogenously and invade surrounding tissue (Tornieporth and Disko, 1994; Thompson, 1995). The parasite is also capable of metastasis via the blood and lymphatic vessels, and secondary cyst development may occur in a variety of sites, including bone, lungs, spleen and brain (Kasai *et al.*, 1980; Amman and Eckert, 1995, 1996; Merkle *et al.*, 1997). Proliferation occurs endogenously as well, with the germinal layer invaginating into the central matrix and creating small rootlike cellular protrusions (Amman and Eckert, 1996). It is from undifferentiated germinal cells in the walls of these protrusions that the protoscoleces begin to develop.

Although rare, humans can become infected with the metacestodes of *E. multilocularis* and the resulting disease is known as alveolar hydatidosis (Schmidt and Roberts, 1989). In humans, along with other accidental intermediate hosts, protoscolex development is infrequent, with reported rates of only 10-15% (Fujioka *et al.*, 1993; Tornieporth and Disko, 1994; Amman and Eckert, 1996). In order to become infected, a human must come into contact with viable eggs. Because the normal parasite life cycle is sylvatic, those people who are most at risk are those who live in rural areas or those who regularly handle wild canids, such as professional trappers (Stehr-Green *et al.*, 1988; Schmidt and Roberts, 1989; Amman and Eckert, 1996). Many researchers have also stressed the importance of domestic dogs in transmission of the disease to humans, with emphasis on those animals that are allowed to roam free and hunt wild prey (Wilson and

Rausch, 1980; Schmidt and Roberts, 1989; Petavy *et al.*, 1991; Schantz, 1993; Tornieporth and Disko, 1994). A notable example are the sled dogs of certain Inuit communities in Alaska which live in close association both with humans and the voles that serve as intermediate hosts in the region (Wilson and Rausch, 1980; Stehr-Green *et al.*, 1988; Gottstein, 1992). When a human does become accidentally infected, the presence of the metacestode will generally go undetected for some time, as the progression of the disease is slow in the initial stage, and always asymptomatic (Kasai *et al.*, 1980; Wilson and Rausch, 1980; Amman and Eckert, 1995). This initial, or latent, phase is believed to last about 10 years following infection, although estimates of the duration range from 5-15 years (Kasai *et al.*, 1980; Sato *et al.*, 1992a; Tornieporth and Disko, 1994; Amman and Eckert, 1995). Once symptoms do begin to manifest, they tend to be mild and vague, and a correct diagnosis is difficult. Early symptoms include a low-grade fever, epigastric pain and cholestatic jaundice, all of which may be attributed to other maladies (Sato *et al.*, 1992a; Tornieporth and Disko, 1994; Amman and Eckert, 1995, 1996). In later stages of the disease, the clinical symptoms become more pronounced and can include fatigue, weight loss, hepatomegaly, a palpable abdominal mass and progressive distension of the abdomen. In severe cases, ascites and portal hypertension have been reported (Wilson and Rausch, 1980; Tanner, 1987; Tornieporth and Disko, 1994; Amman and Eckert, 1995, 1996). Symptoms can also involve other organs due to the parasite's ability to metastasize. Cysts can develop in the brain, lungs, spleen, bone and other extrahepatic sites resulting in seizures, shortness of breath, splenomegaly, spontaneous bone fractures and a wide variety of other effects (Wilson and

Rausch, 1980; Tanner, 1987; Schmidt and Roberts, 1989; Merckle *et al.*, 1997). Without treatment, alveolar hydatidosis has a mortality rate of over 90% in human patients (Uchino *et al.*, 1993; Malczewski *et al,*, 1995).

As with any disease, the first step towards successful treatment of alveolar hydatidosis is a correct diagnosis. This is often difficult since the symptoms that patients present with are suggestive of more common ailments such as a hepatic carcinoma or cirrhosis (Gottstein, 1992). If a parasitic infection is suspected, a combination of imaging and immunodiagnostic techniques is generally used in order to achieve a firm diagnosis (Amman and Eckert, 1995; WHO, 1996). The most effective imaging techniques currently utilized are ultrasonography (US) and computed tomography (CT). These are both non-invasive modes of examination and are extremely useful for assessing the morphology of the cysts as well as their relationship to surrounding organs (Ogasawara *et al.*, 1993; Amman and Eckert, 1996). Additionally, there is an extensive body of research outlining the typical features of alveolar hydatidosis as it appears with US/CT, which contributes to the reliability of the methods (Amman and Eckert, 1996 and references therein). Other imaging techniques that have proven useful include plain-film X-ray, angiography and cholangiography (Ogasawara *et al.*, 1993; Tornieporth and Disko, 1994). Finally, use of magnetic resonance imaging (MRI) is increasing, but is still not as popular as older techniques owing to the relative newness of the technology. As yet, the characteristic appearance of metacestodes and affected host organs on MR images are not as well known as those on US or CT, but it has been predicted that MRI will continue to increase in popularity as clinicians become more familiar with the technique (Ogasawara

et al., 1993; Tornieporth and Disko, 1994). All of the imaging methods mentioned are useful for initial diagnosis, as well as pre- and post-treatment evaluation of the patient. However, they are all regarded as being rather unspecific (Tornieporth and Disko, 1994), and serological methods are required to confirm the presence of the parasite. There are a number of such tests that are applicable, including the complement fixation test (CFT), indirect hemagglutination (IHA), indirect immunofluorescence (IIF) and immunoelectrophoresis (IE) (Kumagai, 1993; Tornieporth and Disko, 1994), but by far the most widely used technique is the enzyme-linked immunosorbent assay (ELISA) (Gottstein, 1992; Tornieporth and Disko, 1994). Specifically, the Em2-ELISA can differentiate between *E. multilocularis* and other *Echinococcus* species in 95% of human cases by detecting the host response against the *E. multilocularis*-specific antigen Em2 (Gottstein, 1992; Gottstein *et al.*, 1993; Tornieporth and Disko, 1994; Amman and Eckert, 1996).

Once a definite diagnosis is obtained, a mode of treatment may be selected. Whenever possible, the preferred treatment is surgery coupled with chemotherapy. Generally this involves resection of the cysts from affected organs, but in cases where the liver is extensively invaded, liver transplantation is also an option (Schantz, 1982; Uchino *et al.*, 1993; Amman and Eckert, 1995). As surgery is only possible in 20-40% of symptomatic patients (Akinoglu *et al.*, 1991; Uchino *et al.*, 1993; Amman and Eckert, 1995), chemotherapy alone may be used in the remaining 60-80% in an effort to slow or arrest the growth of the metacestodes. Currently, the favoured drugs for treatment of the disease are benzimidazole derivatives (Amman and Eckert, 1996; WHO, 1996), and of

these, albendazole (ABZ) is the drug of choice (Saimot *et al*, 1983; Morris *et al.*, 1985; Sato *et al.*, 1993b). In animal trials ABZ shows a pronounced inhibitory effect on cyst growth and protoscolex formation by arresting parasite cellular proliferation with an efficacy far superior to other compounds tested (Taylor *et al.*, 1989; Sato *et al.*,1993b; Tornieporth and Disko, 1994). In experiments involving *E. multilocularis*-infected jirds, cyst weights in ABZ treated animals were as much as 75% less than those in untreated controls (Modha *et al*, 1997), although intact protoscoleces could still be detected (Taylor *et al.*, 1989). In human trials, ABZ also arrested the growth of metacestodes, and in some cases, resulted in a decrease in lesion size as observed by CT (Wilson *et al.*, 1987; 1992). Samples of parasite tissue isolated from human patients treated with ABZ and inoculated into voles either completely failed to proliferate (Wilson *et al.*, 1987) or else showed a pattern of proliferation indicative of a severely reduced viability (Wilson *et al.*, 1992). The mechanism behind the action of this potent chemotherapeutic agent is not well understood, but experiments carried out on *E. granulosus* suggest that the drug binds to tubulin within parasite microtubules, thus inhibiting cell growth and function (Morris and Smith, 1987). Experimental research completed in our lab revealed that ABZ also modifies the metabolism of *E. multilocularis* (Modha *et al.*, 1997). Metacestodes from ABZ-treated jirds contained less glycogen, glycine, succinate, alanine and acetate, but more taurine, glycerophosphocholine and phosphocreatine/creatine than those from untreated animals. It was hypothesized that the drug induces these changes by inhibiting certain key enzymes of carbohydrate metabolism, as well as by decreasing glycine production and dissipating the transmembrane proton gradient (Modha *et al.*, 1997).

Unfortunately, the same enzymes presumed to be affected by ABZ in the parasite are also present in human hepatocytes (Modha *et al.*, 1997), as is tubulin (Morris and Smith, 1987). This could explain the enzymatic abnormalities and other side effects seen in many treated patients such as inflammation, hepatocyte necrosis, destructive jaundice and hepatitis (Morris and Smith, 1987; Wilson *et al.*, 1992). The hepatotoxicity of ABZ coupled with the need for long-term treatments means that any patient undergoing chemotherapy for alveolar hydatidosis must be closely monitored to insure permanent liver damage does not occur (Morris and Smith, 1987; Wilson *et al.*, 1987).

More recently, some research groups have reported success in using cytokines to treat alveolar hydatidosis (Emery *et al.*, 1998; Jenne *et al.*, 1998). Interleukin-12 (IL-12) treatment cured 37.5% of infected mice and inhibited metastasis in 68.75% (Emery *et al.*, 1998), while interferon gamma (IFN-γ) treatment arrested the growth of metacestodes in the thorax and liver of a 61-year-old woman (Jenne *et al.*, 1998).

In intermediate hosts, the immune response against the parasite is both humoral and cell-mediated. Most human patients will respond to infection with the synthesis of parasite-specific antibodies of all the possible immunoglobulin classes (Vuitton *et al.*, 1984; Tornieporth and Disko, 1994; Gottstein and Felleisen, 1995). Most common are IgE antibodies which have been demonstrated in increased levels in many human cases (Vuitton *et al.*, 1988; Gottstein, 1992; Gottstein and Felleisen, 1995; Jenne *et al.*, 1997). In spite of this expressed humoral response, the secreted antibodies do not seem to have any protective effect for the host (Gottstein, 1992; Tornieporth and Disko, 1994), and may in fact be involved in certain immunopathologic processes (Gottstein, 1992). This is

in contrast to many helminthic infections or infestations where an IgE antibody-dependent, eosinophil-mediated cytotoxicity is effective at killing or damaging the invading worms (Abbas *et al.*, 1994; Kuby, 1994). In alveolar hydatidosis however, increased numbers of eosinophils are only seen in the peritoneums of experimentally infected mice (Devouge and Ali-Khan, 1983; Playford and Kamiya, 1992). Eosinophilia has not yet been seen in human patients (Vuitton *et al.*, 1984; Jenne *et al.*, 1997). However, an antibody-mediated complement interaction has been shown to lyse protoscoleces and oncospheres *in vitro*, and components of the complement system have been detected on the surface of metacestodes in mice *in vivo* (Tanner, 1987; Gottstein, 1992; Playford and Kamiya, 1992; Heath, 1995). So far, this is thought to be the most effective method of host defence observed in mice (Tanner, 1987; Heath, 1995) but there are no comparable studies on complement interaction in human hydatidosis.

A specific cellular immune response has been demonstrated by the *in vitro* proliferation of peripheral blood mononuclear cells (PBMC) in serum exposed to *E. multilocularis* antigen (Bresson-Hadni *et al.*, 1989; Gottstein *et al.*, 1991). The lab of Vuitton *et al.* (1989) has shown that in infected humans the periparasitic granuloma - the aggregation of mononuclear inflammatory cells at the host/parasite interface - is composed mainly of macrophages, T-cells and myofibroblasts. A similar cellular make-up is seen in the granulomas of experimentally infected mice (Bresson-Hadni *et al.*, 1990). Animals considered genetically susceptible to *E. multilocularis* infections have a higher proportion of the $CD8^+$ subpopulation of T-cells within the granuloma than do controls, while genetically resistant animals have a higher proportion of the $CD4^+$

subpopulation (Bresson-Hadni *et al.*, 1990). $CD8^+$ T-cells are cytotoxic cells that play an essential role in cell-mediated immunity while $CD4^+$ T-cells are the "helper T" cells involved in humoral immunity. In humans, a comparable effect is seen where patients with cysts that naturally "died out" have large numbers of $CD4^+$ cells in the granuloma, while high proportions of $CD8^+$ cells are seen in patients with active metacestodes (Vuitton *et al.*, 1989). Along similar lines, Gottstein *et al.* (1991) showed that the serum of "cured" patients is characterized by a high *in vitro* lymphoproliferative response and low antibody concentrations while that of patients with progressive hydatidosis is characterized by a low lymphoproliferative response and high antibody concentrations. This suggests that actively growing metacestodes markedly alter the host's cellular immune response. In mice the parasite growth is controlled by T-cells in the early stages of infection (Ali-Khan, 1978; Emery *et al.*,1998) but later the parasite is able to overcome the host's cellular defences and accelerates its proliferation (Ali-Khan, 1978; Emery *et al.*, 1996).

E. multilocularis metacestodes seem to have two general strategies for survival: evasion of the host's immune system and suppression of certain immune responses (Tornieporth and Disko, 1994; Gottstein and Felleisen, 1995). The laminated layer surrounding the developing metacestodes plays a major role in parasite survival within the host. While unprotected protoscoleces can be destroyed by a number of mechanisms, including complement proteins (Heath, 1995), activated macrophages (Kanazawa *et al.*, 1993), ivermectin (Ochieng-Mitula *et al.*, 1994) and the benzimidazole derivatives (Taylor and Morris, 1988), the metacestodes within a laminated layer remain viable even

when subjected to the same agents. Furthermore, the laminated layer can persist in host tissues long after the parasite itself has died out (Gottstein and Felleisen, 1995). Metacestode lesions that do not contain any living parasite cells will continue to stimulate a humoral immune response for an indefinite period, which gives an indication as to the inability of the host to remove this material (Rausch *et al.*, 1987). The juvenile worms also seem to have the ability to alter the immune response directly. Peritoneal macrophages from experimentally infected mice lose their accessory cell activity over the course of the disease (Rakha *et al.*, 1991), including their ability to activate T-cells. There is impairment of cellular mechanisms of recognition and neutrophil chemotaxis as well (Alkarmi and Behbehani, 1989), and it is thought that immunosuppression is due to certain factors secreted by the metacestode (Tornieporth and Disko, 1994). Persat *et al.* (1996) found that neutral glycosphingolipids found in metacestode surface membranes inhibit the human PBMC proliferative response by mechanisms that include cell lysis and inhibition of antibody synthesis.

Meanwhile, *E. multilocularis* infections are still extremely serious and a more thorough understanding of alveolar hydatidosis is essential if we ever hope to eradicate it. Research conducted in our lab investigates the metabolic interaction between parasite and host, and it was revealed that in the case of *E. multilocularis* metacestodes induce a systemic starvation effect in infected jirds (Novak *et al.*, 1989; 1993; 1995; Modha *et al*, 1997). The sera of infected animals showed a significant decrease in the levels of unbound fatty acid chains and glucose when compared to uninfected controls (Novak *et al.*, 1989), and glucose levels were seen to be lower in the liver, kidneys and spleen of

infected animals as well (Novak *et al.*, 1993). The presence of the parasite also led to a depletion of hepatic glycogen stores, a metabolic state that is characteristic of long-term starvation (Hunt and Groff, 1990). An examination of the lipid profile of livers from *E. multilocularis*-infected jirds showed that the parasite affects concentrations of lipid metabolites as well (Schoen, 1997). Infected livers had lower levels of total glycerophospholipid (GPL), and the individual GPLs phosphatidylinositol (PTI) and phosphatidylcholine (PTC). A decrease was also seen in the concentration of hepatic cholesterol (CTL), while tissue concentrations of phosphatidylethanolamine (PTE) increased with infection.

When the ratio of fatty acid moiety : total fatty acid was compared for various fatty acid (FA) components, increases were seen in the ratios of arachidonic acid, linoleic acid and one other polyunsaturated moiety in infected livers (Schoen, 1997).

In an effort to expand upon the knowledge accrued in our lab, I chose to continue to study the effect of *E. multilocularis* on host lipids by examining two other organs, kidneys and adrenal glands, of the jird *M. unguiculatus*.

II. Lipid Metabolism

1. Host: general aspects

Lipids are a large, heterogenous group of biomolecules that are characterized by their insolubility in water, but that can be extracted from cells and tissues by organic

solvents such as chloroform and benzene. In the living body, lipids have many diverse functions. They serve as sources of metabolic fuel and are structural components of all membranes. They also fulfill other biologically important roles including acting as enzyme cofactors and intracellular messengers (Shiau, 1987; Lehninger *et al.*, 1993).

The mammalian body is able to synthesize all of the lipids necessary for survival except for linoleic and α-linolenic acid (Longmuir, 1987; Hunt and Groff, 1990). Therefore, these FAs must be acquired from the diet. Additionally, mammalian cells lack the enzymes necessary for the synthesis of FAs with double bonds located beyond the ninth position from the carboxyl terminus, so these molecules are obtained by elongation of existing FAs or by dietary uptake (Longmuir, 1987). The digestion of ingested fats occurs primarily in the small intestine, and is facilitated, under the influence of bile, by the process of emulsification (Hunt and Groff, 1990; Guyton and Hall, 1996). This process results in a drastic increase in the surface area of the lipids, allowing the water-soluble lipase enzymes ready access to the molecules. There are several different lipases that contribute to the digestion of lipids, and the majority are secreted into the duodenum by the pancreas (Guyton and Hall, 1996). Triacylglycerols (TAGs), a class of neutral lipids consisting of three FA chains esterified to a molecule of glycerol, are broken down by the action of pancreatic lipase into a mixture of diacylglycerols (DAGs), monoacylglycerols (MAGs) and free FAs (Guyton and Hall, 1996). GPLs present in the mammalian diet consist of two FA chains esterified to a glycerol backbone at the C-1 and C-2 positions with a phosphate headgroup at C-3 (Longmuir, 1987). These molecules are hydrolyzed by phospholipase A_2, while cholesterol ester hydrolase is responsible for the

cleaving of ingested CTL esters into their component parts (Longmuir, 1987; Guyton and Hall, 1996). Once the lipases have completed the partial digestion of the fat molecules, the resulting digestates combine with bile salts to form water-soluble micelles which transport lipid moieties to the intestinal wall for absorption (Hunt and Groff, 1990; Guyton and Hall, 1996). The MAGs, free FAs, CTL and other products of digestion enter the mucosal cells by passive diffusion while the bile salts are "recycled" by the digestive system to be re-used in further lipid breakdown (Hunt and Groff, 1990; Brindley, 1991). In the smooth endoplasmic reticulum (ER) of the mucosal cells, TAGs, GPLs and CTL esters are reformed from their component parts and aggregate into globules along with phospholipids and free CTL (Shiau, 1987; Hunt and Groff, 1990; Guyton and Hall, 1996). Apoproteins coat the surfaces of these globules, and they enter the lymphatic system as lipoprotein particles to be transported throughout the body. The small intestine produces two types of lipoprotein particles: chylomicrons and very low density lipoproteins (VLDL) (Shiau, 1987; Hunt and Groff, 1990; Brindley, 1991). Additionally, short-chain free FAs can enter the portal blood vessels directly where they are bound to albumin and carried to the liver for oxidation (Hunt and Groff, 1990; Brindley, 1991). Once in the lymphatic system, chylomicrons and VLDLs are released into the bloodstream gradually to be carried to various organs for further metabolism. Lipoproteins undergo intravascular hydrolysis within certain tissues, such as skeletal muscle and adipose tissue, whereby TAGs are broken down to MAGs and free FAs. These molecules are quickly absorbed by the tissue cells and will either be oxidized for energy (as in muscle), or stored as TAGs for future use (as in adipocytes) (Hunt and Groff, 1990; Brindley, 1991;

Lehninger *et al.*, 1993; Guyton and Hall, 1996). Due to this intravascular hydrolysis, chylomicrons are reduced to small TAG-depleted, CTL-rich particles called chylomicron remnants that are removed from the blood and metabolized in the liver. At the same time, VLDLs are transformed to intermediate density lipoproteins (IDL) and then to CTL-rich low density lipoproteins (LDL) which carry CTL to peripheral tissues (Hunt and Groff, 1991; Deckelbaum *et al.*, 1992; Lehninger *et al.*, 1993).

The liver plays a vital role in mammalian lipid and lipoprotein metabolism. It is involved in the uptake of lipids, as well as their storage and metabolic conversion. It can release these molecules into the body because it is able to convert the hydrophobic lipids into water-soluble forms that can be transported to other tissues and organs in blood or bile (Desmet, 1994). Chylomicron remnants and the CTL they contain are quickly metabolized and any TAGs left in the lipoproteins of intestinal origin will also be used by hepatocytes and either oxidized to create energy or used in the synthesis of new lipids (Hunt and Groff, 1990). This is also the fate of those free FAs that are carried directly to the liver by the portal circulation (Hunt and Groff, 1990; Brindley, 1991; Seifter and Englard, 1994). The liver is capable of synthesizing new FAs either *de novo* from the products of carbohydrate and protein catabolism, or by modification of existing FAs (Hunt and Groff, 1990; Lehninger *et al.*, 1993). These FAs can then be incorporated into new TAGs, GPLs or CTL esters and transported to other tissues as hepatic lipoproteins. Finally, although many tissues in the body are capable of the *de novo* synthesis of CTL from units of acetyl coenzyme A (acetyl-CoA), the liver is considered to be the major site for this reaction (Vlahcevic *et al.*, 1994).

The process by which FAs are catabolized in the liver and other organs to produce metabolic energy is called β-oxidation (Figure 2) (Lehninger *et al.*, 1993; Guyton and Hall, 1996). This set of reactions represents a greater source of energy than the oxidation of carbohydrates because FAs exist in a more reduced state. Therefore, they must undergo a greater degree of oxidation in order to reach the ultimate endpoint of CO_2 and H_2O (Hunt and Groff, 1990). The FAs destined for β-oxidation are transported between organs either as free FAs bound to albumin, or as TAGs contained within lipoproteins such as VLDL (Brindley, 1991). These TAGs are hydrolyzed outside of cells by the enzyme lipoprotein lipase to yield glycerol and free FAs (Hunt and Groff, 1990; Brindley, 1991). The glycerol moiety can be utilized by any tissue possessing the enzyme glycerol kinase, which converts glycerol to a form that can enter glycolysis (Hunt and Groff, 1990; Lehninger *et al.*, 1993). However, the breakdown of glycerol releases only 5% of the energy that is biologically available in a TAG, and it is the oxidation of FAs that is the more important reaction (Lehninger *et al.*, 1993). The enzymes necessary for β-oxidation are localized within the mitochondria of cells, therefore once a FA enters the cytosol, it must be transported into the mitochondrial matrix (Hunt and Groff, 1990; Lehninger *et al.*, 1993; Seifter and Englard, 1994). The FA chains are first activated by a chain length-specific fatty acyl-CoA synthetase which catalyzes the formation of a thioester linkage between the FA carboxyl group and the thiol group of CoA. This energy-dependent reaction produces a fatty acyl-CoA intermediate that can then be carried across the mitochondrial membrane by facilitated diffusion (Lehninger *et al.*, 1993). The fatty acyl-CoA is transiently attached to the hydroxyl group of a molecule of carnitine by carnitine

Figure 2

β-oxidation of fatty acids and ketogenesis.

The following enzymes are involved:

1. Fatty acyl-CoA ligase
2. Carnitine acyltransferase I
3. Carnitine acyltransferase II
4. Fatty acyl-CoA dehydrogenase, enoyl-CoA hydratase, β-hydroxyacyl-CoA dehydrogenase and acyl-CoA acyltransferase
5. HMG-CoA synthase
6. HMG-CoA lyase
7. β-hydroxybutyrate dehydrogenase
8. β-ketothiolase

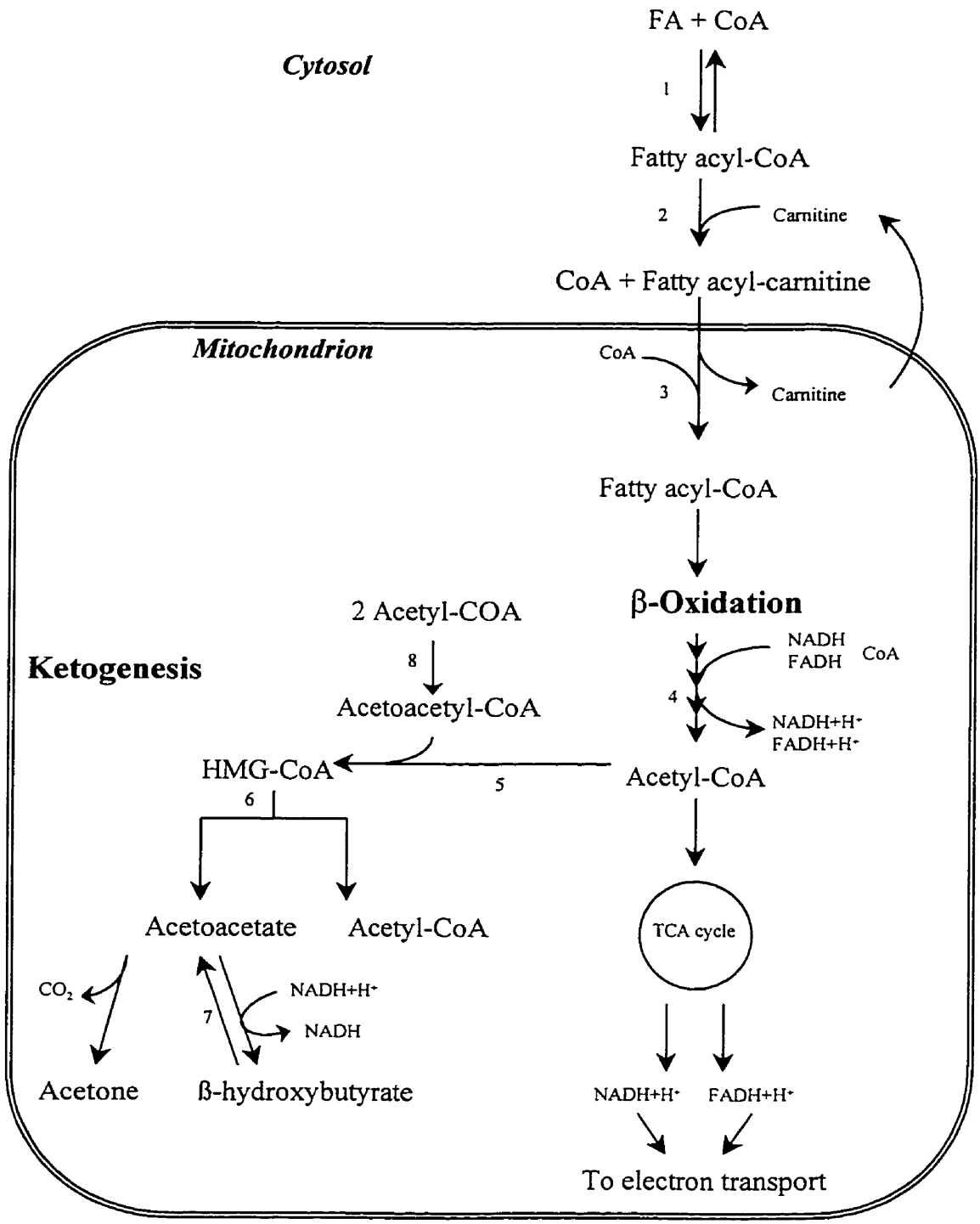
FA + CoA
Cytosol
1
Fatty acyl-CoA
2
Carnitine
CoA + Fatty acyl-carnitine
Mitochondrion
CoA
3
Carnitine
Fatty acyl-CoA
β-Oxidation
2 Acetyl-COA
NADH
FADH
CoA
Ketogenesis
8
4
Acetoacetyl-CoA
NADH+H+
FADH+H+
HMG-CoA
5
Acetyl-CoA
6
Acetoacetate
Acetyl-CoA
TCA cycle
CO2
NADH+H+
7
NADH
Acetone
ß-hydroxybutyrate
NADH+H+
FADH+H+
To electron transport

acyl transferase I in a reaction that displaces the CoA moiety (Hunt and Groff, 1990; Lehninger *et al.*, 1993). The fatty acyl-carnitine ester is carried through the membrane by the acylcarnitine/carnitine transporter, and the fatty acyl-CoA is reformed with intramitochondrial CoA by carnitine acyltransferase II (Schulz, 1991; Lehninger *et al.*, 1993). Once inside the mitochondrion, the fatty acyl-CoA can enter the β-oxidation sequence, essentially a series of enzyme-mediated dehydrogenation reactions and thiolytic attacks by CoA molecules. With saturated FA chains composed of an even number of carbon atoms, successive repetitions of the reactions produce numerous acetyl-CoA molecules (Lehninger *et al.*, 1993). Saturated FAs with an odd number of carbons are broken down to several acetyl-CoAs and one propionyl-CoA (Hunt and Groff, 1990). The acetyl-CoA produced enters the tricarboxylic acid (TCA) cycle where it is completely oxidized to CO_2, thus producing ATP and the reduced electron carriers $NADH+H^+$ and $FADH+H^+$. These flavoproteins go on to donate electrons to the mitochondrial electron transport chain (ETC), which itself produces H_2O and ATP (Lehninger *et al.*, 1993). Meanwhile, the propionyl-CoA resulting from the oxidation of odd-chain FAs is enzymatically converted to succinyl-CoA which enters the TCA cycle (Hunt and Groff, 1990; Schulz, 1991). Unsaturated FAs are also catabolized via β-oxidation, but additional reactions are required in order to move or remove the double bonds (Brindley, 1991). The auxiliary enzymes necessary are enoyl-CoA isomerase and 2,4-dienoyl-CoA reductase, respectively (Lehninger *et al.*, 1993).

Owing to the fact that the energetic returns obtained from FA oxidation are far greater than those obtained from the metabolism of other compounds, the catabolism of

FAs becomes crucial during periods of prolonged stress (Lehninger *et al.*, 1993; Seifter and Englard, 1994). During long-term starvation, the concentrations of carbohydrates in the body drop, and the rate of lipolysis in hepatic and adipose tissues increases (Hunt and Groff, 1990; Seifter and Englard, 1994). Large quantities of free FAs are released into tissues where energy is generated from the oxidation of acetyl-CoA in the TCA cycle. The liver, however, has the option of shuttling FA-derived acetyl-CoA into the synthesis of compounds known as ketone bodies (Figure 2) (Lehninger *et al.*, 1993; Seifter and Englard, 1994). During starvation, increased concentration of free FAs in the body leads to increased β-oxidation in the liver, but the hepatic TCA cycle can't handle the excessive amounts of acetyl-CoA produced. There is a limited supply of TCA cycle intermediates such as oxaloacetate (OAA) because these compounds are in turn shunted towards gluconeogenesis as the organism attempts to compensate for the drop in blood glucose levels (Lehninger *et al.*, 1993). Within hepatocyte mitochondria, two molecules of acetyl-CoA are acted upon by a thiolase enzyme to produce acetoacetyl-CoA. This molecule then condenses with another acetyl-CoA to form β-hydroxy-β-methylglutaryl-CoA (HMG-CoA), which is cleaved to produce acetoacetate and acetyl-CoA. The two previous reactions are catalyzed by HMG-CoA synthase and HMG-CoA lyase, respectively. Acetoacetate may be reversibly reduced by β-hydroxybutyrate dehydrogenase to form β-hydroxybutyrate (β-HB) or decarboxylated by acetoacetate decarboxylase to form acetone. Acetoacetate may also be directly exported from the liver along with the other ketone bodies β-HB and acetone to be catabolized in other tissues (Lehninger *et al.*, 1993). The liver lacks the enzyme that is essential for a tissue to utilize

ketone bodies for energy production, therefore it derives no direct energetic benefit from ketogenesis (Lehninger *et al.*, 1993; Seifter and Englard, 1994). Many other tissues do possess the enzyme, and can convert acetoacetate and β-HB back to acetyl-CoA. In organs with high energy demands, ketone bodies become the major source of ATP when glucose is no longer available. The brain requires approximately 25% of all metabolic energy produced to meet its needs (Hellerstein and Munro, 1994), and due to the presence of the blood-brain barrier, the necessary energy substrates must be water-soluble. Thus, during prolonged starvation, the brain depends on ketone bodies to fill a role that is occupied by glucose in the healthy animal. These compounds can cross the barrier of the CNS and be oxidized via the TCA cycle, providing energy returns that are comparable to those of short chain FAs (Hellerstein and Munro, 1994).

In addition to its role as an energy-producing product of FA oxidation, acetyl-CoA can also serve as a precursor in the synthesis of various lipids. When glucose is present in excess, acetyl-CoA may be used in the *de novo* synthesis of FAs (Figure 3). Most tissues are capable of this synthesis, but the liver is the major site of lipid production (Goodridge, 1991). FA synthesis occurs in the cytosol, but the needed acetyl-CoA is located in the mitochondria. Therefore, intramitochondrial acetyl-CoA combines with OAA to form citrate which can be transported across the mitochondrial membrane. Once in the cytosol, citrate lyase cleaves the citrate molecule releasing acetyl-CoA and OAA (Hunt and Groff, 1990; Goodridge, 1991). OAA is recycled back into the mitochondrion while acetyl-CoA is converted into the three carbon molecule malonyl-CoA by the activity of acetyl-CoA carboxylase. The new acyl chain is synthesized on a

Figure 3

Fatty acid synthesis.

The following enzymes are involved:

1. Citrate lyase
2. Acetyl-CoA carboxylase
3. Malonyl-CoA-ACP transferase
4. Acetyl-CoA-ACP transacetylase
5. FA synthase

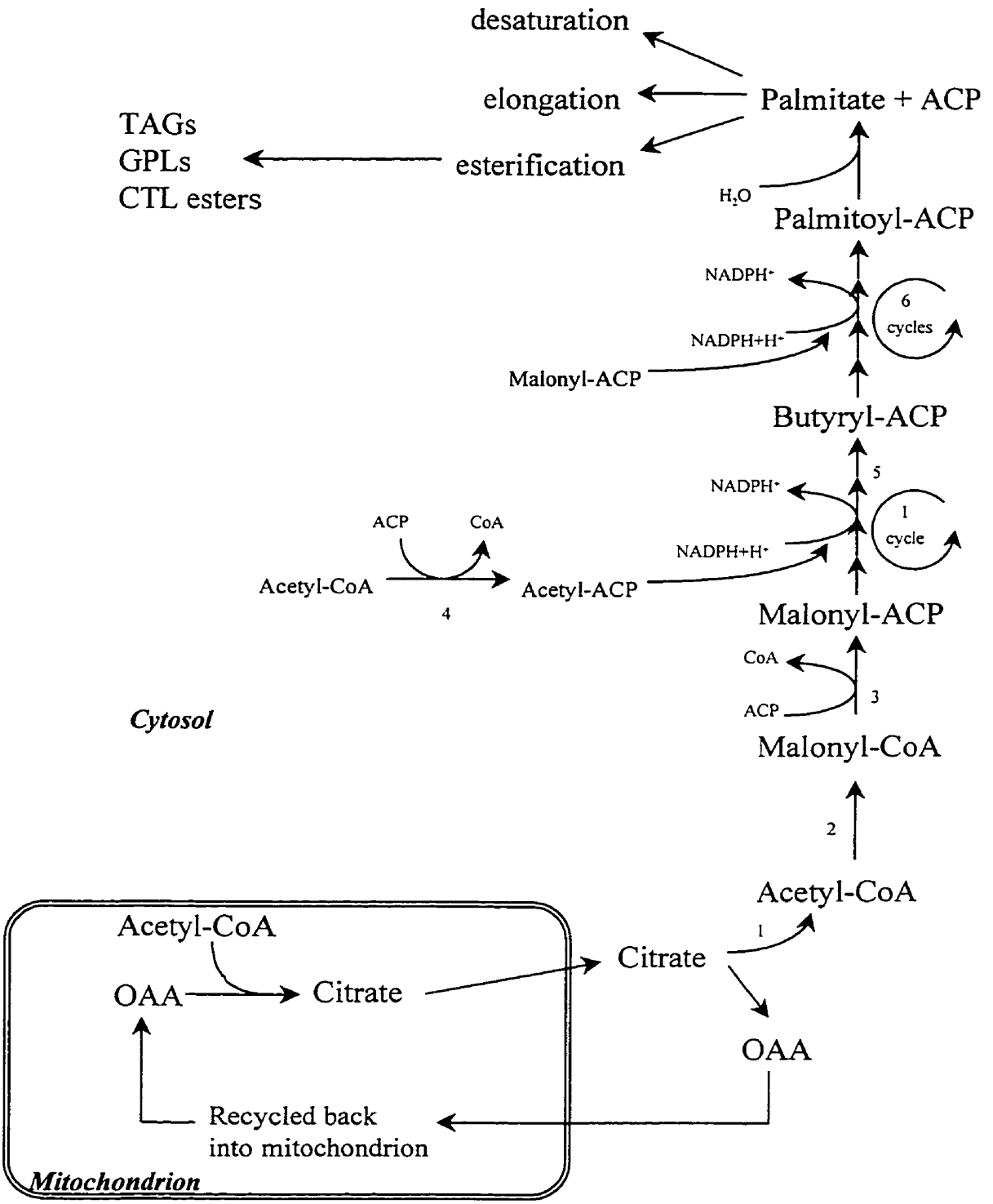
desaturation
elongation
Palmitate + ACP
TAGs
GPLs
CTL esters
esterification
H2O
Palmitoyl-ACP
NADPH+
6
cycles
NADPH+H+
Malonyl-ACP
Butyryl-ACP
5
NADPH+
1
cycle
ACP
CoA
NADPH+H+
Acetyl-CoA
Acetyl-ACP
4
Malonyl-ACP
CoA
3
ACP
Cytosol
Malonyl-CoA
2
Acetyl-CoA
Acetyl-CoA
1
OAA
Citrate
Citrate
OAA
Recycled back
into mitochondrion
Mitochondrion

multifunctional peptide enzyme called FA synthase (Goodridge, 1991). This complex polypeptide exhibits seven separate enzyme activities even though it is a single protein encoded by a single gene. The first step in the sequence of reactions is the activation of two acyl groups by FA synthase: the malonyl-CoA formed by the activity of acetyl-CoA carboxylase, and another molecule of acetyl-CoA. Each of these acyl molecules is transferred to a separate domain of the peptide by a specific enzyme. Acetyl-CoA-ACP transacetylase transfers the acetyl group of acetyl-CoA to the β-ketoacyl acyl carrier protein (ACP) synthase domain, while malonyl-CoA-ACP transferase transfers the malonyl group of malonyl-CoA to the ACP domain. These acyl-ACP derivatives undergo a condensation reaction that produces acetoacetyl-ACP with the release of a molecule of CO_2. Reduction of the carbonyl group to form β- hydroxybutyryl-ACP, followed by a dehydration reaction results in the creation of trans-Δ^2-butenoyl-ACP which undergoes a reduction to produce butyryl-ACP. The four carbon butyryl group is transferred from the ACP domain to the β-ketoacyl ACP synthase domain that was originally occupied by the acetyl group. A new malonyl group is attached to the ACP domain and the entire set of reactions is repeated resulting in a lengthening of the acyl chain by two more carbons. The acyl-ACP remains attached to the β-ketoacyl ACP domain and cycles through five more times, with two new carbons added each time. The final product of these reactions is the 16-carbon, saturated FA palmitate that is released from FA synthase by the action of a hydrolase (Goodridge, 1991; Lehninger *et al.*, 1993). Palmitate then becomes the precursor for other FAs (Longmuir, 1987). It may be elongated by the FA elongation systems present in the ER and mitochondria, or have cis double bonds introduced by a

number of different desaturase enzymes. The enzymes can insert a double bond at positions 9, 6, 5 and 4 from the carboxyl end of an FA and are therefore called Δ^9, Δ^6, Δ^5 and Δ^4 desaturases. As mentioned previously, mammalian cells do not possess any enzymes able to introduce a double bond beyond position 9, so any FAs with such a bond must be obtained either by elongation of an existing unsaturated FA or by dietary uptake (Longmuir, 1987; Cook, 1991).

Once synthesized, FAs may be incorporated into TAGs or GPLs (Figure 4). In order to be incorporated into a TAG, FAs must first be converted to their CoA esters by various acyl-CoA synthetase enzymes . They can then be esterified to the two free carbons of a molecule of glycerol-3-phosphate (G3P) by acyl transferases, producing a phosphatidate (diacylglycerol-3-phosphate). This intermediate is hydrolyzed to form a 1,2-diacylglycerol which is converted into a TAG by transesterification with a third fatty acyl-CoA (Brindley, 1991; Lehninger *et al.*, 1993). The G3P required for the formation of both TAGs and GPLs is created in one of two ways. It may be formed in the cytosol from the dihydroxyacetone phosphate (DHAP) generated during glycolysis in a reaction catalyzed by G3P dehydrogenase. Alternatively, in liver and kidney, it may be generated from glycerol by glycerol kinase. The biosynthesis of GPLs begins with the same reactions that initiate TAG synthesis. The exception is that instead of a third fatty acyl-CoA, a polar headgroup is attached to the C-3 of glycerol via a phosphodiester bond (Lehninger, 1993). Four of the most abundant GPLs in cellular membranes are PTC, PTE, PTI and phosphatidylserine (PTS) (Longmuir, 1987). Each of these GPLs can synthesized by more than one route, and many of the pathways are interrelated

Figure 4

Simplified overview of TAG and GPL synthesis.

A. Reactions of TAG and GPL synthesis

1. G3P dehydrogenase
2. Glycerol kinase
3. Acyl-CoA synthetase
4. Acyl transferase
5. Phosphatidate phosphatase

B. Structures of selected polar headgroups of GPLs

A.

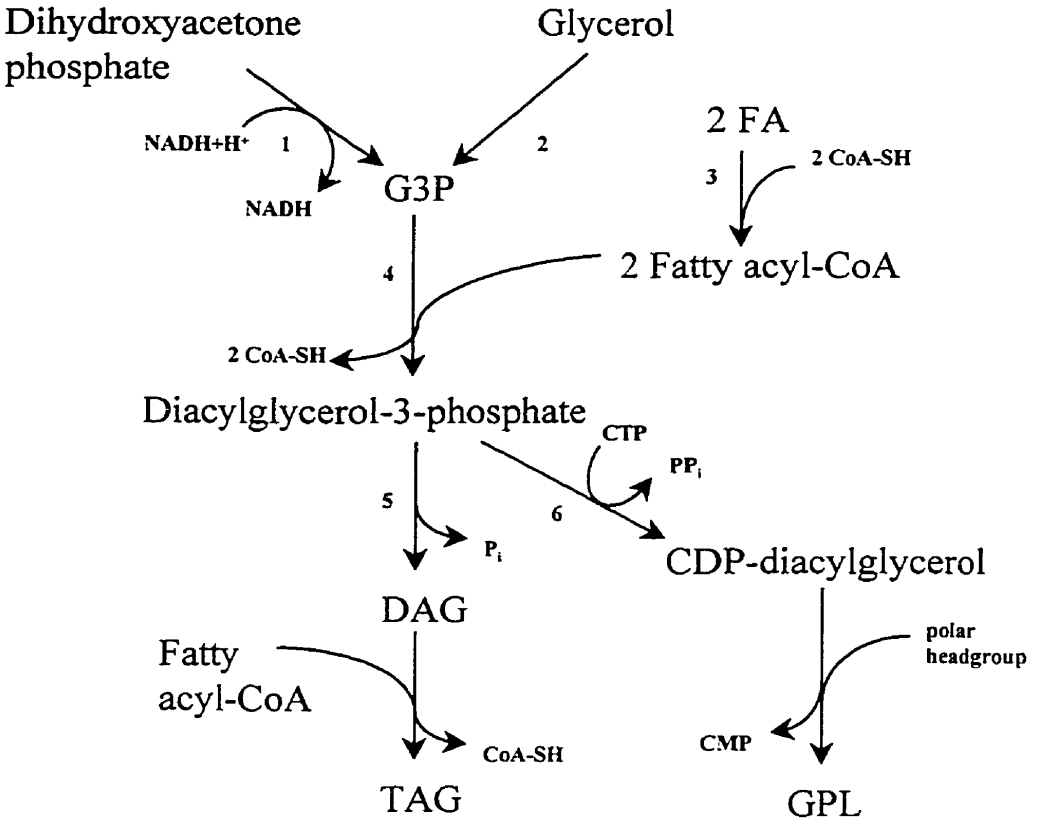

B.

Choline:

Ethanolamine:

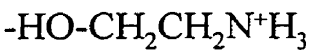

Serine:

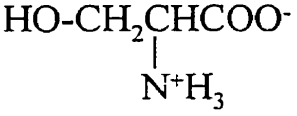

Inositol:

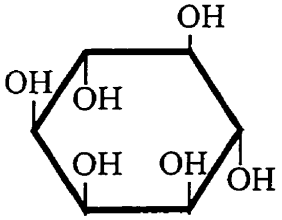

(Longmuir, 1987; Ansell and Spanner, 1982; Lehninger *et al.*, 1993). Following the synthesis of a 1,2-DAG, a polar headgroup can be attached through a molecule of phosphoric acid. The acid moiety forms two ester bonds: one with the hydroxyl group of glycerol C-3 and the other with a hydroxyl moiety located on the headgroup itself (Lehninger, 1993). One of the hydroxyls involved in the soon-to-be-formed phosphodiester bond must first be activated by the attachment of the nucleotide cytidine diphosphate (CDP). A cytidine monophosphate is displaced by the nucleophilic attack of the other hydroxyl group, and the bond is formed. The CDP nucleotide may activate either of the two hydroxyls, thus there are two general strategies for the attachment of a headgroup (Ansell and Spanner, 1982; Lehninger *et al.*, 1993). The primary intracellular location for the biosynthesis of GPLs is the ER, and they are transported to other membrane sites in ER-derived vesicles (Longmuir, 1987). GPLs and TAGs synthesized in the liver can also be transported to other locations in the body, but most tissues have at least a limited capacity to produce lipids *in situ* (Longmuir, 1987; Lehninger *et al.*, 1993).

The final important class of lipid found in mammalian cells is the sterols: CTL and its derivatives. CTL is obtained in the diet and transported through the body in lipoprotein particles, but it is also readily formed *de novo* in most mammalian tissues (Hunt and Groff, 1990). The liver and small intestine are responsible for the bulk of endogenous CTL produced. Biosynthesis involves 30 distinct enzymatic steps, starting with the formation of mevalonate from three molecules of acetyl-CoA (Vlahcevic *et al*, 1994). This set of reactions occurs in the cytosol and involves an HMG-CoA intermediate. Mevalonate is then converted into activated isoprene units, six of which

polymerize to form the 30-carbon, linear molecule called squalene. The final series of steps is the cyclization of squalene that produces the 4-ring steroid nucleus which is modified to form CTL (Pedersen, 1988; Lehninger *et al.*, 1993; Vlahcevic *et al.*, 1994). Once synthesized, CTL has several possible fates. It is an important component of membranes where it regulates membrane fluidity, and it is the sole precursor for bile acid and the steroid hormones (Lehninger *et al.*, 1993; Vlahcevic *et al.*, 1994). It may be converted to CTL esters by the action of acyl-CoA-CTL acyltransferase (ACAT) and either stored or transported to other tissues in lipoprotein particles (Pedersen, 1988; Lehninger *et al.*, 1993).

2. Host: kidneys

The kidneys fulfill a variety of functions within the mammalian body that are essential for the maintenance of a stable metabolic environment. These functions include the regulation of water and electrolyte balances in the blood, the excretion of metabolic waste products and foreign chemicals in urine, the regulation of arterial blood pressure, the secretion of hormones, and the synthesis of glucose (gluconeogenesis) (Guyton and Hall, 1996). Lipids play an important role in renal metabolism, as they do in other organs. Kidney cells are known to contain the enzyme glycerolphosphate acyltransferase which is essential for the synthesis of TAGs and GPLs (Longmuir, 1987; Brindley, 1991; Cook, 1991), and they can also synthesize FAs *de novo*. However, the rate of synthesis of these compounds is minimal when compared to that in the liver. With respect to

catabolic pathways, kidney cells rely heavily on the oxidation of FAs and ketone bodies to produce adequate ATP to fuel energy-requiring processes like the absorption of H_2O and solutes (Gullans and Hebert, 1996). Most of the various kidney cell types possess the enzymes of β-oxidation and in general, short-chain FAs like butyrate and valerate are preferentially utilized. Ketone bodies generated in the liver are even more readily oxidized than FAs, and in the absorptive cells of the nephron, β-hydroxybutyrate and acetoacetate alone are capable of supporting maximal rates of cellular activity. The substrates oxidized in renal cells are, for the most part, absorbed by the cells from blood plasma. The lipids generated endogenously are used in membrane synthesis or for the storage of particular FAs (Gullans and Hebert, 1996).

Renal interstitial cells fill the spaces within the kidney that are not occupied by nephrons or capillaries (Tisher and Madsen, 1996). These cells contain large lipid droplets that consist mainly of TAGs, CTL esters and GPLs, and because of the presence of a prominent ER, it is thought that the cells have a secretory function. The TAGs and GPLs in the droplets are rich in unsaturated FAs, including arachidonic acid (AA), a 20-carbon polyunsaturated molecule with four double bonds (Breyer and Badr, 1996; Tisher and Madsen, 1996). This FA is of particular interest as it is the precursor for a large group of biologically active molecules called eicosanoids (Lands, 1991; Smith *et al.*, 1991; Breyer and Badr, 1996). These molecules include the prostaglandins (PG), thromboxanes (TX), leukotrienes (LT), lipoxins (LX) and the mono-, di- and trihydroxyeicosatetraenoic acids (HETE), and they are all derived from AA (Breyer and Badr, 1996). Prior to conversion, the AA is stored as part of more complex lipid

molecules, primarily esterified at the 2 position of PTI, PTC and PTE (Schlondorff and Ardaillou, 1986; Smith *et al.*, 1991; Breyer and Badr, 1996). Appropriate stimuli - generally hormonal in nature - activate cellular phospholipase enzymes that liberate AA, and the free FA can enter one of three enzymatic pathways (Breyer and Badr, 1996). The actions of the renal eicosanoids are varied and complex. Products of one of the pathways (the cyclooxygenase (COX) pathway) act as both vasodilators and vasoconstrictors, depending on the specific type and circumstance. They also stimulate the release of renin, an enzyme that in turn stimulates an increase in arterial blood pressure (Breyer and Badr, 1996; Guyton and Hall, 1996), and are thought to have a role in the control of urine concentration, sodium excretion and blood flow through the kidney (Venuto and Ferris, 1982). All of these effects are achieved through the mediation or modulation of hormone action. LTs are potent vasoconstrictors and leukocyte activating agents, while LXs seem to act as vasodilators. HETEs are vasoactive as well, and seem to have an effect on sodium transport (Breyer and Badr, 1996).

It has been proposed that renal eicosanoids have one, all-encompassing function: cytoprotection (Schlondorff and Ardaillou, 1986). By constantly adjusting renal blood flow, interstitial ion concentration and pH, these compounds serve to protect renal cells from the drastic changes that can occur in their environments. It is known that PGs play a role in controlling renal hemodynamics and physiology in humans with advanced liver disease (Epstein, 1986), so it is logical to assume that they do so with any illness with systemic effects. Eicosanoids have also been implicated in the immune response to injury or the presence of a pathogen. Once an inflammatory response has been triggered,

eicosanoid production in surrounding cells increases and they contribute to the defence by promoting tissue swelling, triggering pain impulses and attracting platelets and leukocytes (Alberts, *et al.*, 1994). Eicosanoid synthesis is stimulated by a number of intercellular messengers, including the protein bradykinin and some of the adrenal steroid hormones (Breyer and Badr, 1996). Because the plasma concentrations of these compounds is drastically altered as a result of disease or prolonged stress, it is possible that eicosanoid levels throughout all body tissues are also altered, even if some of these tissues are not themselves directly traumatized (Alberts *et al.*, 1994).

Therefore, alterations to the renal lipid profile of *E. multilocularis*-infected jirds are anticipated even though the parasite is not known to invade the substance of the kidney. Systemic starvation conditions induced by the parasite within the host affecting glucose availability and the catabolism of FAs, coupled with suspected changes in eicosanoid production should produce alterations significant enough to be detectable by nuclear magnetic resonance (NMR) spectroscopy.

3. Host: adrenal glands

The adrenal glands are endocrine organs that are involved in the maintenance of homeostasis. Lipids have a central role in these glands, not only as major components of all membranes, but also as precursors for the main adrenal product: the steroid hormones. These hormones are synthesized in the outer cortex region of the organ, and they are all derived from CTL (Figure 5) (McNicol, 1992; Guyton and Hall, 1996). The cells of the

Figure 5

Synthesis of the corticosteroids.

A. Reactions of hormone synthesis

1. 20-22 desmolase
2. 3β-hydroxysteroid dehydrogenase
3. 21-hydroxylase
4. 11β-hydroxylase
5. 18-hydroxylase
6. 17α-hydroxylase
7. 3β-hydroxysteroid dehydrogenase
8. 21-hydroxylase
9. 11β-hydroxylase

B. Structures of some common corticosteroids

a. Progesterone

b. Corticosterone

c. Cortisol

d. Aldosterone

A.

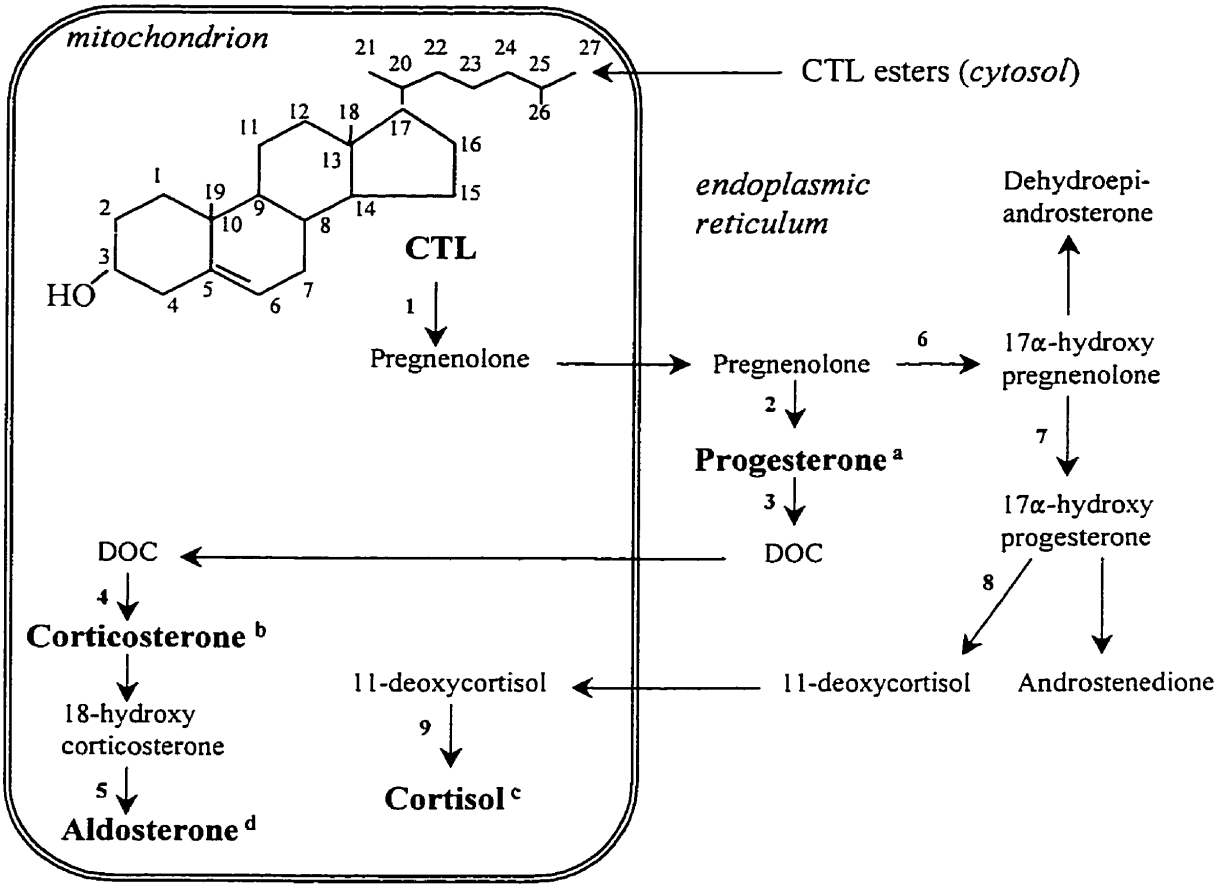
mitochondrion
CTL esters (cytosol)
endoplasmic reticulum
CTL
Pregnenolone
Progesterone a
DOC
Corticosterone b
18-hydroxy corticosterone
Aldosterone d
11-deoxycortisol
Cortisol c
Pregnenolone
17α-hydroxy pregnenolone
Dehydroepi-androsterone
17α-hydroxy progesterone
11-deoxycortisol
Androstenedione
HO

B.

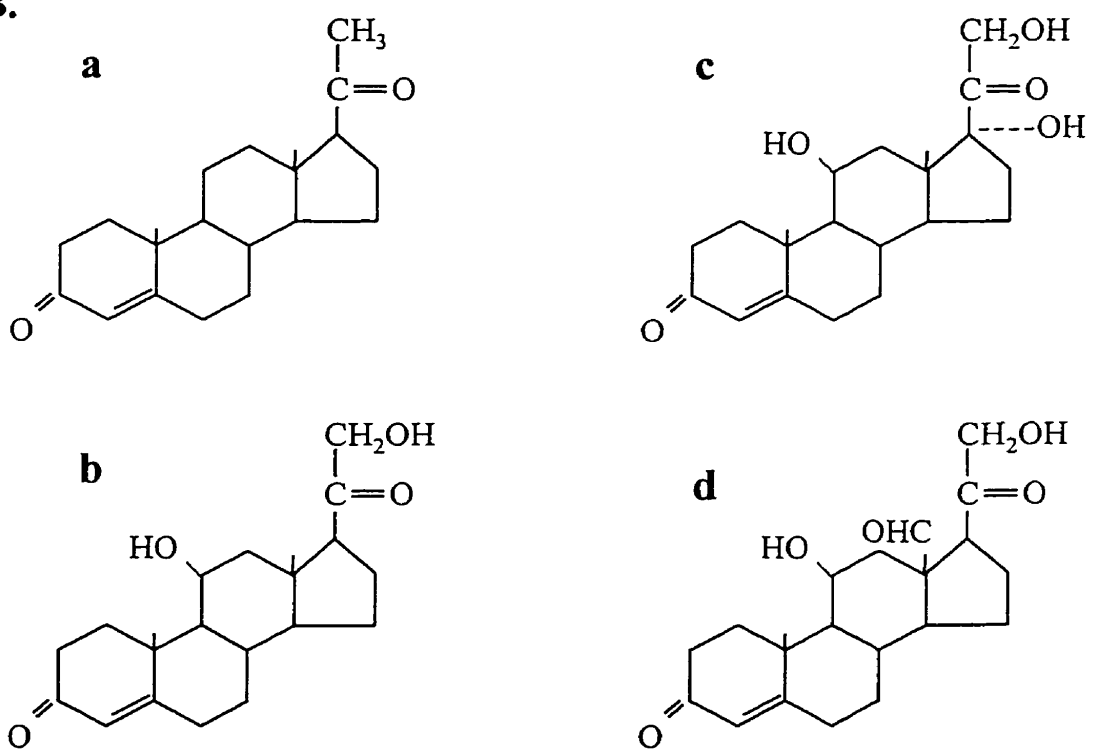
a
CH3
C=O
O
c
CH2OH
C=O
----OH
HO
O
b
CH2OH
C=O
HO
O
d
CH2OH
C=O
HO
OHC
O

adrenal cortex are characterized by the presence of large lipid droplets in which the majority of adrenal lipids are stored (Moore *et al.*, 1989). Droplets contain mainly free CTL and its derivatives, although other lipid species are present (McNicol, 1992). The steady-state concentration of intracellular CTL is maintained at a relatively low and constant level, and any excess is stored within the lipid droplets as CTL esters (Pedersen, 1988). The FAs in the esters are predominantly long-chain and unsaturated (Pedersen, 1988), although they can also contain FAs with as few as six carbons (Guo and Hamilton, 1993). Like most other mammalian tissues, the adrenal cortex is capable of synthesizing CTL *de novo*, but under normal conditions corticosteroidogenesis depends largely on exogenous sources of CTL derived from plasma LDL (Fraser, 1992). However, when plasma lipoprotein levels are limiting, as might be expected under conditions of systemic starvation, cortical CTL synthesis rates increase and endogenous CTL becomes the predominant substrate for hormone production (Pedersen, 1988).

The adrenal cortex produces three main classes of steroid hormones: mineralcorticoids, glucocorticoids and the sex steroids. The mineralcorticoids affect electrolyte and water balance in extracellular fluids, and are able to regulate the excretion of sodium and potassium in the kidney. The most potent member of this group is aldosterone, but there are several other, less important mineralcorticoids as well (Guyton and Hall, 1996). The glucocorticoids include cortisol and corticosterone, and their main effect is the raising of blood glucose levels (Munck and Náray-Fejes-Tóth, 1995) which is achieved through both a stimulation of gluconeogenesis and an inhibition of glucose utilization. They are also known to have anti-inflammatory actions and play a very

important role in the body's response to stress. In the healthy animal, glucocorticoids have a minimal effect on physiological processes, but in conditions of stress, their plasma levels increase and their effects become more pronounced. The final group of steroid hormones are the sex hormones, including progesterone and the estrogens, which affect sexual development and reproduction (Guyton and Hall, 1996). The adrenals are not the major sites for the production of these hormones, however, as the bulk are secreted from the gonads.

The pathways for the synthesis of the corticosteroids are illustrated in Figure 5. All of the steps, save the hydrolysis of the CTL esters, occur in two organelles, the mitochondrion and the ER. The mobilization of CTL esters from the lipid droplets is a process dependent on adrenocorticotropin (ACTH), a hormone secreted by the anterior pituitary gland, and it is mediated by cyclic AMP (cAMP) (Fraser, 1992). The synthesis of all the adrenal hormones is very tightly regulated, by other hormones and intercellular messengers, and by biofeedback mechanisms of the steroid hormones themselves (Guyton and Hall, 1996).

The adrenal hormones have profound effects on the functioning of the body, and their effects are tightly intertwined with the effects of other hormones, and the functioning of numerous other organs. For this reason, I expect that alveolar hydatidosis, a disease that produces profound systemic changes in metabolism, will have an equally profound effect on these glands. Using proton NMR spectroscopy, I have attempted to characterize some of these changes, focussing my attention on the lipid profile of the organs.

4. Parasite lipid metabolism

Cestodes are incapable of the *de novo* synthesis of sterols and FAs (Frayha and Smyth, 1983; Smyth and McManus, 1989; McManus and Bryant, 1995), but are still dependent on lipids for membrane synthesis and cellular proliferation. As obligate parasites they rely completely on the host to supply those compounds that they themselves cannot make, and therefore free FAs, GPLs, CTL and TAGs are all taken up through a combination of diffusion and mediated transport mechanisms (Smyth and McManus, 1989). Once the host-derived lipids have been absorbed, they are incorporated into various metabolic pathways in parasite tissues. There is no evidence to suggest that cestodes possess an active β-oxidation sequence, so they obtain little if any energy from lipid catabolism (Smyth and McManus, 1989). However several species are known to exhibit the activity of lipase enzymes that catalyse the breakdown of complex lipids to free FAs, glycerol and other moieties. Thus, while host lipids do not represent a source of metabolic energy for parasitic cestodes, they are important precursors for complex lipids of parasite origin.

Surveys conducted on the lipid profile of various juvenile taeniid tapeworms have shown that the major FAs present in lipids are the even-chain moieties palmitic, stearic, oleic and linoleic acid (Kassis and Frayha, 1973; Mills *et al.*, 1981; Smyth and McManus, 1989). These and other FAs found in cestode tissues are the result of either direct uptake from the host or the modification of host-derived lipids. Cestodes can liberate FAs from GPLs, acylglycerols and CTL esters (Smyth and McManus, 1989), and they are also capable of elongating FAs through the sequential addition of individual units of acetyl-

CoA (Frayha, 1971; Mills *et al.*, 1981; Barrett, 1983). Their ability to modify FAs ends here however, as they lack the enzymes necessary to add or remove double bonds from acyl chains (Barrett, 1983).

The FAs in cestode tissues may be incorporated into more complex lipid molecules, as occurs in mammalian tissues (Barrett, 1983). They are capable of incorporating free FAs and glycerol into their MAG, DAG and TAG fractions, just as they can synthesize GPLs and CTL esters. *Echinococcus* species are not able to synthesize sterols *de novo*, but it has been shown that they will readily produce CTL esters once the appropriate precursors have been absorbed from the host (Frayha, 1971; Barrett, 1983; Richards *et al.*, 1987). CTL is an important membrane constituent that has been detected in metacestodes of *E. granulosus* (Richards *et al.*, 1987) and *E. multilocularis* (Schoen, 1997) along with another important group of structural lipids: GPLs. Previously published research has demonstrated the presence of PTI and PTC in *E. granulosus* cysts (Richards *et al.*, 1987), and work completed more recently in our lab showed that *E. multilocularis* contains these molecules as well, and in addition, PTE (Schoen, 1997). It is known that cestodes are able to synthesize GPLs *de novo* from exogenous precursors that include glucose, FAs, glycerol and amino acids (Barrett, 1983; Smyth and McManus, 1989), but little is known about the actual synthetic pathways.

Recently, there has been considerable interest in the hypothesis that cestodes are able to synthesize eicosanoids, similar to those produced in the mammalian kidney (Belley and Chadee, 1995). The enzymes of the COX pathway have not yet been characterized in parasites, but at least two species of cestodes are known to produce PGs

and TXs (Leid and McConnell, 1983; Belley and Chadee, 1995). It has been speculated that eicosanoids of parasite origin may have a role in the successful evasion of the host immune response, but considerably more research needs to be done in this field before any definite conclusions may be drawn.

The direct uptake of host lipid by the juvenile stage of *E. multilocularis* coupled with the metabolic consequences of the systemic starvation conditions it induces suggests that infection with the metacestodes will have a profound effect on the overall lipid profile of the infected host. I examined two organs from intermediate hosts in an effort to describe some of the changes and learn more about the relationship that exists between parasite and host.

Hypothesis

Infection of *Meriones unguiculatus* with *Echinococcus multilocularis* will result in alterations to lipid metabolism in kidneys and adrenal glands of affected hosts.

III. Carbohydrate Metabolism

1. Host liver

As discussed above, the mammalian liver plays an integral part in the storage and metabolism of lipids, but this is far from the sum total of its duties. The liver also has a number of specific functions with respect to carbohydrate metabolism, including:

synthesis and storage of the polysaccharide glycogen, conversion of the monosaccharides galactose and fructose to glucose, gluconeogenesis and, finally, formation of many important biomolecules from intermediate products of carbohydrate metabolism (Guyton and Hall, 1996). In addition to the importance of their own direct consequences, these individual functions can be regarded as contributors to a more fundamental task carried out by the liver: the maintenance of glucose homeostasis (Hers, 1990; Seifter and Englard, 1994; Guyton and Hall, 1996). Free monosaccharides like glucose are not present in the mammalian diet in significant quantities (Hunt and Groff, 1990). Instead, the bulk of dietary carbohydrates are ingested in the form of polysaccharides such as starch and glycogen, or disaccharides such as lactose. These compounds are then broken down by hydrolytic enzymes within the gut and the products, principally glucose, fructose and galactose, are absorbed by the small intestine and enter the bloodstream (Seifter and Englard, 1994; Guyton and Hall, 1996). The level of glucose in the blood (glycemia) is an extremely important metabolic parameter, and as such, is tightly regulated by a number of different mechanisms (Guyton and Hall, 1996). When the level of glycemia is high, as is the case following a meal, glucose is taken up by hepatocytes and either converted to glycogen or oxidized to pyruvate via the glycolytic pathway (Hers, 1990; Seifter and Englard, 1994). The incorporation of glucose monomers into the glycogen polymer is a vital set of reactions that allows a large amount of the monosaccharide to be stored intracellularly in an insoluble form. This eliminates the possibility of glucose loss due to diffusion out of cells, and prevents the detrimental osmotic consequences that manifest when the level of glycemia exceeds normal limits (Lehninger, *et al.*, 1993; Seifter and

Englard, 1994). In contrast, when the level of glycemia is low, as occurs during fasting or systemic starvation, the hepatocytes are stimulated to release free glucose into the blood (Hers, 1990). This glucose is derived from the breakdown of glycogen (glycogenolysis) by the enzyme glycogen phosphorylase, or from *de novo* synthesis (gluconeogenesis) from lactate, pyruvate, amino acids and other substrates (Van den Burghe, 1991; Seifter and Englard, 1994). The maintenance of normal levels of glycemia is essential as certain tissues are obligate users of glucose for energy production (blood cells, retina and renal medulla), while others use it preferentially (brain) (Hers, 1990; Seifter and Englard, 1994). There is sufficient glucose located within hepatic glycogen stores to supply the body for approximately 12 hours, and so during short-term fasting, glycogenolysis is the primary source for the monosaccharide (Hellerstein and Munro, 1994). Long-term starvation, however, results in a severe depletion of hepatic glycogen and under these conditions, the body relies upon gluconeogenesis to maintain a supply of glucose in the blood (Hellerstein and Munro, 1994; Seifter and Englard, 1994).

The production of glucose via the reactions of gluconeogenesis occurs solely in the liver and renal cortex (Seifter and Englard, 1994), with the liver capable of producing considerably more of the hexose than kidney tissue (Van den Burghe, 1991; Seifter and Englard, 1994). The reactions of gluconeogenesis are very closely related to those of glycolysis, and the two processes share most of their enzymatic steps (Figure 6) except for three irreversible steps in each pathway that minimize futile cycling of carbohydrate through glucose synthesis and breakdown (Lehninger *et al.*, 1993). The first irreversible reaction of glycolysis is the phosphorylation of free glucose by the enzyme glucokinase,

Figure 6

Glycolysis and gluconeogenesis.

The following enzymes are involved:

1. Hexokinase
2. Glucose-6-phosphatase
3. Phosphoglucose isomerase
4. Phosphofructokinase-1
5. Fructose-1,6-bisphosphatase
6. Aldolase
7. Triose phosphate isomerase
8. G3P dehydrogenase
9. Phosphoglycerate kinase
10. Phosphoglycerate mutase
11. Enolase
12. PEP carboxykinase
13. Malate dehydrogenase (cytosolic)
14. Malate dehydrogenase (mitochondrial)
15. Pyruvate carboxylase
16. Pyruvate kinase
17. Glycogen phosphorylase
18. Phosphoglucomutase

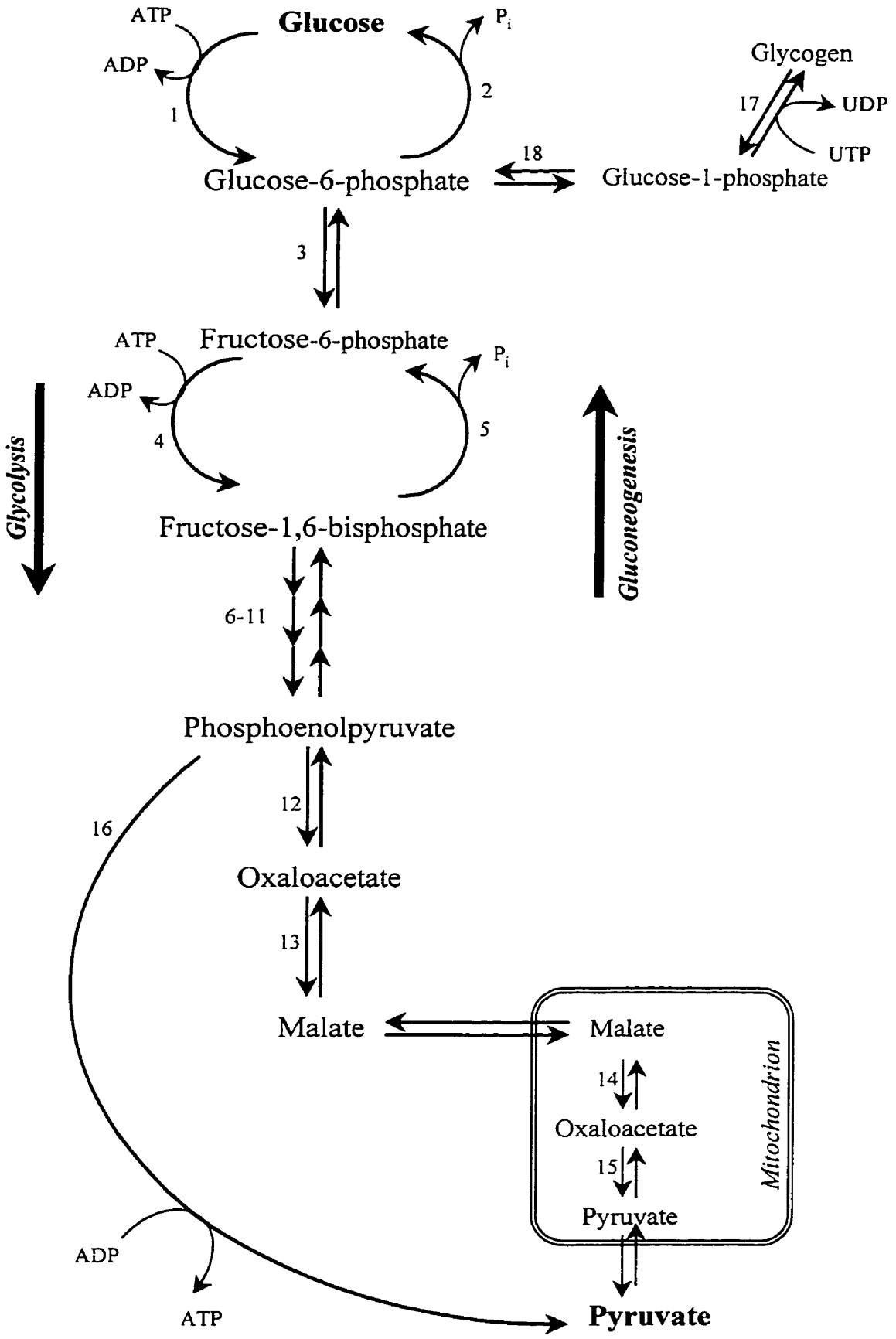
ATP
Glucose
P_i
ADP
1
2
Glycogen
17
UDP
UTP
18
Glucose-6-phosphate
Glucose-1-phosphate
3
ATP
Fructose-6-phosphate
P_i
ADP
4
5
Glycolysis
Gluconeogenesis
Fructose-1,6-bisphosphate
6-11
Phosphoenolpyruvate
12
16
Oxaloacetate
13
Malate
Malate
14
Oxaloacetate
15
Pyruvate
Mitochondrion
ADP
ATP
Pyruvate

(Fig. 6, [1]) The second of these steps is the phosphorylation of fructose-6-phosphate by phosphofructokinase-1 (Fig. 6, [4]) to yield fructose-1,6-bisphosphate, and the last is the conversion of phosphoenolpyruvate (PEP) to pyruvate catalyzed by pyruvate kinase (Fig. 6, [16]). Owing to the existence of these three irreversible steps in glycolysis, gluconeogenesis requires three corresponding by-pass reactions to function *in vivo*. First is the conversion of pyruvate to PEP via a series of reactions occurring in both mitochondrion and cytosol (Fig. 6, [12-15]), followed by the hydrolysis of fructose-1,6-bisphosphate by fructose-1,6-bisphosphatase (Fig. 6 [5]) to form fructose-6-phosphate. The final by-pass of gluconeogenesis involves the dephosphorylation of Glc-6-phosphate to yield free glucose in a reaction catalyzed by glucose-6-phosphatase (Fig. 6, [2]) (Lehninger *et al.*, 1993).

In order for hepatocytes to synthesize glucose, there must be a supply of appropriate precursor molecules. The principle substrates used in gluconeogenesis are lactate and alanine which, along with certain other amino acids such as serine and glycine, enter the pathway directly following their conversion to pyruvate (Lehninger *et al.*, 1993; Seifter and Englard, 1994). Other compounds can also serve as precursors. Glycerol and propionyl-CoA formed during the breakdown of lipids enter the reactions of gluconeogenesis in an indirect manner once they have been converted to glyceraldehyde-3-phosphate and succinyl-CoA, respectively (Lehninger *et al.*, 1993). Although FA-derived acetyl-CoA is not considered to be gluconeogenic as there can be no net synthesis of glucose from acetate, carbon atoms from acetyl-CoA can end up in glucose following their incorporation into TCA cycle intermediates that enter the pathway in the same way

as amino acids such as glutamate (Glu), proline, valine and phenylalanine (Lehninger *et al.*, 1993; Seifter and Englard, 1994).

Under normal metabolic conditions, the lactate present in the liver is derived principally from the anaerobic catabolism of glucose that occurs in certain extrahepatic tissues (Lehninger *et al.*, 1993; Hellerstein and Munro, 1994), in a reaction the results in a net gain of two molecules of ATP. Erythrocytes, retinal cells and brain tissue all ferment glucose to lactate, even under aerobic conditions, and skeletal muscle will produce lactate when the oxygen (O_2) supply is insufficient to support the oxidation of pyruvate via the TCA cycle. This is generally the case during short periods of strenuous muscle activity during which O_2 cannot be carried to muscles quickly enough to produce the ATP required to fuel the movements. The lactate produced is transported in blood to the liver where lactate dehydrogenase (Fig. 7, [1]) catalyzes its conversion to pyruvate (Lehninger *et al.*, 1993; Seifter and Englard, 1994), which in turn can enter either gluconeogenesis or other metabolic pathways (Rehbinder, 1971). The bulk of lactate delivered to hepatocytes is used in glucose synthesis, thus completing the Cori cycle: the interorgan glucose/lactate cycle that exists between liver and skeletal muscle (Seifter and Englard, 1994). However, not all lactate is destined for carbohydrate biosynthesis. Once incorporated into pyruvate, the carbon atoms derived from lactate can also enter the reactions of the TCA cycle and contribute to the formation of any of the TCA cycle intermediates, or any of the biomolecules synthesized from these intermediates (Rehbinder, 1971). Experiments in which ^{13}C-labeled lactate was perfused through intact hearts demonstrated label in succinate and glutamate, an amino acid formed from the transamination of

α-ketoglutarate (Sherry *et al.*, 1985; Malloy *et al.*, 1990a; Jones *et al.*, 1993), thus proving the incorporation of lactate into reactions other than those of gluconeogenesis.

The 2-carbon carboxylic acid acetate is another of the many compounds that may contribute to energy generation by entry into the TCA cycle. Free acetate must be converted to acetyl-CoA by the activity of acetyl-CoA synthetase (Fig. 7, [3]) prior to its incorporation into any metabolic pathway (Crabtree *et al.*, 1990; Lehninger *et al.*, 1993), and this reaction is known to occur readily in hepatocytes (Crabtree *et al.*, 1990; Seifter and Englard, 1994). In the normal, healthy mammalian liver, acetyl-CoA has three possible fates: lipid biosynthesis, ketogenesis or aerobic oxidation (Lehninger *et al.*, 1993). In an animal suffering from long-term starvation, it seems improbable that a significant amount of the organic acid would be shuttled into FA synthesis since it is the oxidative breakdown of these compounds that serves as the main source of acetyl-CoA under such conditions (Seifter and Englard, 1994). Instead, we expect the bulk of hepatic acetyl-CoA to be directed towards the TCA cycle and synthesis of ketone bodies. Ketogenesis and the importance of ketone bodies for the generation of energy under starvation conditions was addressed in the section on lipid metabolism, and the discussion will not be repeated here.

The well-known reactions of the TCA cycle (Figure 7) are localized within the mitochondria of hepatocytes (Lehninger *et al.*, 1993). Acetyl-CoA enters the pathway by combining with a molecule of OAA to form citrate in a reaction catalyzed by citrate synthase (Fig. 7, [4]). The six carbons of citrate pass through successive steps that lead to

Figure 7

The tricarboxylic acid cycle

This figure demonstrates the reactions of the TCA cycle as well as the entry points for lactate, acetate and alanine, and the formation of glutamate.

The following enzymes are involved:

1. Lactate dehydrogenase
2. Pyruvate dehydrogenase
3. Acetyl-CoA synthetase
4. Citrate synthase
5. Aconitase
6. Isocitrate dehydrogenase
7. α-ketoglutarate dehydrogenase
8. Succinyl-CoA synthetase
9. Succinate dehydrogenase
10. Fumarase
11. Malate dehydrogenase
12. Glutamate dehydrogenase

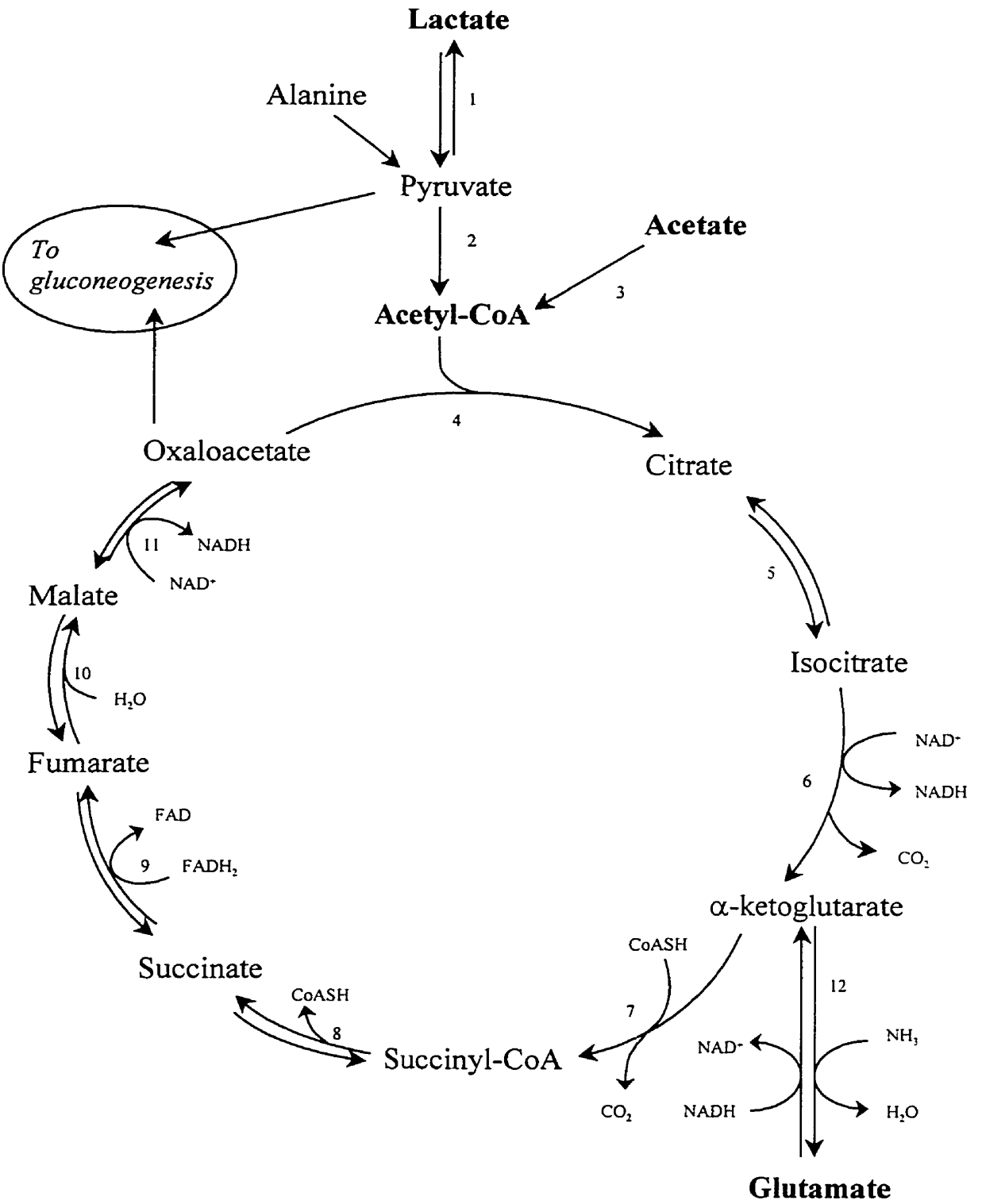
Lactate
Alanine
1
Pyruvate
To gluconeogenesis
2
Acetate
3
Acetyl-CoA
4
Oxaloacetate
Citrate
11
NADH
NAD+
Malate
5
Isocitrate
10
H2O
Fumarate
NAD+
6
NADH
CO2
FAD
9
FADH2
α-ketoglutarate
CoASH
Succinate
CoASH
7
12
8
Succinyl-CoA
NAD+
NH3
CO2
NADH
H2O
Glutamate

the eventual regeneration of OAA and the start of another turn of the cycle. The products of the eight enzyme-catalyzed reactions include one molecule of the high-energy compound GTP, three molecules of $NADH+H^+$ and one molecule of $FADH+H^+$. GTP is a carrier of the chemical energy needed to fuel many metabolic processes, while $NADH+H^+$ and $FADH+H^+$ are used to produce more of these high-energy phosphate compounds via the electron transport chain. Owing to the amphibolic nature of the TCA cycle, it is responsible for much more than just the oxidation of acetyl-CoA. The various intermediates themselves are precursors for other biomolecules which include amino acids, FAs, sterols, glucose and heme.

2. Parasite carbohydrate metabolism

Metacestodes of *E. multilocularis* readily absorb glucose from their hosts, and when its supply is plentiful it is incorporated into glycogen that is stored within protoscoleces to be mobilized in times when host glucose levels are low (McManus and Bryant, 1995). The hexose is catabolized through predominantly anaerobic pathways, starting with glycolysis, to produce energy (Figure 8). The bulk of the PEP produced by glycolysis is further broken down either by homolactic fermentation or a series of reactions involving malate dismutation. In homolactic fermentation, PEP is dephosphorylated by pyruvate kinase to produce pyruvate, which is then reduced by lactate dehydrogenase to form lactate. These reactions occur within the cytosol of parasite cells, and the lactate is excreted as a waste product into host tissues. In the reactions of malate dismutation, PEP

Figure 8

Carbohydrate metabolism in cestodes.

The following enzymes are involved:

1. Pyruvate kinase
2. Lactate dehydrogenase
3. Transaminase
4. PEP carboxykinase
5. Malate dehydrogenase (cytosolic)
6. Malic enzyme (cytosolic)
7. Malic enzyme (mitochondrial)
8. Pyruvate dehydrogenase
9. Unknown in cestodes
10. Malate dehydrogenase (mitochondrial)
11. Citrate synthase
12. Fumarase
13. Fumarate reductase

* reactions of glycolysis (as seen in mammals)

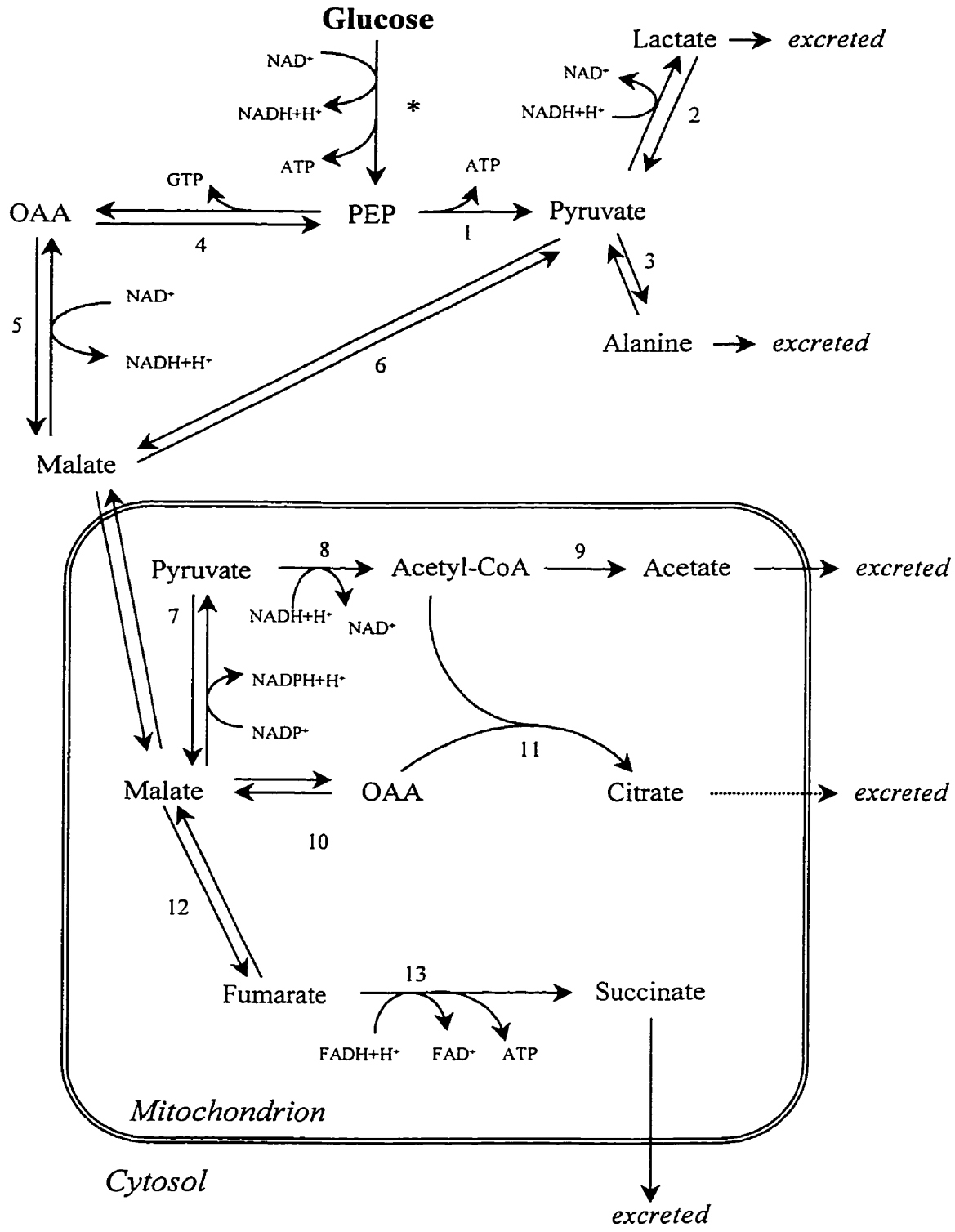
Glucose
NAD+
NADH+H+
ATP
*
Lactate
excreted
NAD+
NADH+H+
2
GTP
ATP
OAA
PEP
Pyruvate
4
1
3
5
NAD+
NADH+H+
6
Alanine
excreted
Malate
Pyruvate
8
Acetyl-CoA
9
Acetate
excreted
7
NADH+H+
NAD+
NADPH+H+
NADP+
11
Malate
OAA
Citrate
excreted
10
12
13
Fumarate
Succinate
FADH+H+
FAD+
ATP
Mitochondrion
Cytosol
excreted

is converted to OAA within the cytosol by the activity of PEP carboxykinase, and then malate is generated by malate dehydrogenase. The cytosolic malate is transported into mitochondria where it undergoes a dismutation to pyruvate via the action of malic enzyme, and fumarate in a reaction catalyzed by fumarase (McManus and Bryant, 1995). Pyruvate is oxidized to acetate via the action of pyruvate dehydrogenase and an unknown enzyme, while fumarate is converted to succinate by fumarate reductase. Both succinate and acetate cannot be efficiently metabolized by the parasite, so they are treated as waste and excreted. Each of these three fermentation pathways can generate only two molecules of ATP, so a considerable amount of glucose must be taken up and utilized by the metacestodes in order to produce adequate energy to fuel their metabolic needs (McManus and Bryant, 1995).

There is evidence to suggest that certain reactions associated with the aerobic catabolism of glucose function within cestodes as well. Following the injection of [2-^{13}C]acetate into livers of *E. multilocularis*-infected jirds, ^{13}C-label was detected in the TCA cycle intermediate citrate in perchloric acid (PCA) extracts of metacestode tissue (Schoen, 1997). Furthermore, when cysticerci of *Taenia crassiceps* were incubated with [3-^{13}C]pyruvate, they also produced ^{13}C-labeled citrate in addition to the usual excretory products succinate, lactate, acetate and alanine (Corbin *et al.*, 1998a). Similarly, when incubated with OAA, metacestodes of *Mesocestoides vogae* produced and excreted citrate into their incubation medium (Corbin *et al.*, 1998b). These results show that citrate synthase is active at least in metacestode tissues in addition to many other TCA cycle enzymes whose activities have also been detected. However, research completed in our

lab (Corbin, 1997; Schoen, 1997; Corbin *et al.*, 1998c) failed to detect any products of citrate catabolism in cestode tissues which suggests that the TCA cycle reactions between citrate and succinate are either absent in these organisms or operate very slowly. Evidence of citrate excretion by tetrathyridia of *M. vogae* (Corbin *et al.*, 1998b) supports this conclusion. The precise role of TCA cycle reactions in *E. multilocularis* is not yet fully understood, but it is known that the anaerobic pathways yielding lactate, acetate, succinate and alanine occur even under aerobic conditions (McManus and Bryant, 1995) which suggests that the parasites have a limited dependence on aerobic catabolism.

The end products of cestode carbohydrate metabolism are excreted by the parasites into host tissues (Smyth and McManus, 1989; McManus and Bryant, 1995), and it has been suggested that they may be incorporated into host synthetic pathways (Novak *et al.*, 1995). This is due to the fact that as metacestodes of *E. multilocularis* remove essential nutrients from the host they induce systemic starvation conditions within the infected animal. The starvation of the host results in significant changes to the homeostatic regulation of carbohydrates within the liver, leading to an increase in the rate of gluconeogenesis as the host tries to compensate for the glucose removed by the parasite. The newly synthesized glucose is catabolized in extra-hepatic host tissues via glycolysis, the TCA cycle and electron transport to produce metabolic energy, or else absorbed by the parasite for use in its own energy-producing pathways (Novak *et al.*, 1995). Thus the gluconeogenic precursors under these conditions can be compounds of both host and parasite origin. In the liver, acetyl-CoA derived from the β-oxidation of FAs will enter the TCA cycle and its carbon atoms may eventually end up in glucose. The lactate,

acetate, succinate and alanine of parasite origin can enter host hepatic biosynthetic pathways in a manner reminiscent of the glucose-alanine cycle and Cori cycle that function within mammalian tissues. In these two pathways, the alanine and lactate produced in muscle as a result of protein degradation and anaerobic glucose catabolism, respectively, are carried to the liver and incorporated into the reactions of gluconeogenesis (Hellerstein and Munro, 1994). These dual-purpose cycles serve to produce new glucose that is exported back to muscle cells, and to remove the organic acids from tissues before they can accumulate to harmful levels (Ampola, 1994).

In two separate experiments, Corbin (1997) studied the metabolism of [3-^{13}C]alanine and [3-^{13}C]lactate in livers of mice infected with cysticerci of the taeniid tapeworm *T. crassiceps*. Both labeled compounds were injected into the duodena of infected and uninfected animals, and metabolism was allowed to proceed for two hours. In the case of [3-^{13}C]alanine, there was less label in the alanine present in the livers of infected animals which clearly indicates an increased rate of alanine utilization. In addition, infected mice had lower concentrations of hepatic glucose and Glu. When the effects of parasite-induced starvation on the regulation of the enzymes and transport mechanisms involved in alanine metabolism were considered, it was concluded that the observed differences between the two experimental groups were due to an increase in the rate of gluconeogenesis in infected animals. Cysticercus tissue was also examined, and ^{13}C-labeled glucose was detected along with labeled acetate, alanine and lactate. Like all cestodes, *T. crassiceps* cannot synthesize glucose *de novo*, therefore the labeled glucose present in the parasite had to be of host origin and the result of the incorporation of

[3-^{13}C]alanine into host gluconeogenic pathways. At the time the experiment was terminated, the cysticerci contained 1.4 times as much glucose as the host liver, an indication of the parasite's glucose uptake ability. Although the ^{13}C-labeled acetate, alanine and lactate detected in cysticerci were due primarily to the uptake and conversion of exogenous [3-^{13}C]alanine, it is likely that their presence was also due, in part, to the catabolism of labeled glucose. Cestodes can absorb alanine from the host and convert it, through a pyruvate intermediate, to lactate via lactate dehydrogenase (McManus and Bryant, 1989). No further metabolism of these compounds in cestode tissues is possible, however, and they are excreted. Similarly, the pyruvate derived from alanine can be converted to both acetate and succinate (Corbin *et al.*, 1998a), but these products are again both excreted since cestodes lack the mechanisms necessary to utilize them further.

Similar results were seen when [3-^{13}C]lactate was injected into the duodena of infected mice (Corbin, 1997). Once again, hepatic levels of glucose were lower in infected mice than in controls, and there was also less ^{13}C label in the hepatic lactate of infected animals. As with [3-^{13}C]alanine, the latter observation indicates an increased utilization of the exogenous substrate within host hepatocytes. In addition, while there was no significant difference in the concentration of total hepatic glycogen between the two groups of mice, there was a decrease in the percent label in glycogen in the infected group. These results indicate that both the acceleration of gluconeogenesis and its related reactions (such as the conversion of pyruvate to OAA), as well as the inhibition of certain reactions that compete with gluconeogenesis for substrates (such as the conversion of pyruvate to acetyl-CoA by the pyruvate dehydrogenase complex) had to have happened.

It is likely that [3-^{13}C]lactate was converted to glucose more rapidly in infected animals due to the accelerated rate of gluconeogenesis and decelerated rate of competing reactions such as those of the TCA cycle. The newly synthesized glucose was rapidly exported from hepatocytes to supply the host's nutrient-deprived tissues, and once in circulation, was absorbed by the parasite. Evidence to support this theory arises from the fact that ^{13}C-labeled glucose was detected in metacestode tissue and, as discussed earlier, could only be present there as a result of uptake from the host. Additionally, less label was detected in hepatic succinate and glutamate in infected mice which suggests a decreased flux of labeled substrates through the TCA cycle (Corbin, 1997).

Schoen (1997) investigated the fate of [2-^{13}C]acetate in jirds infected with *E. multilocularis*. Following portal vein injections of labeled acetate and either 30 or 120 minutes of metabolism, it was possible to describe the flow of carbon between parasite and host. After 30 minutes, label was detected in hepatic acetate, β-HB, succinate, alanine, lactate and glucose in both infected and uninfected animals as well as in parasite cysts. Infected jirds had a higher percentage of ^{13}C in hepatic glycogen than controls, and while there was no change in the concentrations of total hepatic lactate and alanine between the two experimental groups, the percent ^{13}C enrichment in these two compounds was lower in the infected group. After 120 minutes, there was a decrease in the amount of label present in hepatic acetate, β-HB, succinate, alanine, lactate and glucose of infected animals, but more label was present in most of the parasite metabolites. In addition, the label in hepatic glycogen was gone, and was located instead in parasite glycogen. These results show that the carbon atoms of acetate do eventually

end up in host glucose, and that the newly synthesized glucose, when released into circulation, is readily absorbed by the metacestodes.

To follow up on the information obtained by Corbin (1997) and Schoen (1997), I elected to study the effect of *E. multilocularis* infection on the hepatic metabolism of [3-^{13}C]lactate and [1,2-$^{13}C_2$]acetate when introduced as a mixture. Using ^{13}C NMR spectroscopy, I examined the incorporation of these compounds into the TCA cycle and their relative contributions and that of endogenous, unlabeled metabolites to cycle intermediates. I wished to determine whether substrate competition in the feeder pathways of the TCA cycle is altered by this parasitic infection, with my focus being the competition between lactate and acetate for conversion to the acetyl-CoA that enters the cycle at the citrate synthase step. The results obtained by previous researchers in our lab led me to believe that livers of *E. multilocularis*-infected jirds experience increased rates of gluconeogenesis and decreased TCA cycle activity. Therefore, these changes, coupled with the presence of parasite-derived lactate and acetate, should be expected to produce alterations to the hepatic metabolite profile of infected animals profound enough to be detected by ^{13}C NMR spectroscopy.

3. Isotopomer analysis of metabolism

NMR spectroscopy is widely recognized as a very powerful tool for studying the biochemistry and physiology of living systems. The popularity of the technique is primarily due to its non-invasive nature which allows for the analysis of metabolism *in vivo*, but additional appeal lies in the fact that a number of different tissue metabolites can

be detected and quantified from a single NMR spectrum (Bader-Goffer and Bachelard, 1991). The basic principle of NMR spectroscopy is the measurement of the energy released when the magnetic moment of a particular nucleus changes its alignment in a magnetic field (Malloy, 1990), and there are several nuclei of biological importance that can be detected in this way. The most common nucleus used in NMR studies is ^{1}H, the most abundant isotope of hydrogen, but analyses of the ^{13}C isotope of carbon have been increasing in popularity over the past decade because of some unique advantages that this nucleus offers. The most abundant isotope of carbon is ^{12}C, a nucleus that is undetectable by NMR. In contrast, ^{13}C represents only 1% of all naturally occurring carbon so only those compounds that are present in tissues in high concentrations (like lipids) can be detected in natural abundance studies (Malloy, 1990). The advantage of ^{13}C NMR lies in the fact that ^{13}C-enriched substrates can be added to living systems and their metabolism along particular pathways may be mapped with little or no background interference from endogenous compounds (Bader-Goffer and Bachelard, 1991; Malloy, 1990).

Several techniques incorporating ^{13}C-NMR spectroscopy to study biological systems have been developed over the years, and one of them, the technique of isotopomer analysis, I chose to use in my own research. Isotopomers are molecules of the same compound that differ from each other solely with respect to the number and location of atomic isotopes they contain (isotope + isomer = isotopomer) (Bader-Goffer and Bachelard, 1991). For example, [3-^{13}C]lactate is an isotopomer of lactate as it has one ^{13}C isotope located at position 3 of the molecule, but it behaves in exactly the same way as unlabeled lactate in biochemical pathways. One of the most important NMR phenomena

in isotopomer analyses is coupling. If a ^{13}C atom in a molecule has another ^{13}C located adjacent to it, the isotope experiences coupling, its resonance will be split and appear as a doublet of peaks in the NMR spectrum. If a third ^{13}C nucleus is added, this doublet will be futher split into a doublet of doublets. Therefore, when the sample under investigation contains a mixture of isotopomers of a particular compound, the signals originating from the various carbon atoms in the compound will appear as complex multiplets of peaks in the final NMR spectrum.

The lab of A.D. Sherry and C.R. Malloy has published the results of numerous experiments in which they used isotopomer analysis to study the fate of labeled compounds as they pass through the reactions of the TCA cycle (Sherry *et al.*, 1985; Malloy *et al.*, 1987; Malloy *et al.*, 1988; Malloy *et al.*, 1990a; Jones *et al.*, 1993). One such set of experiments showed how the relative contributions of exogenous substrates to acetyl-CoA can be determined through examination of the resonances due to various Glu isotopomers (Malloy *et al.*, 1990). The make-up of the Glu isotopomers is dependent on the position of the ^{13}C label in the exogenous substrates. Malloy *et al.* (1990) perfused guinea pig hearts with a solution containing both [3-^{13}C]lactate and [1,2-$^{13}C_2$]acetate. Under these conditions, only three possible acetyl-CoA isotopomers may be formed; unlabeled acetyl-CoA derived from endogenous sources, [2-^{13}C]acetyl-CoA from [3-^{13}C]lactate and [1,2-$^{13}C_2$]acetyl-CoA from [1,2-$^{13}C_2$]acetate. The relative concentrations of these three isotopomers are defined as Fc_0, Fc_2 and Fc_3, respectively, (F_U, F_{LL} and F_{LA} in the present experiment) the chance that a molecule of OAA will condense with one of them to form citrate is proportional to its relative concentration within the acetyl-CoA

pool. This fact makes it possible to calculate Fc_0, Fc_2 and Fc_3 by analyzing the labeling pattern seen in compounds that are derived from citrate and the reactions of the TCA cycle. One such compound is the amino acid Glu, large pools of which exist within cells owing to the rapid equilibrium between it and α-ketoglutarate. Because only three acetyl-CoA isotopomers are formed under these experimental conditions, only 24 out of a possible 32 Glu isotopomers will be synthesized. As each individual Glu isotopomer has a different pattern of ^{13}C-labeling amongst its five constituent carbon atoms, each Glu carbon resonance will appear as a cluster of peaks instead of the singlet that would be observed in a natural-abundance spectrum. By measuring the areas of the various peaks in two of these multiplet resonances, it is possible to determine the relative concentrations of the different isotopomers in the sample that are contributing to that resonance. You can then work backwards in order to determine the original substrate sources of each isotopomer, and what their relative concentrations are. Malloy *et al.* (1990) derived mathematical equations that allow for the calculation of Fc_0, Fc_2 and Fc_3 from information garnered from the carbon 3 (C3) and carbon 4 (C4) resonances in a ^{13}C NMR spectrum of Glu. By measuring the doublet in the C4 resonance (C4D34) that arises as a result of coupling between C3 and C4 ($J_{C3, C4}$), the doublet of doublets in the C4 resonance due to $J_{C3, C4}$ and $J_{C4, C5}$, and the total areas of the C3 and C4 resonances, the relative concentrations of acetyl-CoA isotopomers can be calculated.

The analysis of Glu isotopomers using ^{13}C-NMR spectroscopy has been applied to metabolism in heart muscle (Malloy *et al.*, 1990a; 1990b), kidney tissue (Jans and Leibfritz, 1989; Jans and Kinne, 1991), brain tissue (Bader-Goffer *et al.*, 1990; Shank *et*

al., 1993) and liver (Cohen, 1987). I elected to use the specific method developed by Malloy *et al.* (1990) in an effort to study changes in hepatic metabolism that occur as a result of an alveolar hydatidosis infection.

Hypothesis

Infection of *Meriones unguiculatus* with *Echinococcus multilocularis* will result in alterations to the substrate competition in the TCA cycle reactions occurring within host hepatocytes.

Materials and Methods

I. Lipid Metabolism

1. Infection and Tissue Collection

Thirty-four, six month old *M. unguiculatus* males were used in this experiment. All animals were cared for and utilized in accordance with the principles of the Canadian Council on Animal Care as stated in Guide to the Care and Use of Experimental Animals, and were allowed to feed on commercial pellets and water *ad libitum*. Seventeen jirds were infected with *E. multilocularis* (Alaskan strain) by an intraperitoneal injection of 0.5 ml of cyst cell suspension each, prepared according to the method of Lubinsky (1960). The other 17 animals served as uninfected controls. On days 38-42 post-infection (p.i.), the jirds were anaesthetized with an intramuscular injection of sodium pentobarbitol (60 mg/kg) (MTC Pharmaceuticals), their abdomens opened and the kidneys and adrenal glands removed. Each organ pair was rinsed in sterile saline, frozen in liquid nitrogen (N_2) and then weighed. All organ pairs were stored at -70°C until preparation of the lipid extracts. Parasite cysts were also removed and weighed in order to determine the degree of infection, but they were not retained. To insure the metabolic rate of each animal was similar, all jirds were dissected between 9:00 a.m. and 12 noon. It is also important to note that the parasite, located in the peritoneal cavity, had not invaded the kidneys or adrenal glands of any of the animals used in this experiment at this time of infection.

2. Lipid Extraction and NMR Sample Preparation

The lipid extraction protocol utilized in this experiment was that developed by Folch *et al.* (1957) in which tissue is homogenized in a solution of chloroform, methanol and water (H_2O). In order to extract the maximum amount of lipid using this method, Folch *et al.* (1957) emphasize the importance of maintaining the correct ratio of the three solvents throughout. To do this, it is essential that the H_2O content of the sample tissues be known. Although the weight percent (%) of H_2O in kidneys and adrenal glands of many different animals is available in the literature, no such information could be found for desert-dwelling rodents like *M. unguiculatus*. One study demonstrated that bone tissue obtained from desert rodents has a significantly lower H_2O content than that obtained from non-desert rodents (Sokolov, 1966), and for this reason, it was considered prudent to determine the % H_2O in kidneys and adrenal glands of jirds rather than rely on values reported for rodents such as rats and mice (Altman and Dittmer, 1972).

Kidneys and adrenal glands were collected from uninfected jirds and frozen in liquid N_2. Each pair of frozen organs was crushed in liquid N_2 using a precooled mortar and pestle. Total lipids were extracted using a 2:1 (v/v) chloroform : methanol (C:M) mixture as suggested by Folch *et al.* (1957), and described below. The chloroform was HPLC grade from EM Industries (Merck, CX1050-1), while the methanol was reagent grade from Mallinckrodt. It is important to note that for the purposes of NMR analysis, the chloroform used should not contain ethanol, and should have a low concentration of hydrocarbon stabilizer.

Kidney tissue was extracted in 20 ml of the C:M solution per gram of sample, while

the adrenal glands were extracted in 25 ml per gram. A greater volume was used for extraction of the adrenals owing to their lesser weight. Without the larger volume of solution, the final extract volume would have been too small to work with comfortably. Each sample was homogenized using either a Brinkman Polytron homogenizer (kidneys) or a hand-held glass homogenizer (adrenal glands), and then vacuum filtered through a ceramic, 43 mm Büchner funnel using quantitative filter paper (VWR). The filtrate was collected and the tissue residue resuspended in the same volume of 2:1 C:M solution, re-homogenized and re-filtered. The first and second filtrates were then combined.

To determine the % H_2O, a portion of the filtrate was transferred, undiluted, to a 5 mm NMR tube for proton NMR analysis. Samples were run unlocked on a Gemini 200 NMR spectrometer operating at 200 MHZ with minimum receiver gain and the pulse width reduced to the point at which the receiver channel is no longer overloaded. Only one scan was acquired, and the mole % of chloroform, methanol and water in each filtrate sample was determined by integration of the corresponding resonances. Each integral value was corrected for the number of protons contributing to the signal and, in addition, the integral value for the H_2O resonance was adjusted to take into account the contribution from the hydroxyl proton of methanol. This procedure was repeated three times for kidneys and four times for adrenals, and the mean mole % of H_2O calculated. Based on the results obtained, all lipid extractions were performed making the assumption that each kidney pair was 84% H_2O by weight, and each adrenal pair was 69% H_2O by weight.

In the case of the organs used for the actual lipid analyses, the lipid extraction

procedure was followed as described above to the point of combining the two filtrates. At this stage, the tissue extract was washed with an appropriate volume of a 0.12 M potassium chloride (KCl) (Fisher Scientific) solution in order to remove all water soluble, therefore non-lipid, compounds. The volume of KCl required was calculated according to the method devised by Folch *et al.* (1957) which requires that the volume ratio of C : M : H_2O be 8 : 4 : 3, and where H_2O includes that already present in tissues. After washing, the phases were allowed to separate and the upper aqueous layer was removed and discarded. The washing was repeated a second time using an appropriate volume of a solution made to replicate the composition of the initial upper phase as described in Folch *et al.* (1957). Once again, the upper aqueous layer was removed and discarded and the lower layer, containing chloroform and lipids, was transferred to a round-bottom flask and rotary evaporated to dryness under $N_2(g)$. The sample was at room temperature or below until the final stage of evaporation when it was warmed very slightly by pouring warm water over the flask. The lipid residue was then resuspended in three ml of benzene (thiophene free, Fisher Scientific) and rotary evaporated to dryness in order to remove any remaining water by azeotropic distillation. The dry residue was resuspended in deuterated chloroform ($CDCl_3$) (99.8 atom % D, CDN Isotopes) with either 2.5 ml (kidneys) or 15 ml (adrenals) per gram of original tissue. Once again, the greater volume of solvent used in the case of the adrenal samples was a result of the relatively smaller size of the glands. To use the same proportion of solvent as was used with the kidney samples would produce volumes too small to work with. A known amount of tetrakis(trimethylsilyl)silane (TMSS) (98 atom % D, Aldrich Chemical Co.) was added to

each sample to act as an intensity standard. Following centrifugation at 2500 rpm (840 g) for 10 minutes, the supernatant was removed from each sample and combined with sufficient deuterated methanol (CD_3OD) (99.8 atom % D, CDN Isotopes) to produce a 1.75:1 (v/v) $CDCl_3$: CD_3OD ratio in the final NMR samples. In general, the addition of CD_3OD results in decreased line widths, and the relative amount of CD_3OD determines the position of the water peak; this particular ratio allowed for unhindered measurement of the CTL ester resonance. Lipid samples were stored in glass culture tubes at -70°C, and then transferred to 5 mm NMR tubes for proton NMR analysis.

3. NMR Spectroscopy and Quantification of Lipids

The lipid content and concentration of each sample were determined by quantitative and qualitative analysis of proton NMR spectra obtained from a Bruker AMX 500 NMR spectrometer operating at 500.14 MHZ for this nucleus. All samples were analysed at 27°C (300 K), and spectra were accumulated with the spectrometer locked on the methyl deuterons of CD_3OD. A spectral width of 5000.00 Hz, 32 K data points and a flip angle of 78° were used in data acquisition. The recycle time was 10.24 seconds and each sample was scanned 240 times. All chemical shifts were assigned relative to the C-18 methyl of CTL at 0.68 ppm. Peak identifications were based on published data (Sparling *et al.*,1989; Sze and Jardetzky, 1990; Casu *et al.*, 1991; Adosraku *et al.*, 1993; Choi *et al.*, 1993; Adosraku *et al.*, 1994) and spectra of authentic compounds.

The concentrations of individual lipids, total FA and various FA components (μmol/g of tissue) were calculated from integration data of spectral peaks relative to

TMSS, and the recorded weight of the original tissue. FA moieties that were studied included those from AA, docosahexaenoic acid (DHA) and linoleic acid (LA), as well as other, unspecified FA. Integration of peaks was carried out using a sub-routine of the UXNMR 980101.3 software on the AMX 500 spectrometer. All integration values were corrected for the number of protons contributing to the corresponding resonances. Total FA concentration was calculated from the combined integration values for the resonances of the ω-CH_3 protons of FA chains (δ = 0.87 ppm) and the protons of ω-CH_3 groups β to a double bond in FA chains (δ = 0.96 ppm). In addition, FA chain composition was analysed by calculating ratios of individual FA components to total FA. The following ratios were studied:

Saturated FA components

-$(C\underline{H}_2)_n$- (δ=1.29 ppm) : total FA

-$C\underline{H}_2COO$ (δ=2.32 ppm): total FA

-$C\underline{H}_2CH_2COO$ (δ=1.61 ppm) : total FA

Unsaturated FA components

-$C\underline{H}_2CH$=CH- (δ=2.02 ppm) : total FA

-CH=CH$(C\underline{H}_2CH$=CH$)_n$- (δ=2.81 ppm) : total FA

-CH=CH$CH_2C\underline{H}_2CH_2COO$ of AA (δ=1.68 ppm) : total FA

-CH=CH$C\underline{H}_2C\underline{H}_2COO$ of DHA (δ=2.39 ppm) : total FA

-CH=CH$C\underline{H}_2$CH=CH- of LA (δ=2.76 ppm) : total FA

The underlined H's represent those protons whose resonances were integrated for each lipid or lipid moiety.

The average number of double bonds per FA chain (degree of unsaturation, DU) and the average FA chain length (AFACL) were also determined for each sample.

$$DU = \underline{H}C{=}C\underline{H}\ (\delta{=}5.34\ ppm) : \text{total FA}$$

$$\begin{aligned} AFACL = {} & 1_a + 1_b + 2(DU) + 2(\text{-CH=CHC}\underline{H}_2\text{C}\underline{H}_2\text{COO of DHA : total FA}) + \\ & 2(\text{-CH=CHCH}_2\text{C}\underline{H}_2\text{CH}_2\text{COO of AA : total FA}) + (\text{-(C}\underline{H}_2)_n\text{- : total FA}) + \\ & (\text{-C}\underline{H}_2\text{COO : total FA}) + (\text{-C}\underline{H}_2\text{CH}_2\text{COO : total FA}) + \\ & (\text{-C}\underline{H}_2\text{CH=CH- : total FA}) + (\text{-CH=CH(C}\underline{H}_2\text{CH=CH)}_n\text{- : total FA}) \\ & + (\text{-CH=CHC}\underline{H}_2\text{CH=CH- of LA : total FA}) \end{aligned}$$

Where 1_a and 1_b are equal to one terminal methyl group (ω-CH_3) and one carbonyl group (C=O) per FA chain respectively.

Statistical analysis was performed using the SAS statistical computer program. Data were analysed by an analysis of variance (ANOVA) procedure where a value of $\alpha \leq 0.05$ was deemed significant.

II. Carbohydrate Metabolism

1. Preliminary Experiments

Over the course of planning this experiment, a decision had to be made regarding

the ratio of labeled compounds that should be used in order to obtain the best results. Two ratios of [1,2-$^{13}C_2$]acetate : [3-^{13}C]lactate were tested: 1 : 1 and 4 : 1. Nine, uninfected *M. unguiculatus* males were fasted overnight (~18 hours), and portal vein injections with the two mixtures of [1,2-$^{13}C_2$]acetate and [3-^{13}C]lactate were performed as described below. Five animals received the 4 : 1 mixture and four received the 1 : 1 mixture. PCA extracts of individual livers were prepared, and ^{13}C NMR analysis completed as described below. Examination of the resultant spectra of the individual samples revealed that there was no discernable difference between the two metabolite ratios, therefore the 1 : 1 solution was selected for the sake of economy. In addition, it was obvious that integration of all peaks in the Glu C3 and C4 resonances would be extremely difficult and inaccurate, so a decision was made to combine three extracts prepared from livers that were injected with the 1 : 1 solution and run the NMR analysis again. The combined sample produced a spectrum with a much improved signal : noise ratio, but integration of the smallest peak was still quite error-prone, which raised the question of whether or not the animals should be starved overnight prior to injection of the labeled compounds. In experiments completed previously in our lab in which hepatic carbohydrate metabolism was studied (Novak *et al.*, 1995; Corbin, 1997; Schoen, 1997), animals were fasted for 18 hours before labeled compounds were administered. The purpose was to insure host glycogen levels were depleted so that the exogenous, labeled substrates would be taken up into host metabolic pathways in place of endogenous products of glycogen catabolism. However, the current experiment studied the competition between lactate and acetate for entry into the TCA cycle, and there was

concern that for the purposes of ^{13}C NMR analysis, insufficient label would be incorporated into the pathway if the animals were starved. The reason is that when blood glucose levels are low (as in starvation) the oxidation of FAs that occurs produces large amounts of acetyl-CoA that are then available for entry into the TCA cycle. In the case of this experiment, this would result in a decrease in the proportion of labeled acetyl-CoA reacting with OAA, and a concomitant decrease in the ^{13}C labeling of TCA cycle intermediates and Glu. Therefore, in order to determine if this decrease in labeling would affect the peak intensities in the NMR spectra to an extent that would render data analysis impossible, more preliminary trials were done.

Three additional *M. unguiculatus* males were used and were allowed free access to food until the time of surgery and hepatic portal vein injections. The PCA extracts of all three livers were combined, and an NMR sample prepared. After acquisition of the ^{13}C NMR spectrum it could be seen that the signal : noise ratio was vastly improved over the sample prepared from starved animals, and so the decision was made to not starve the animals in future trials. It was also decided that all PCA extracts should be combined such that each final NMR sample would contain metabolites derived from three individual livers.

2. Infection and Tissue Collection

In this experiment, two groups of 21, six month old *M. unguiculatus* males were used. One group was infected with *E. multilocularis* by an intraperitoneal injection of cyst cell suspension as described above. The other group served as uninfected controls.

Throughout the course of the experiment, all animals were allowed to feed on commercial pellets and water *ad libitum*. Between 28 and 33 days p.i., each animal was anaesthetized with an intramuscular injection of sodium pentobarbitol (60 mg/kg). Their abdomens were opened and 0.1 cc of a solution containing a mixture of [1,2-$^{13}C_2$]acetate (3.5 mol/L) (99 atom % ^{13}C, MSD Isotopes) and [3-^{13}C]lactate (3.5 mol/L) (99.5 atom % ^{13}C, Isotec Inc.) was injected into the hepatic portal vein over a period of four minutes. In the case of the infected jirds, it was checked that the livers were completely free of parasite invasion. All animals were left to metabolize the labeled compounds for a period of one hour, after which time the livers were excised. The organs were rinsed in sterile saline, gallbladders were removed and discarded and the liver tissue was frozen in liquid N_2 and weighed. All organs were stored at -70°C until preparation of the perchloric acid (PCA) (Fisher Scientific) extracts. Parasite cysts were also removed and weighed in order to determine the degree of infection, and then frozen and stored for use in future studies. All jirds were dissected between 9:00 a.m. and 12 noon to minimize any effects of temporal differences in metabolism.

3. Preparation of PCA Extracts and NMR Samples

Each liver was crushed in liquid N_2 using a precooled mortar and pestle. The finely ground sample was then transferred into a 50 ml homogenizing tube with 4 ml of cold, 0.5 M PCA added per gram of tissue. The sample was homogenized while surrounded by an ice bath, and the resulting tissue suspension was centrifuged at 15000 rpm (27100 g) for 10 minutes at -2°C. The supernatant was decanted into a 30 ml beaker, neutralized

using potassium hydroxide (KOH) (Fisher Scientific) solutions, and centrifuged again under the aforementioned conditions to remove any precipitated potassium perchlorate. At this point in the procedure, three liver extracts were combined and frozen at -70°C so that each of the final NMR samples contained metabolites derived from three individual livers.

The frozen samples were lyophilized to dryness and prepared for ^{13}C NMR analysis by resuspension in 2.8 ml deuterium oxide (D_2O) (99.9 atom % D, CDN Isotopes) and 0.2 ml of a solution containing sodium [2,2,3,3-$^2H_4$]-3-trimethyl-silylpropionate (TSP) (MSD Isotopes) in D_2O (0.045 g/ml). The TSP served as a chemical shift and intensity standard. In addition, 0.15 g of ethylenediaminetetraacetate (EDTA) (J.T. Baker Chemical Co.) was added to each sample in order to chelate paramagnetic ions that can lead to line broadening in NMR spectra. Samples were stirred for a minimum of two hours, and the pH meter reading adjusted to 8.0-8.3 using sodium deuteroxide (NaOD) (99 atom % D, Aldrich Chemical Co.). At this pH meter reading, both the C3 and C4 resonances of Glu are clear of overlapping peaks that interfere under more acidic conditions. Following refrigeration for one hour, each sample was centrifuged for 30 minutes at 35000 rpm (119000 g) and 4°C. The supernatant was then transferred to a 10 mm NMR tube for ^{13}C NMR analysis.

4. NMR Spectroscopy and Data Analysis

Proton decoupled, ^{13}C NMR spectra were obtained from a Bruker AMX 500 NMR spectrometer operating at 125.77 MHZ for this nucleus. Proton decoupling was achieved

using the WALTZ-16 decoupling routine with the decoupler power set to 13dB for the acquisition and 20 dB for the relaxation. All spectra were acquired at 300 K (27°C). A spectral width of 26315.79 Hz, 64 K data points zero-filled to 128 K prior to transformation and a recycle time of 11.25 seconds were applied during data accumulation. The flip angle was 90°, acquisition time was 1.2452 seconds and each sample was scanned 8000 times. In addition, 32 dummy scans were added on to the beginning of each analysis to reduce any temperature gradients in the sample that could affect spectral resolution. Chemical shift values were assigned relative to the TSP resonance at 0.00 ppm, and peak assignments were based on published data (Malloy *et al.*, 1990a; Malloy *et al.*, 1990b) and spectra of authentic compounds. Quantification of the various glutamate isotopomers was achieved by measuring the heights of the component peaks in the glutamate C3 and C4 resonances, at 29.78 ppm and 36.27 ppm respectively. It should be noted that as peak heights are proportional to areas, providing line widths are constant, and as peak heights are often more reliable (Bain *et al.*, 1991), we elected to use the former for this study. The relative contributions of exogenous [1,2-$^{13}C_2$]acetate and [3-^{13}C]lactate to the acetyl-CoA used in the hepatic citrate synthase reactions was determined through use of the following mathematical equations. Equation (**3**) was derived by Malloy *et al.* (1990b), while equations (**1**) and (**2**) were adapted from the original Malloy *et al.* (1991) equations by our lab. Equation (**4**) was also derived in our lab for the purposes of this experiment.

(**1**) Mole fraction of acetyl-CoA derived from [3-^{13}C]lactate (i.e. labeled lactate)

$$= \mathbf{F_{LL}} = \mathbf{(A4S/A4D45)(A4Q/C3)}$$

(2) Mole fraction of acetyl-CoA derived from [1,2-$^{13}C_2$]acetate (i.e. labeled acetate)
$= \mathbf{F_{LA} = A4Q/C3}$

(3) Mole fraction of acetyl-CoA derived from endogenous sources (i.e. unlabeled sources)
$= \mathbf{F_U = 1 - (F_{LL} + F_{LA})}$

(4) % Glu molecules labeled with ^{13}C at C3 = **(A4D34/A4D34 + A4S) x 100**

Where: C3 represents the total area of the resonance due to carbon 3 of Glu

A4S represents the area of the singlet due to C4 of Glu (uncoupled)

A4D45 represents the area of the doublet due to coupling between carbons 4 and 5 (i.e. $J_{C4, C5}$) in the C4 resonance

A4D34 represents the area of the doublet due to $J_{C3, C4}$ in the C4 resonance

A4Q represents the area of the doublet of doublets due to $J_{C3, C4}$ and $J_{C4, C5}$ in the C4 resonance

Flow of label in the citrate synthase reaction

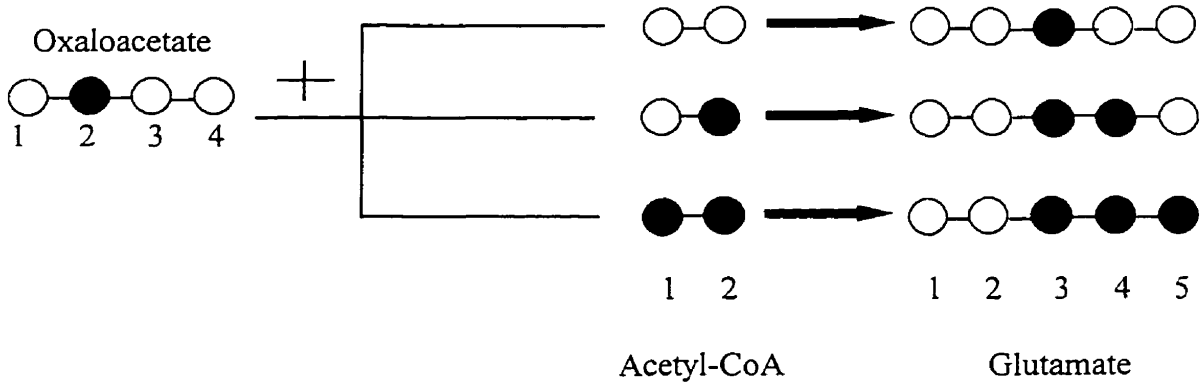

Where the open circles represent ^{12}C and the shaded circles represent the ^{13}C label.

Statistical analysis was performed using the SAS computer program. All data were analysed by an ANOVA procedure, with an α value of ≤ 0.05 deemed significant.

Results

I. Lipid Metabolism

In this experiment, the uninfected control animals had an average body mass of 70.91 ±7.43 g while the infected jirds had an average body mass of 66.14 ± 6.05 g. The body weight of infected animals was determined by subtracting the cyst weight from the host's total weight prior to organ removal. The mean weight of cysts was 17.76 ± 3.05 g. The difference between the mean body mass of control and infected animals was statistically significant.

1. Kidneys

The kidney pairs collected from uninfected jirds had a mean mass of 0.595 ± 0.068 g, while those collected from infected animals had a mean mass of 0.622 ● 0.056 g. There was no significant difference in the mean organ weights between the two groups.

Representative ^{1}H NMR spectra of C:M extracts of kidneys from an uninfected control jird and a jird infected with *E. multilocularis* are shown in Figures 9 and 10, respectively. The resonances that were integrated are labeled as follows: **1**, -C<u>H</u>=C<u>H</u>- of FA chains; **3**, C<u>H</u> of carbons 1 and 3 in glycerol of TAG; **4**, -C<u>H</u>$_2$OPO$_2$ in glycerol of GPL; **5**, C<u>H</u>OP in the ring of PTI; **6**, (C<u>H</u>$_3$)$_3$N$^+$ of PTC; **7**, $^+$NH$_3$C<u>H</u>$_2$ in PTE; **8**, -HC=CH(C<u>H</u>$_2$CH=CH)$_n$- of FA chains; **9**, -HC=CHC<u>H</u>$_2$CH=CH- of linoleic acid (LA); **10**, -HC=CHC<u>H</u>$_2$C<u>H</u>$_2$COO of docosahexaenoic acid (DHA); **11**, -C<u>H</u>$_2$COO of FA chains; **12**, -C<u>H</u>$_2$CH=CH- of FA chains; **13**, HC=CHCH$_2$C<u>H</u>$_2$CH$_2$COO of AA;

Figure 9

^{1}H NMR spectrum of a C:M extract of kidneys collected from an uninfected *M. unguiculatus*.

Peak assignments:

1. -C<u>H</u>=C<u>H</u>- of FA chains
3. C<u>H</u> of C-1and C-3 in glycerol of TAG
4. -C<u>H</u>$_2$OPO$_2$ in glycerol of GPL
5. C<u>H</u>OP in ring of PTI
6. (C<u>H</u>$_3$)$_3$N$^+$ of PTC
7. N$^+$H$_3$C<u>H</u>$_2$ of PTE
8. -HC=CH(C<u>H</u>$_2$CH=CH)$_n$- of FA chains
9. -HC=CHC<u>H</u>$_2$CH=CH- of LA
10. -HC=CHC<u>H</u>$_2$C<u>H</u>$_2$COO of DHA
11. -C<u>H</u>$_2$COO of FA chains
12. -C<u>H</u>$_2$CH=CH- of FA chains
13. -HC=CHCH$_2$C<u>H</u>$_2$CH$_2$COO of AA
14. -C<u>H</u>$_2$CH$_2$COO of FA chains
15. (-C<u>H</u>$_2$-)$_n$ of FA chains
16. -HC=CHCH$_2$C<u>H</u>$_3$ of ω-3 FA chains
17. ω-C<u>H</u>$_3$ of FA chains
18. C<u>H</u>$_3$ of C-18 of CTL

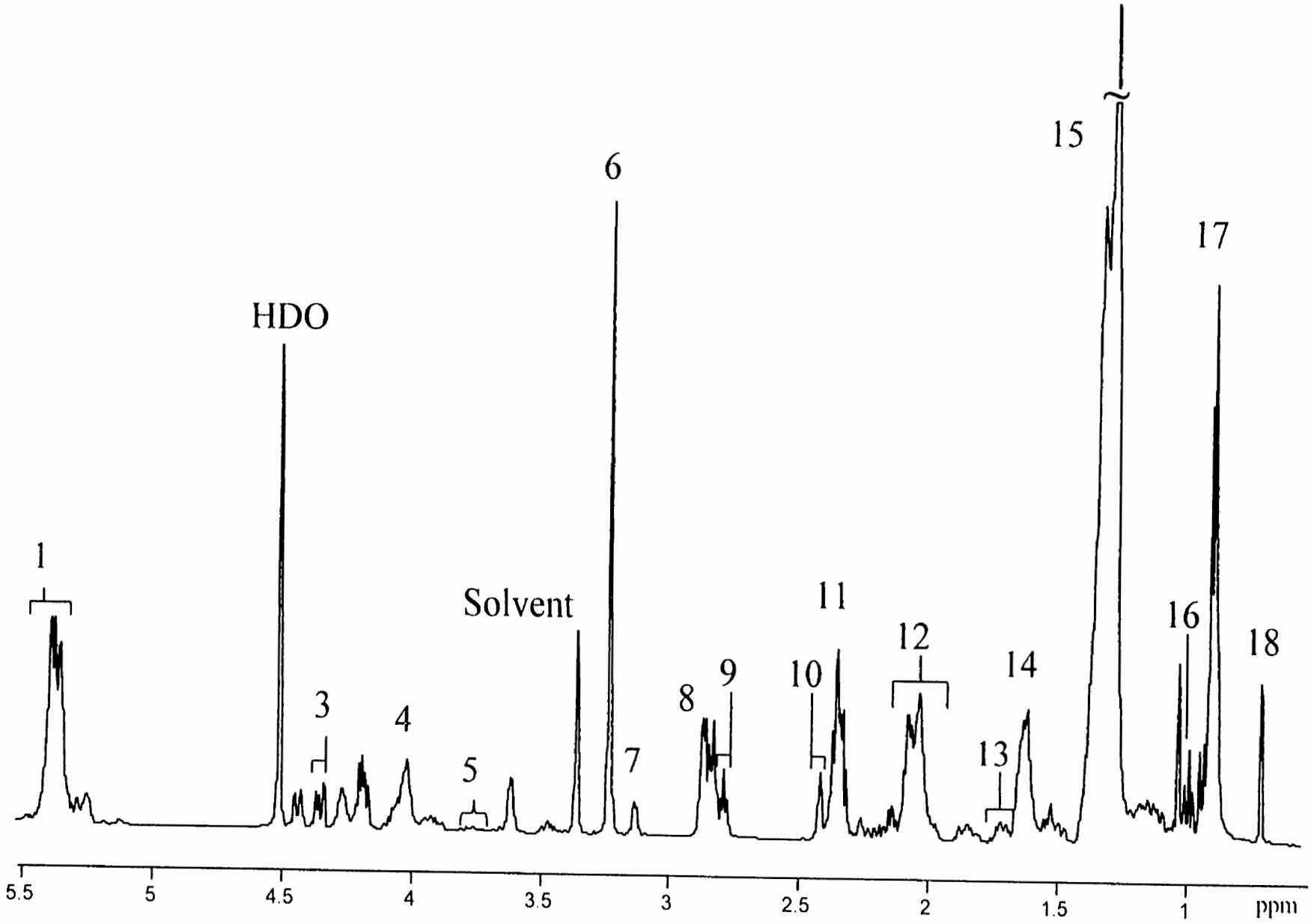
1
HDO
3
4
5
Solvent
6
7
8
9
10
11
12
13
14
15
16
17
18
5.5
5
4.5
4
3.5
3
2.5
2
1.5
1
ppm

Figure 10

^{1}H NMR spectrum of a C:M extract of kidneys collected from *M. unguiculatus* infected with *E. multilocularis*.

Peak assignments:

1. -C<u>H</u>=C<u>H</u>- of FA chains
3. C<u>H</u> of C-1 and C-3 in glycerol of TAG
4. -C<u>H</u>$_2$OPO$_2$ in glycerol of GPL
5. C<u>H</u>OP in ring of PTI
6. (C<u>H</u>$_3$)$_3$N$^+$ of PTC
7. N$^+$H$_3$C<u>H</u>$_2$ of PTE
8. -HC=CH(C<u>H</u>$_2$CH=CH)$_n$- of FA chains
9. -HC=CHC<u>H</u>$_2$CH=CH- of LA
10. -HC=CHC<u>H</u>$_2$C<u>H</u>$_2$COO of DHA
11. -C<u>H</u>$_2$COO of FA chains
12. -C<u>H</u>$_2$CH=CH- of FA chains
13. -HC=CHCH$_2$C<u>H</u>$_2$CH$_2$COO of AA
14. -C<u>H</u>$_2$CH$_2$COO of FA chains
15. (-C<u>H</u>$_2$-)$_n$ of FA chains
16. -HC=CHCH$_2$C<u>H</u>$_3$ of ω-3 FA chains
17. ω-C<u>H</u>$_3$ of FA chains
18. C<u>H</u>$_3$ of C-18 of CTL

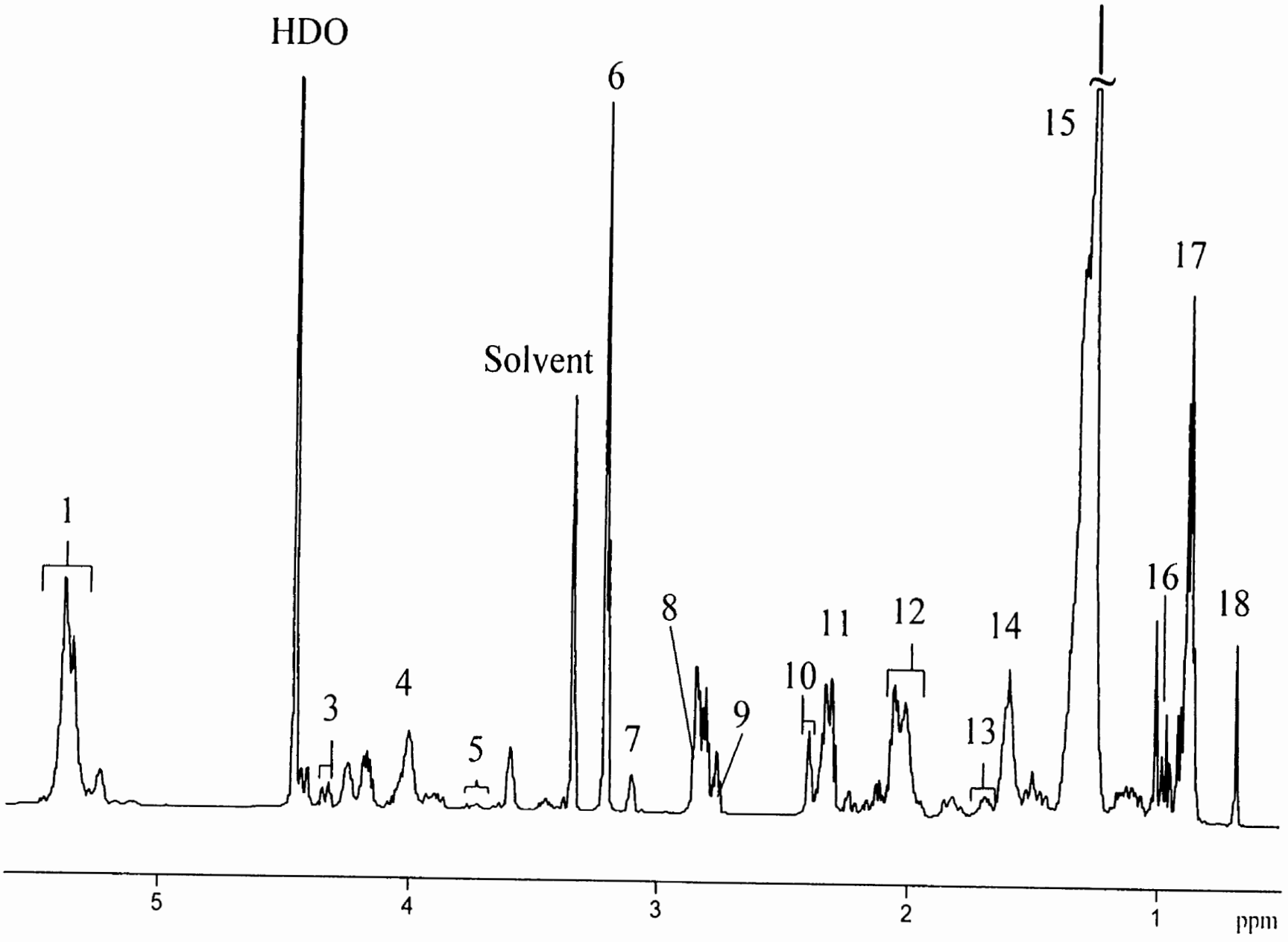
HDO
Solvent
1
3
4
5
6
7
8
9
10
11
12
13
14
15
16
17
18
5
4
3
2
1
ppm

14, -C$\underline{H}_2$CH$_2$COO of FA chains; **15**, -(C$\underline{H}_2$)$_n$- of FA chains; **16**, HC=CHCH$_2$C$\underline{H}_3$ of FA chains; **17**, ω-C$\underline{H}_3$ of FA chains; **18**, C$\underline{H}_3$ of C-18 of CTL.

The concentrations of various classes of lipids, total FA and FA moieties are presented in Table 1. The kidneys from infected jirds had lower concentrations of PTE, PTC, total GPL, the polyunsaturated FA moiety -HC=CH(C$\underline{H}_2$CH=CH)$_n$- and AA than those from control animals.

Ratios of individual FA moieties were also calculated (Table 2), and only two differences were found between the groups. The ratios of the polyunsaturated moiety -HC=CH(C$\underline{H}_2$CH=CH)$_n$- and -HC=CHCH$_2$C$\underline{H}_2$CH$_2$COO$^-$ of AA were both lower in the kidneys from infected animals. There were no other statistically significant differences between the two groups, including the degree of unsaturation and the average FA chain length.

2. Adrenal glands

The adrenal pairs collected from the uninfected controls had a mean mass of 58.0 ± 14.0 mg which was not significantly different from the mean mass of the adrenals from infected animals (55.0 ± 12.0 mg).

Representative ^{1}H NMR spectra of C:M extracts of adrenal glands from an uninfected control and an infected jird are shown in Figures 11 and 12, respectively. The peaks that were integrated and analyzed were the same as those studied in the kidney spectra, with one exception. Peak number **2** in the adrenal spectrum was not present in kidney spectra and represents the signal from the C$\underline{H}$ of carbon 3 in esterified CTL.

Table 1: Concentrations of lipid metabolites from kidneys of *Meriones unguiculatus* infected with *Echinococcus multilocularis*.

Lipid or Lipid Component	Concentration (μmol/g wwt.) Mean±SD	
	control (n=17)	infected (n=17)
Cholesterol	11.04 ± 2.84	10.86 ± 3.10
Phosphatidylethanolamine	9.13 ± 0.81	8.46 ± 0.48*
Phosphatidylcholine	17.06 ± 1.42	16.04 ± 0.78*
Phosphatidylinositol	4.55 ± 1.30	5.06 ± 1.45
Total Glycerophospholipid	43.22 ± 3.69	40.33 ± 2.23*
Triacylglycerol	9.66 ± 2.49	11.60 ± 3.42
Total Fatty Acid	122.50 ± 10.26	124.17 ± 17.12
$C\underline{H}_2$ in $-(CH_2)_n-$	925.46 ± 79.04	934.77 ± 128.40
$-C\underline{H}_2CH_2COO$	83.24 ± 8.60	85.43 ± 12.84
$-C\underline{H}_2COO$	79.10 ± 7.95	80.82 ± 12.41
$-C\underline{H}=C\underline{H}-$	149.37 ± 10.83	147.34 ± 15.86
$C\underline{H}_2$ in $-CH=CH(CH_2CH=CH)_n-$	76.78 ± 6.28	70.72 ± 3.73*
$-C\underline{H}_2CH=CH-$ †	112.00 ± 11.60	115.65 ± 16.86
$-CH=CHC\underline{H}_2C\underline{H}_2COO$ of DHA	7.57 ± 1.05	7.31 ± 0.60
$CH=CHC\underline{H}_2CH=CH-$ of LA	16.86 ± 2.95	18.15 ± 4.26
$-CH=CHCH_2C\underline{H}_2CH_2COO$ of AA	13.85 ± 2.25	12.15 ± 1.31*

* indicates a statistically significant difference

† this includes CH_2 in $-C\underline{H}_2CH=CHCH=CHC\underline{H}_2-$

Table 2: Fatty acid composition of kidney extracts from *Meriones unguiculatus* infected with *Echinococcus multilocularis*.

FA Component	Ratio (FA component : Total FA) Mean ± SD	
	control (n=17)	infected (n=17)
Saturated:		
$C\underline{H_2}$ in $-(CH_2)_n-$	7.56 ± 0.29	7.53 ± 0.19
$-C\underline{H_2}CH_2COO$	0.68 ± 0.03	0.69 ± 0.02
$-C\underline{H_2}COO$	0.65 ± 0.03	0.65 ± 0.02
Unsaturated (Degree of Unsaturation):		
$-C\underline{H}=C\underline{H}-$	1.22 ± 0.07	1.19 ± 0.05
Polyunsaturated:		
$C\underline{H_2}$ in $-CH=CH(CH_2CH=CH)_n-$	0.63 ± 0.06	0.58 ± 0.06*
$-C\underline{H_2}CH=CH-$[†]	0.91 ± 0.04	0.93 ± 0.03
$-CH=CHC\underline{H_2}C\underline{H_2}COO$ of DHA	0.06 ± 0.01	0.06 ± 0.01
$-CH=CHC\underline{H_2}CH=CH-$ of LA	0.14 ± 0.01	0.14 ± 0.02
$-CH=CHCH_2C\underline{H_2}CH_2COO$ of AA	0.11 ± 0.02	0.10 ± 0.01*
Average Fatty Acid Chain Length	15.36 ± 0.49	15.22 ± 0.35

* indicates a statistically significant difference

Figure 11

^{1}H NMR spectrum of a C:M extract of adrenal glands collected from an uninfected *M. unguiculatus*.

Peak assignments:

1. -C<u>H</u>=C<u>H</u>- of FA chains
2. C<u>H</u> of CTL C-3 in CTL esters
3. C<u>H</u> of C-1 and C-3 in glycerol of TAG
4. -C<u>H</u>$_2$OPO$_2$ in glycerol of GPL
5. C<u>H</u>OP in ring of PTI
6. (C<u>H</u>$_3$)$_3$N$^+$ of PTC
7. N$^+$H$_3$C<u>H</u>$_2$ of PTE
8. -HC=CH(C<u>H</u>$_2$CH=CH)$_n$- of FA chains
9. -HC=CHC<u>H</u>$_2$CH=CH- of LA
10. -HC=CHC<u>H</u>$_2$C<u>H</u>$_2$COO of DHA
11. -C<u>H</u>$_2$COO of FA chains
12. -C<u>H</u>$_2$CH=CH- of FA chains
13. -HC=CHCH$_2$C<u>H</u>$_2$CH$_2$COO of AA
14. -C<u>H</u>$_2$CH$_2$COO of FA chains
15. (-C<u>H</u>$_2$-)$_n$ of FA chains
16. -HC=CHCH$_2$C<u>H</u>$_3$ of ω-3 FA chains
17. ω-C<u>H</u>$_3$ of FA chains
18. C<u>H</u>$_3$ of C-18 of CTL

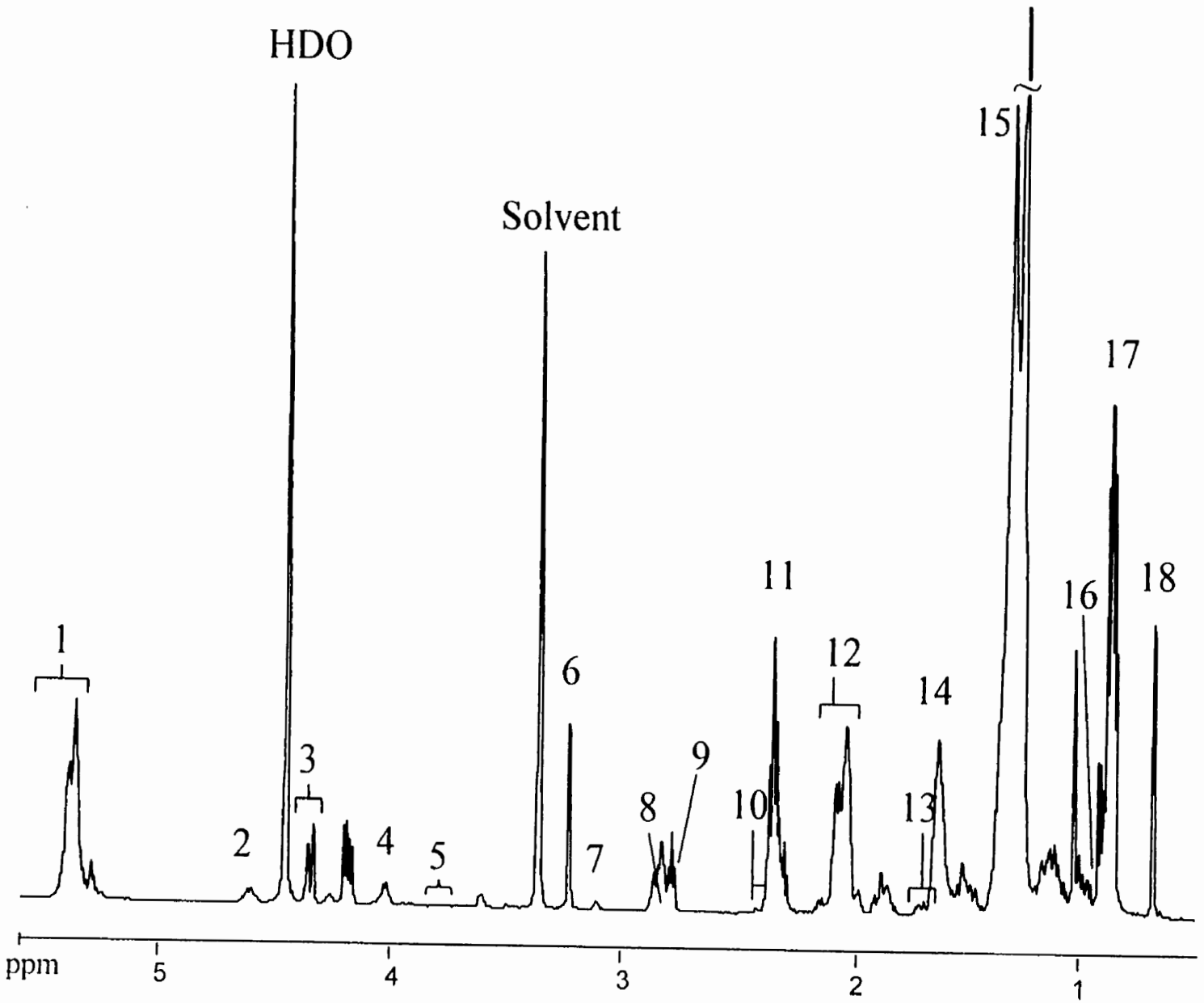
HDO
Solvent
1
2
3
4
5
6
7
8
9
10
11
12
13
14
15
16
17
18
ppm
5
4
3
2
1

Figure 12

^{1}H NMR spectrum of a C:M extract of adrenal glands collected from *M. unguiculatus* infected with *E. multilocularis*

Peak assignments:

1. -C<u>H</u>=C<u>H</u>- of FA chains
2. C<u>H</u> of CTL C-3 in CTL esters
3. C<u>H</u> of C-1 and C-3 in glycerol of TAG
4. -C<u>H_2</u>OPO_2 in glycerol of GPL
5. C<u>H</u>OP in ring of PTI
6. $(C\underline{H_3})_3N^+$ of PTC
7. $N^+H_3C\underline{H_2}$ of PTE
8. -HC=CH(C<u>H_2</u>CH=CH)$_n$- of FA chains
9. -HC=CHC<u>H_2</u>CH=CH- of LA
10. -HC=CHC<u>H_2</u>C<u>H_2</u>COO of DHA
11. -C<u>H_2</u>COO of FA chains
12. -C<u>H_2</u>CH=CH- of FA chains
13. -HC=CHCH$_2$C<u>H_2</u>CH$_2$COO of AA
14. -C<u>H_2</u>CH$_2$COO of FA chains
15. (-C<u>H_2</u>-)$_n$ of FA chains
16. -HC=CHCH$_2$C<u>H_3</u> of ω-3 FA chains
17. ω-C<u>H_3</u> of FA chains
18. C<u>H_3</u> of C-18 of CTL

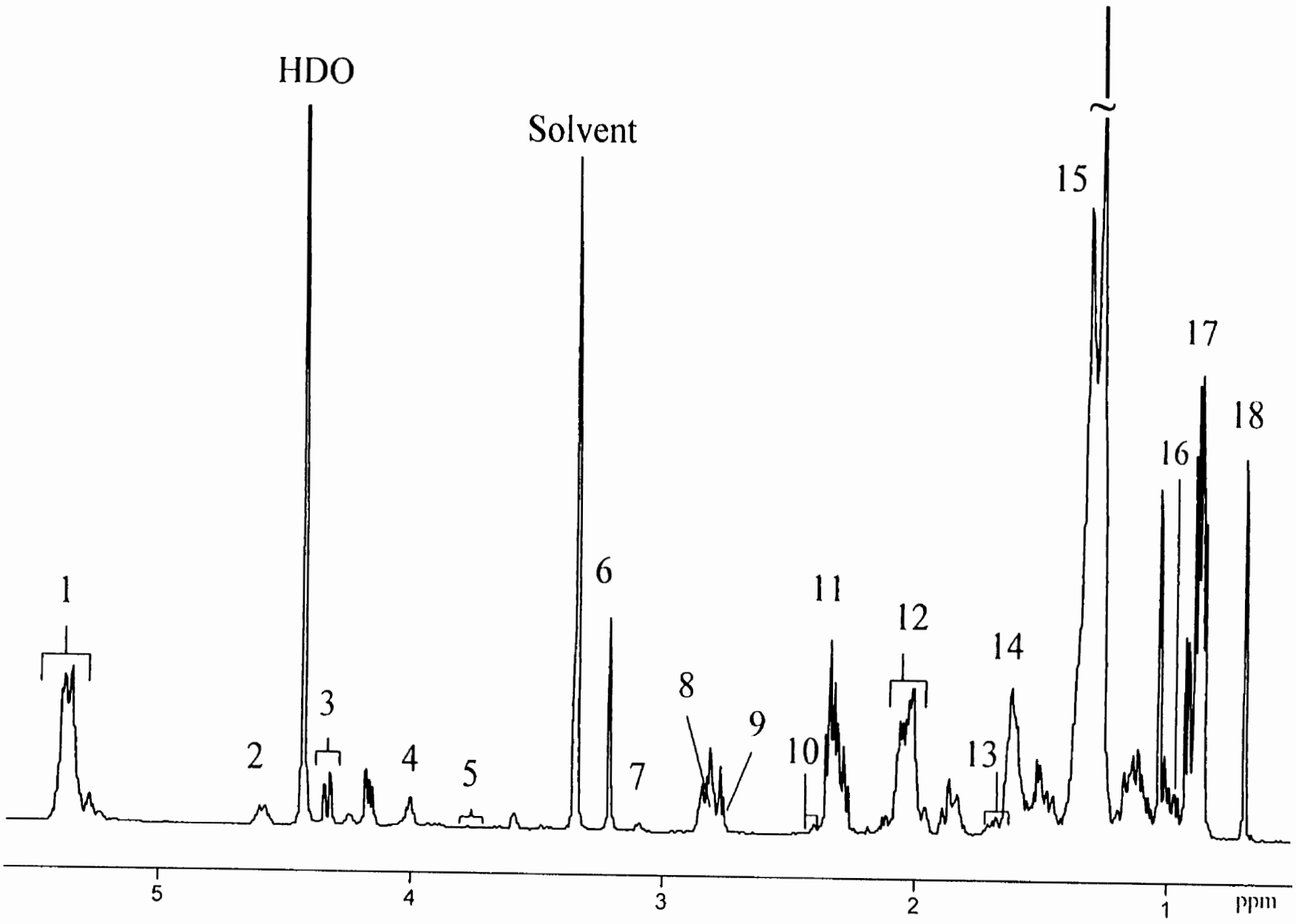
HDO
Solvent
1
2
3
4
5
6
7
8
9
10
11
12
13
14
15
16
17
18
5
4
3
2
1
ppm

The concentrations of all the lipid metabolites studied are presented in Table 3. The adrenals of infected animals had lower concentrations of CTL, PTE, total GPL, total TAG, total FA, the saturated FA moieties -($C\underline{H}_2$)$_n$-, -$C\underline{H}_2CH_2COO$ and -$C\underline{H}_2COO$, and the unsaturated FA moieties -$C\underline{H}$=$C\underline{H}$-, -CH=CH($C\underline{H}_2CH$=CH)$_n$-, -$C\underline{H}_2CH$=CHCH=CH$C\underline{H}_2$- and LA. There were no significant differences in the concentrations of CTL esters, PTC, PTI, DHA or AA between the two groups.

When the ratios of individual FA components to total FA were analyzed, many significant differences were observed (Table 4). Adrenal glands from infected animals had lower ratios of saturated FA moieties -($C\underline{H}_2$)$_n$-, -$C\underline{H}_2CH_2COO$ and -$C\underline{H}_2COO$, and the unsaturated moieties -$C\underline{H}$=$C\underline{H}$-, -$C\underline{H}_2CH$=CH- and -HC=CH$C\underline{H}_2CH$=CH- of LA than uninfected controls. However, the infected jirds had a higher ratio of -CH=CH$C\underline{H}_2C\underline{H}_2COO$ of DHA to total FA. The ratios of the polyunsaturated moiety -HC=CH($C\underline{H}_2CH$=CH)$_n$- and -CH=CH$CH_2C\underline{H}_2CH_2COO$ of AA to total FA were not significantly different between the two groups, but both the degree of unsaturation and the average FA chain length were lower in infected animals.

Table 3: Concentrations of lipid metabolites from adrenal glands of *Meriones unguiculatus* infected with *Echinococcus multilocularis*.

Lipid or Lipid Component	Concentration (μmol/g wwt.) Mean±SD	
	control (n=17)	infected (n=17)
Cholesterol	13.82 ± 4.77	10.15 ± 3.94*
Cholesterol esters	51.80 ± 15.73	49.20 ± 8.88
Phosphatidylethanolamine	5.97 ± 1.17	5.13 ± 0.81*
Phosphatidylcholine	11.83 ± 1.96	11.18 ± 1.52
Phosphatidylinositol	1.22 ± 0.24	1.07 ± 0.27
Total Glycerophospholipid	25.69 ± 3.66	23.33 ± 2.96*
Triacylglycerol	42.29 ± 15.20	26.03 ± 14.19*
Total Fatty Acid	408.21 ± 68.41	334.05 ± 69.56*
$C\underline{H}_2$ in $-(CH_2)_n-$	2329.84 ± 410.14	1775.83 ± 500.05*
$-C\underline{H}_2CH_2COO$	274.26 ± 8.60	214.55 ± 55.12*
$-C\underline{H}_2COO$	241.56 ± 42.56	183.13 ± 51.32*
$-C\underline{H}=C\underline{H}-$	338.57 ± 55.06	265.01 ± 63.55*
$C\underline{H}_2$ in $-CH=CH(CH_2CH=CH)_n-$	110.43 ± 21.34	95.07 ± 15.06*
$-C\underline{H}_2CH=CH-$	349.85 ± 60.95	269.05 ± 72.45*
$-CH=CHC\underline{H}_2C\underline{H}_2COO$ of DHA	2.52 ± 0.64	2.57 ± 0.49
$-CH=CHC\underline{H}_2CH=CH-$ of LA	48.06 ± 12.50	33.66 ± 13.73*
$-CH=CHCH_2C\underline{H}_2CH_2COO$ of AA	23.68 ± 6.15	21.18 ± 3.68

* indicates a statistically significant difference

Table 4: Fatty acid composition of adrenal gland extracts from *Meriones unguiculatus* infected with *Echinococcus multilocularis*.

FA Component	Ratio (FA component : Total FA) Mean ± SD	
	control (n=17)	infected (n=17)
Saturated:		
$C\underline{H}_2$ in $-(CH_2)_n-$	5.74 ± 0.65	5.25 ± 0.51*
$-C\underline{H}_2CH_2COO$	0.67 ± 0.05	0.64 ± 0.04*
$-C\underline{H}_2COO$	0.59 ± 0.07	0.54 ± 0.05*
Unsaturated (Degree of Unsaturation):		
$-C\underline{H}=C\underline{H}-$	0.83 ± 0.04	0.79 ± 0.04*
Polyunsaturated:		
$C\underline{H}_2$ in $-CH=CH(CH_2CH=CH)_n-$	0.27 ± 0.03	0.29 ± 0.03
$-C\underline{H}_2CH=CH-$	0.86 ± 0.08	0.80 ± 0.06*
$-CH=CHC\underline{H}_2C\underline{H}_2COO$ of DHA	0.006 ± 0.001	0.008 ± 0.001*
$-CH=CHC\underline{H}_2CH=CH-$ of LA	0.12 ± 0.03	0.10 ± 0.02*
$-CH=CHCH_2C\underline{H}_2CH_2COO$ of AA	0.06 ± 0.01	0.06 ± 0.01
Average Fatty Acid Chain Length	12.04 ± 0.90	11.40 ± 0.01*

* indicates a statistically significant difference

II. Carbohydrate Metabolism

Uninfected control animals had an average body mass of 72.4 ± 6.5 g, which was significantly different ($\alpha \leq 0.05$) from the average infected jird body mass of 65.6 ± 6.3 g. The body weight of infected animals was determined by subtracting the cyst weight from the total jird weight. The average weight of cyst in infected animals was 8.76 ± 2.52 g. The average mass of the control livers was 3.27 ± 0.46 g, while those from infected animals had an average mass of 2.99 ± 0.33 g. These two means were significantly different. Details of a representative proton-decoupled ^{13}C NMR spectrum of a PCA liver extract (three livers per sample) from uninfected *M. unguiculatus* are shown in Figures 13-15. Figure 13 shows the region between 36.8 ppm and 29.4 ppm, which incorporates the resonances of Glu carbons 3 (C3) and 4 (C4), as well as resonances from glutamine and succinate. Figure 14 is an expanded view of the Glu C4 resonance area at 36.3 ppm, and Figure 15 shows the Glu C3 multiplet at 29.8 ppm. The corresponding regions of a representative spectrum from a liver sample from *E. multilcularis*-infected jirds are shown in Figures 16-18.

Results from the Glu isotopomer analysis of spectra of PCA extracts of livers from uninfected and infected animals are presented in Table 5. The fraction of acetyl-CoA derived from endogenous, unlabeled sources (F_U) was higher in uninfected controls than in infected animals, but the livers of infected animals contained larger fractions of acetyl-CoA derived from both [3-^{13}C]lactate (F_{LL}) and [1,2-$^{13}C_2$]acetate (F_{LA}). The ratio of F_{LA} : F_{LL} was significantly lower in infected animals, but the percentage of Glu labeled with the ^{13}C isotope at carbon 3 was the same in both groups.

Figure 13

^{13}C NMR spectrum of a PCA extract of 3 livers from an uninfected *M. unguiculatus*

This figure shows the area of the spectrum between 29.4 ppm and 36.8 ppm containing the glutamate carbon-3 and carbon-4 resonances. Also shown is a glutamine resonance that was not used in this study

Key:

Glu: glutamate

C3: carbon 3

C4: carbon 4

Gln: glutamine

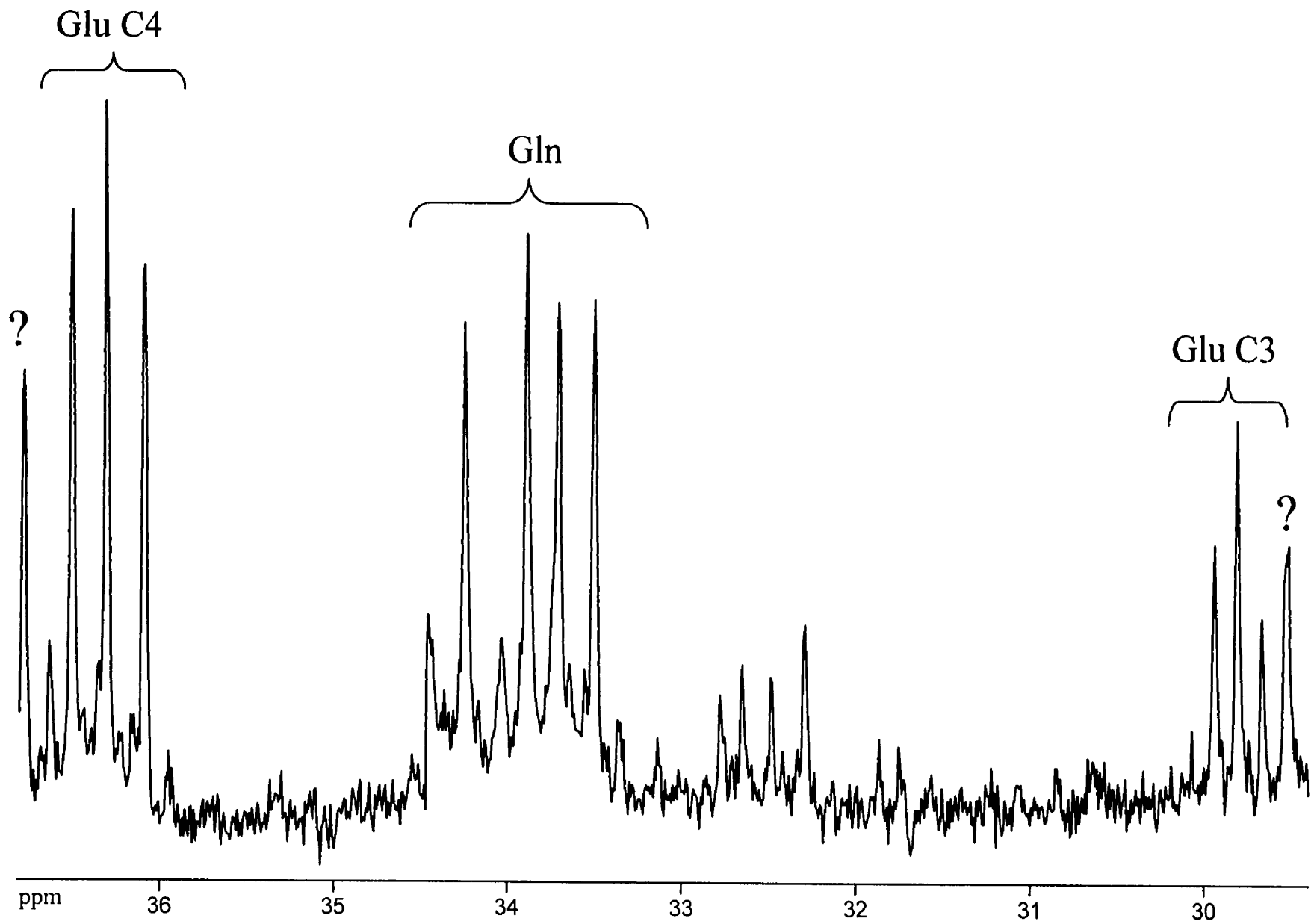
Glu C4
Gln
?
Glu C3
?
ppm
36
35
34
33
32
31
30

Figure 14

^{13}C NMR spectrum of a PCA extract of 3 livers from an uninfected *M. unguiculatus*.

This figure represents an expanded view of the glutamate carbon 4 resonance area.

Key:

C4Q: doublet of doublets due to $J_{C3, C4}$ and $J_{C4, C5}$

C4D45: doublet due to $J_{C4, C5}$

C4D34: doublet due to $J_{C3, C4}$

C4S: carbon 4 singlet

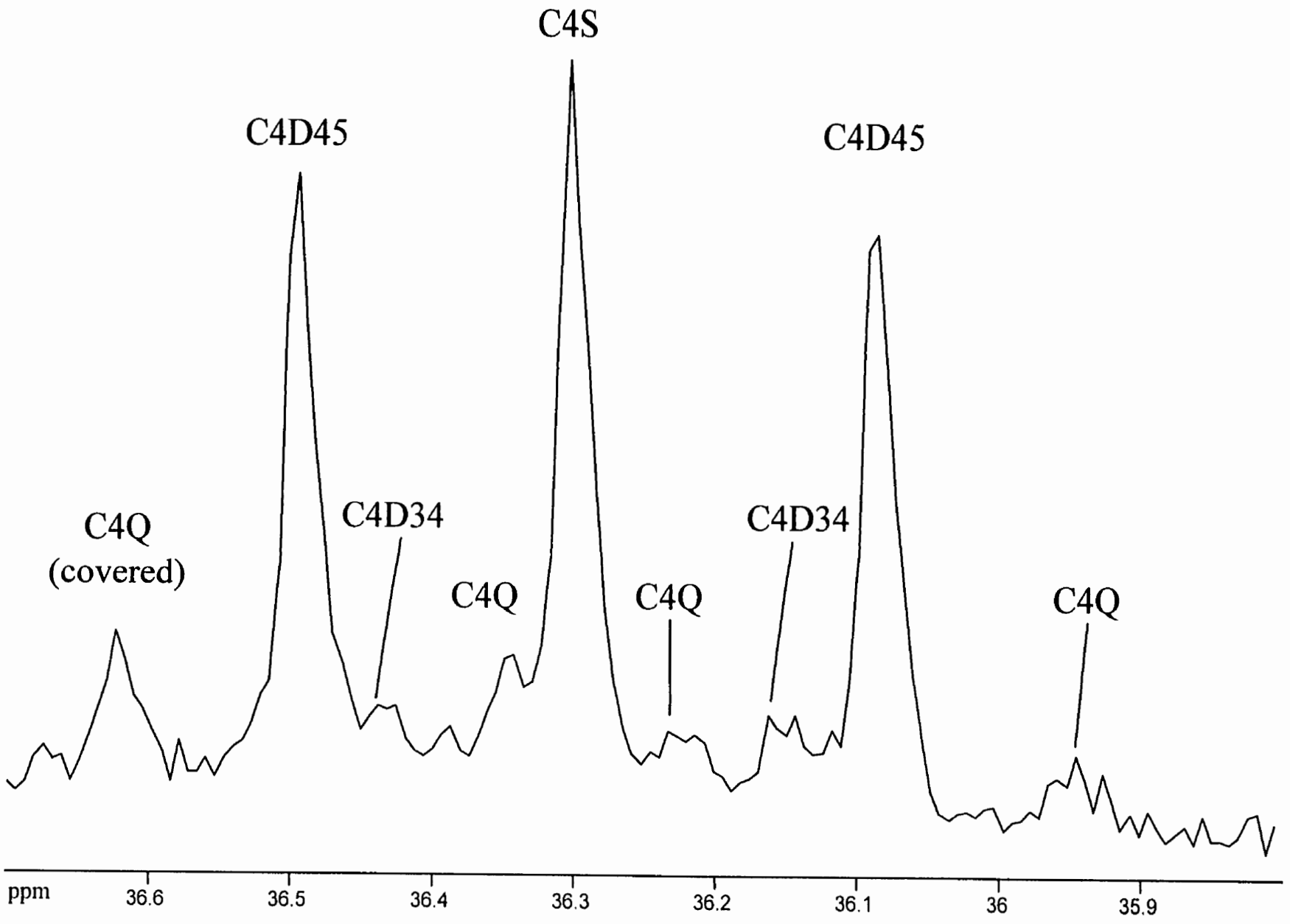
C4S
C4D45
C4D45
C4Q
(covered)
C4D34
C4Q
C4Q
C4D34
C4Q
ppm
36.6
36.5
36.4
36.3
36.2
36.1
36
35.9

Figure 15

^{13}C NMR spectrum of a PCA extract of 3 livers from an uninfected *M. unguiculatus*

This figure shows an expanded view of the glutamate carbon 3 resonance area. For the mode of analysis used in this experiment, the individual resonance components were not measured, just the total area of the carbon 3 resonance.

Key:

C3T: triplet due to $J_{C2, C3}$ and $J_{C3, C4}$

C3D23: doublet due to $J_{C2, C3}$

C3D34: doublet due to $J_{C3, C4}$

C3S: carbon 3 singlet

Note that $J_{C2, C3}$ and $J_{C3, C4}$ have the same value, therefore these two doublets overlap.

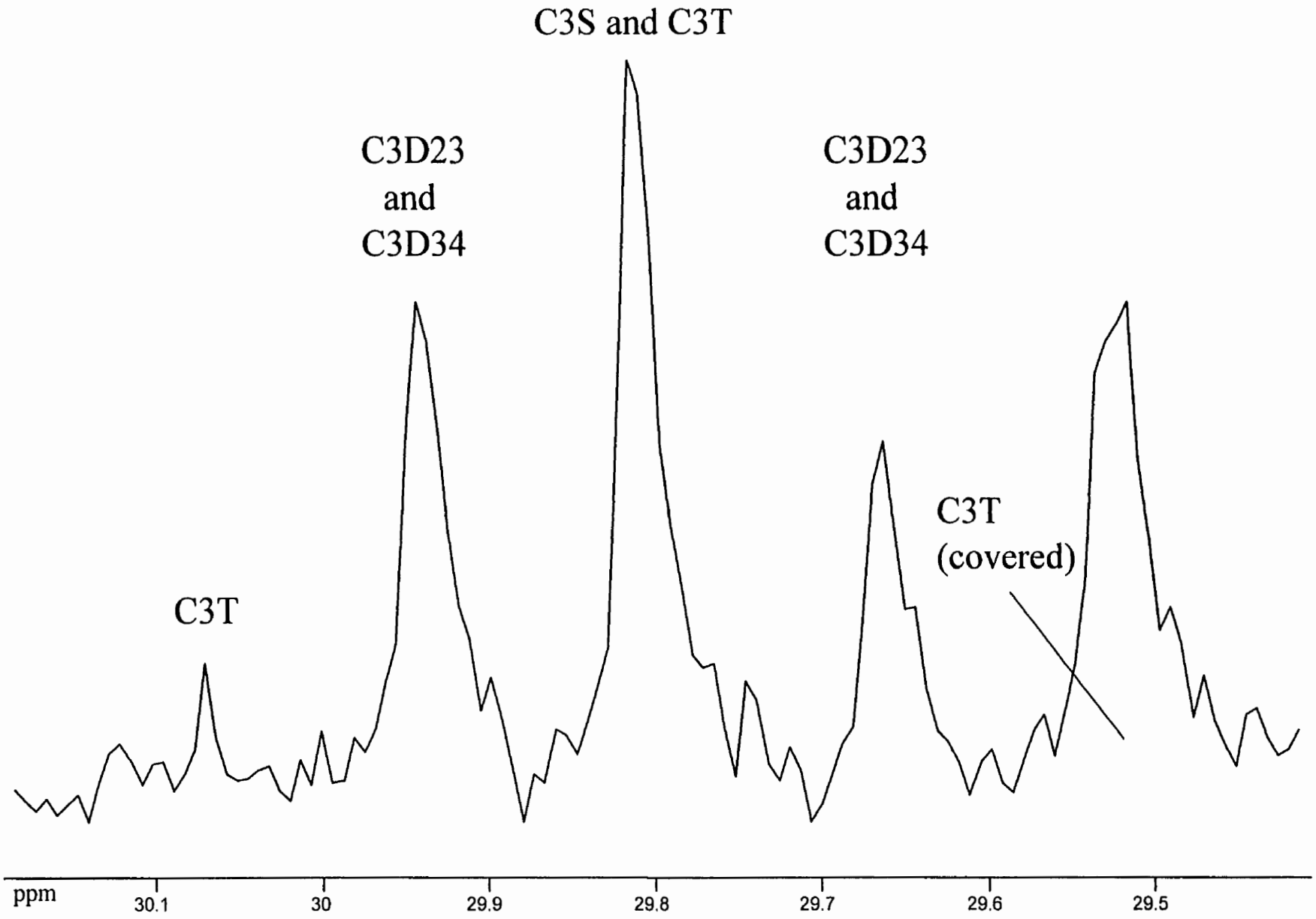
C3S and C3T
C3D23
and
C3D34
C3D23
and
C3D34
C3T
C3T
(covered)
ppm
30.1
30
29.9
29.8
29.7
29.6
29.5

Figure 16

^{13}C NMR spectrum of a PCA extract of 3 livers from *M. unguiculatus* infected with *E. multilocularis*

This figure shows the area of the spectrum between 29.4 ppm and 36.8 ppm containing the glutamate carbon-3 and carbon-4 resonances. Also shown is a glutamine resonance that was not used in this study

Key:

Glu: glutamate

C3: carbon 3

C4: carbon 4

Gln: glutamine

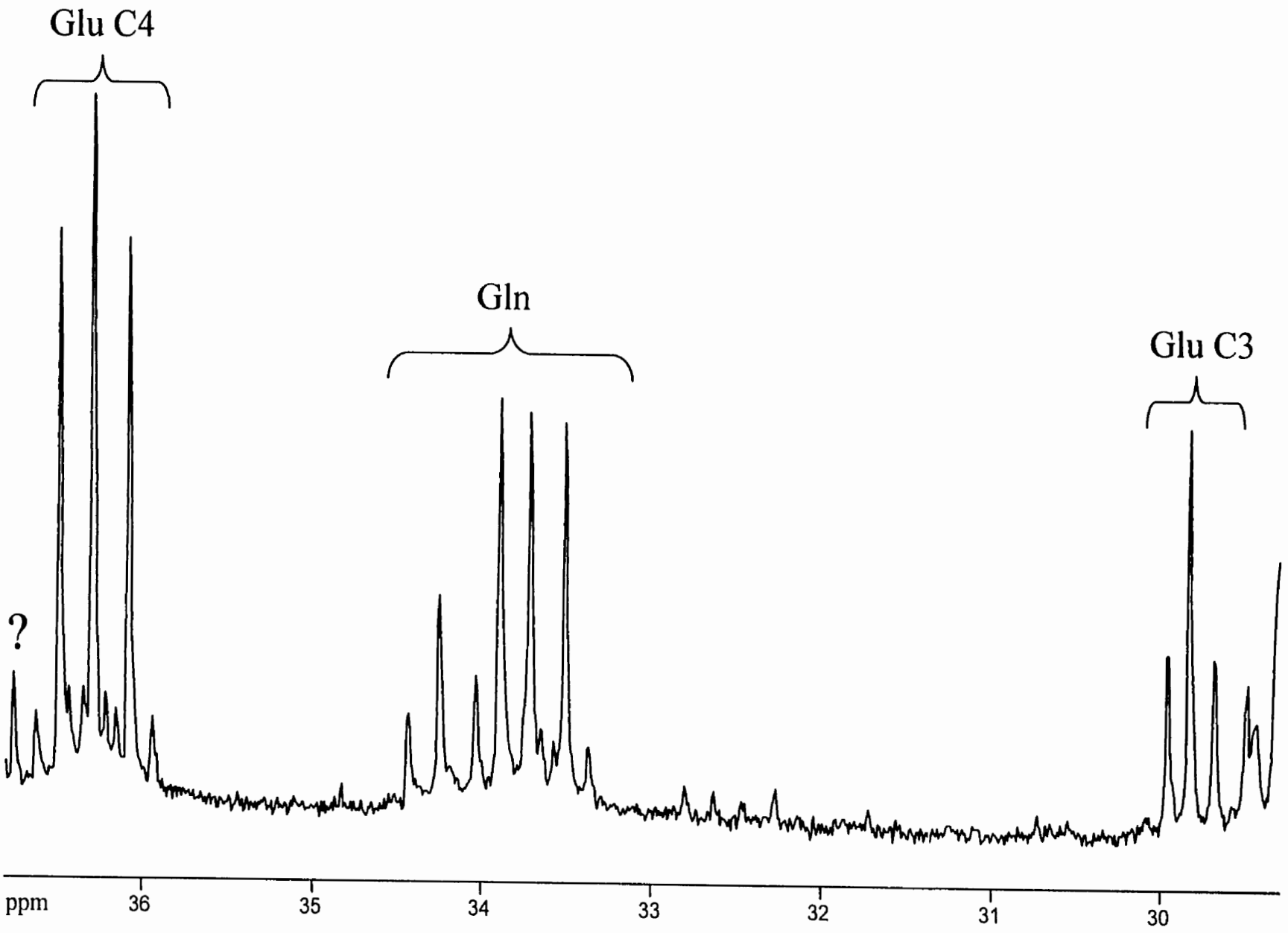
Glu C4
Gln
Glu C3
?
ppm
36
35
34
33
32
31
30

Figure 17

^{13}C NMR spectrum of a PCA extract of 3 livers from *M. unguiculatus* infected with *E. multilocularis*.

This figure represents an expanded view of the glutamate carbon 4 resonance area.

Key:

C4Q: doublet of doublets due to $J_{C3, C4}$ and $J_{C4, C5}$

C4D45: doublet due to $J_{C4, C5}$

C4D34: doublet due to $J_{C3, C4}$

C4S: carbon 4 singlet

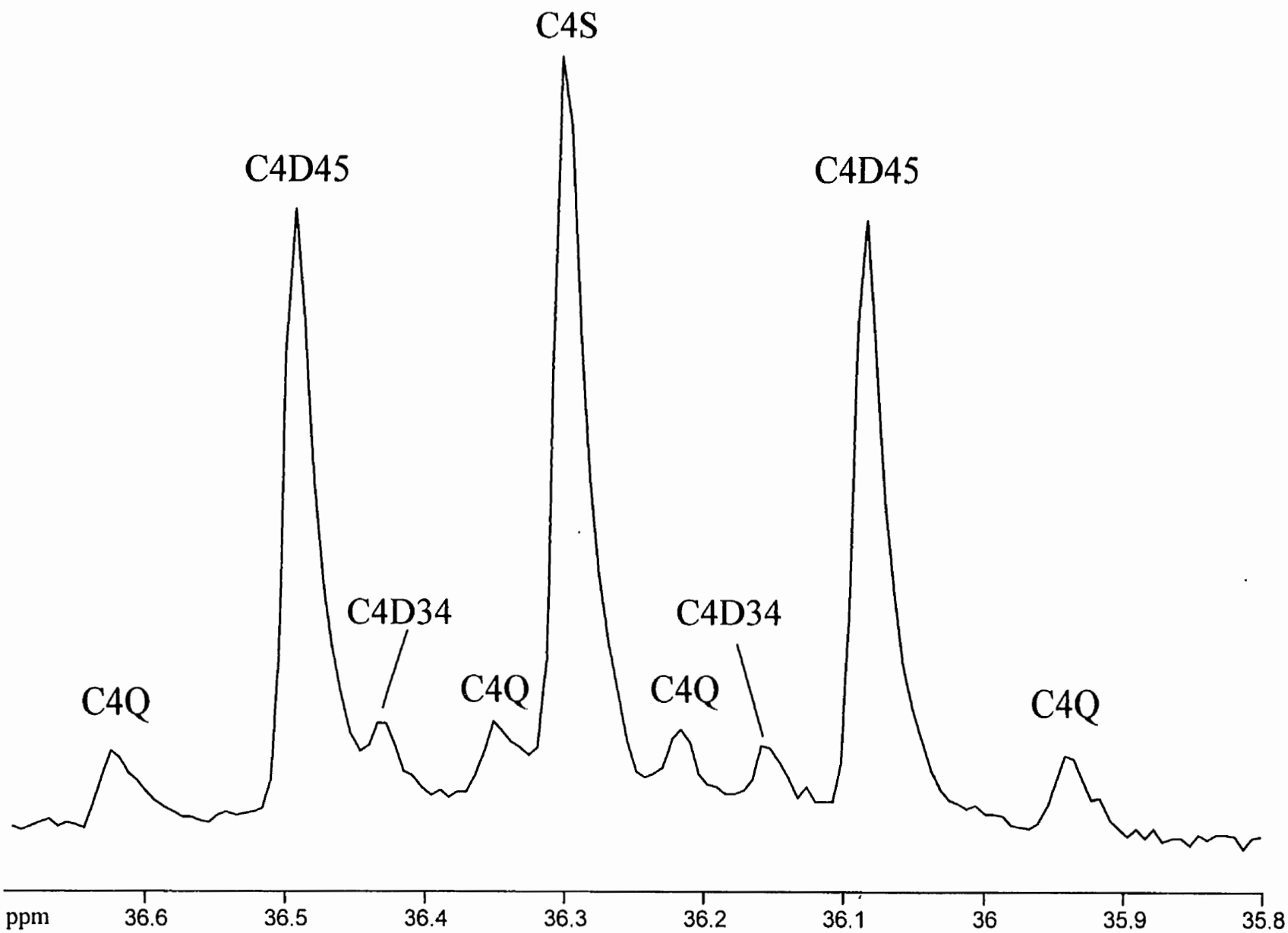
C4S
C4D45
C4D45
C4D34
C4D34
C4Q
C4Q
C4Q
C4Q
ppm
36.6
36.5
36.4
36.3
36.2
36.1
36
35.9
35.8

Figure 18

^{13}C NMR spectrum of a PCA extract of 3 livers from *M. unguiculatus* infected with *E. multilocularis*.

This figure shows an expanded view of the glutamate carbon 3 resonance area. For the mode of analysis used in this experiment, the individual resonance components were not measured, just the total area of the carbon 3 resonance.

Key:

C3T: triplet due to $J_{C2, C3}$ and $J_{C3, C4}$

C3D23: doublet due to $J_{C2, C3}$

C3D34: doublet due to $J_{C3, C4}$

C3S: carbon 3 singlet

Note that $J_{C2, C3}$ and $J_{C3, C4}$ have the same value, therefore these two doublets overlap.

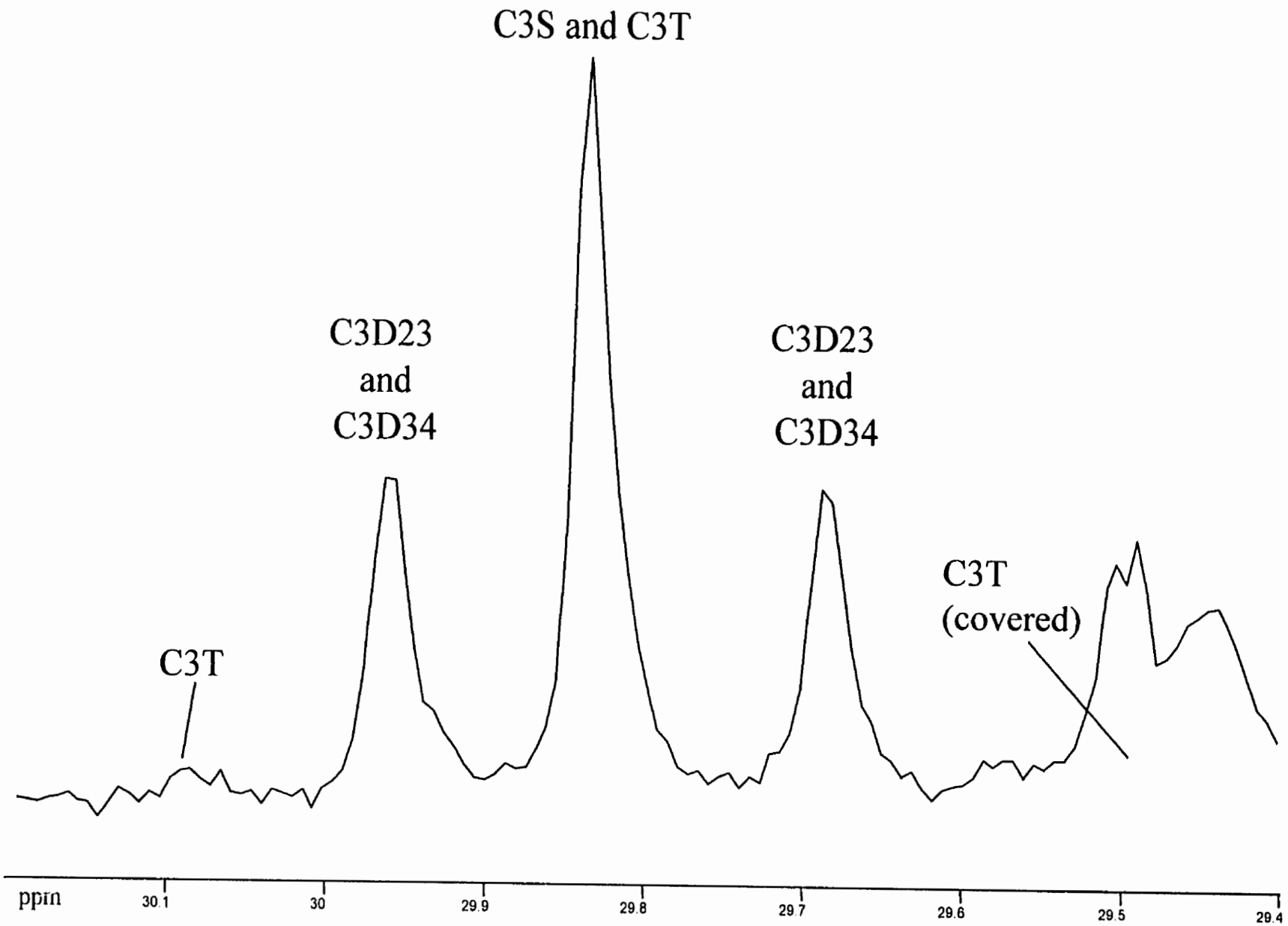
C3S and C3T
C3D23
and
C3D34
C3D23
and
C3D34
C3T
(covered)
C3T
ppm
30.1
30
29.9
29.8
29.7
29.6
29.5
29.4

Table 5: Glutamate isotopomer analysis of ^{13}C NMR spectra of PCA extracts of livers from *Meriones unguiculatus* infected with *Echinococcus multilocularis*.

Acetyl-CoA Isotopomer (and source)	Mole Fraction (Mean ± SD)	
	Control (n=7)	Infected (n=7)
F_U (unlabeled sources)	0.50 ± 0.10	0.34 ± 0.04*
F_{LL} ([3-^{13}C]lactate	0.18 ± 0.04	0.27 ± 0.04*
F_{LA} ([1,2-^{13}C]acetate	0.32 ± 0.07	0.38 ± 0.01*
Ratio F_{LA} : F_{LL}	1.74 ± 0.09	1.42 ± 0.18*
% Glu labeled with ^{13}C at carbon 3	21.53 ± 2.05	21.85 ± 1.46

* indicates a statistically significant difference

Discussion

I. Renal Lipid Metabolism

The results of the present experiment show that alveolar hydatidosis does have an effect on renal lipid metabolism. Significant alterations to the tissue concentrations of PTC, PTE, total GPL, AA and the unsaturated FA moiety -CH=CH(CH_2CH=CH)$_n$- were detected; levels of all of these lipid components decreased as a result of infection. A decrease in the concentration of total renal GPL in infected animals as compared to controls seems to be attributable to the observed depletion of renal PTC and PTE, and the most likely explanation for these changes involves the uptake of lipid precursors by the parasite. Cestodes are unable to synthesize FAs *de novo* and no evidence has yet been published to suggest that *E. multilocularis* metacestodes are able to absorb preformed GPLs from the host circulation. They are, however, able to absorb water-soluble precursors such as glycerol, choline, phosphocholine (PC), ethanolamine, phosphoethanolamine (PE) and inositol and incorporate them, along with host-derived FAs, into complex lipids (Barrett, 1983; Smyth and McManus, 1989; McManus and Bryant, 1995). Detection of resonances due to PTC and PTE in ^{1}H NMR spectra of *E. multilocularis* cysts by Schoen (1997) demonstrates that the parasite removes GPL precursors from the host to synthesize these compounds. The rapid rate of metacestode cellular growth and proliferation creates an enormous demand for membrane biosynthetic substrates, for as is true of most animals (Lehninger *et al.*, 1993), GPLs in cestodes function primarily as structural components of both plasma and organelle membranes

(Barrett, 1983).

Together, PTC and PTE make up over 50% of total phospholipids in all mammalian tissues studied, including the kidney (Ansell and Spanner, 1982). These two compounds are also the dominant phospholipids in metacestodes of *E. multilocularis* (McManus and Bryant, 1995), and indeed, were the only phospholipids detected in cyst tissue by ^{1}H NMR spectroscopy (Schoen, 1997). Corbin (1997) found that the livers of mice infected with *T. crassiceps* cysticerci had a lower concentration of PTC than those from control animals, and a similar observation was reported by Schoen (1997) for livers of *E. multilocularis*-infected jirds. Kidney cells are capable of the *de novo* synthesis of PTC (Longmuir, 1987), and therefore may be affected by a parasite-induced depletion of precursor molecules in the same way as hepatocytes seem to be (Corbin, 1997; Schoen, 1997). It is known that renal cells have the transport mechanisms necessary for the uptake of lipid precursors such as glycerol, FAs, acetate, choline, ethanolamine, methionine and inositol (Bjørnstad and Bremer, 1966; Wirthensohn and Guder, 1983; Wirthensohn *et al.*, 1984; Toback, 1984; Gullans and Hebert, 1996) and that the uptake and metabolism of all substrates by the kidney are dependent on their relative abundance in plasma (Gullans and Hebert, 1996). Therefore when *E. multilocularis* metacestodes remove water-soluble metabolites such as choline from the host, fewer GPL precursors will be delivered to the kidney of the host, and renal PTC synthesis should decrease. In addition to *in situ* formation, renal GPLs may also be supplied by hepatocytes. The liver plays a major role in the processing of dietary lipids, and can synthesize TAGs and GPLs that are then carried to peripheral tissues in the form of lipoproteins such as LDL (Hunt

and Groff, 1990; Desmet, 1994). Certain types of renal cells are known to obtain lipids through the endocytosis of LDL (Ardaillou *et al.*, 1996), so the decrease in the hepatic levels of PTC observed by Schoen (1997) as a result of *E. multilocularis* infection would also have the consequence of less of this lipid being delivered to the kidney.

While substrate supply is a very important parameter in determining the rate of synthesis of PTC, another such factor is pH. It has been hypothesized (Kuesel *et al.*, 1990) that a drop in intracellular pH would alter the activities of several enzymes involved in PTC synthesis and lead to a decrease in the rate of formation of this lipid. Kuesel *et al.* (1990) reported increases in concentrations of glycerophosphocholine (GPC), a product of the breakdown of PTC, and CDPcholine in cultured human tumor cells when the pH of the culture medium was acidified from 7.2 to 5.8. They also observed a decrease in the cellular concentration of PC that correlated with the drop in pH. The drop in PC levels were attributed to a decrease in the activity of choline kinase (Figure 19, [1]), an enzyme that shows maximal activity at pH 8-9 (Pelech and Vance, 1984). The observed change in GPC levels was thought to be a result of stimulation of the lipase enzymes that catabolize PTC to form lysophosphatidylcholine and GPC (Fig. 19, [7 and 8]), as well as an inhibition of the diesterase enzymes that breakdown GPC to form choline and glycerol (Fig. 19, [9 and 10]). The lipase enzymes have acidic pH optima that lie below 7 (Waite, 1991) while the GPC diesterases have alkaline pH optima of 9 or higher (Baldwin and Cornatzer, 1968; Abra and Quinn, 1976). Therefore a decrease in cellular pH would be expected to cause decreases in levels of PTC and choline along with an accumulation of GPC. CDPcholine accumulation at acidic pH was

Figure 19

Metabolism of phosphatidylcholine and phosphatidylethanolamine.

This figure shows the cytidine pathways for the *de novo* synthesis of PTC and PTE, and the PEMT pathway leading to the formation of PTC by the methylation of PTE. Also shown is one pathway leading to the breakdown of PTC.

The following enzymes are involved:

1. Choline kinase (also known as ethanolamine kinase)
2. CTP : phosphoethanolamine cytidyltransferase
3. CDPethanolamine : 1,2 DAG ethanolamine phosphotransferase
4. CTP : phosphocholine cytidyltransferase
5. CDPcholine : 1,2 DAG choline phosphotransferase
6. Phosphatidylethanolamine-N-methyltransferase (PEMT)
7. Phosphatidylcholine 1-acylhydrolase or 2-acylhydrolase
8. Lysophosphatidylcholine acylhydrolase (a lipase)
9. *sn*-glycero-3-phosphocholine glycerophosphohydrolase (a diesterase)
10. *sn*-glycero-3-phosphocholine cholinephosphohydrolase (a diesterase)
11. Acyltransferase
12. Acyl-CoA : 1-acyl-*sn*-glycero-3-phosphocholine-*O*-acyltransferase or
    Acyl-CoA : 2-acyl-*sn*-glycero-3-phosphocholine-*O*-acyltransferase

Abbreviations:

AdoMet: S-adenosylmethionine AdoHcy: S-adenosylhomocysteine

All other abbreviations are explained in the text.

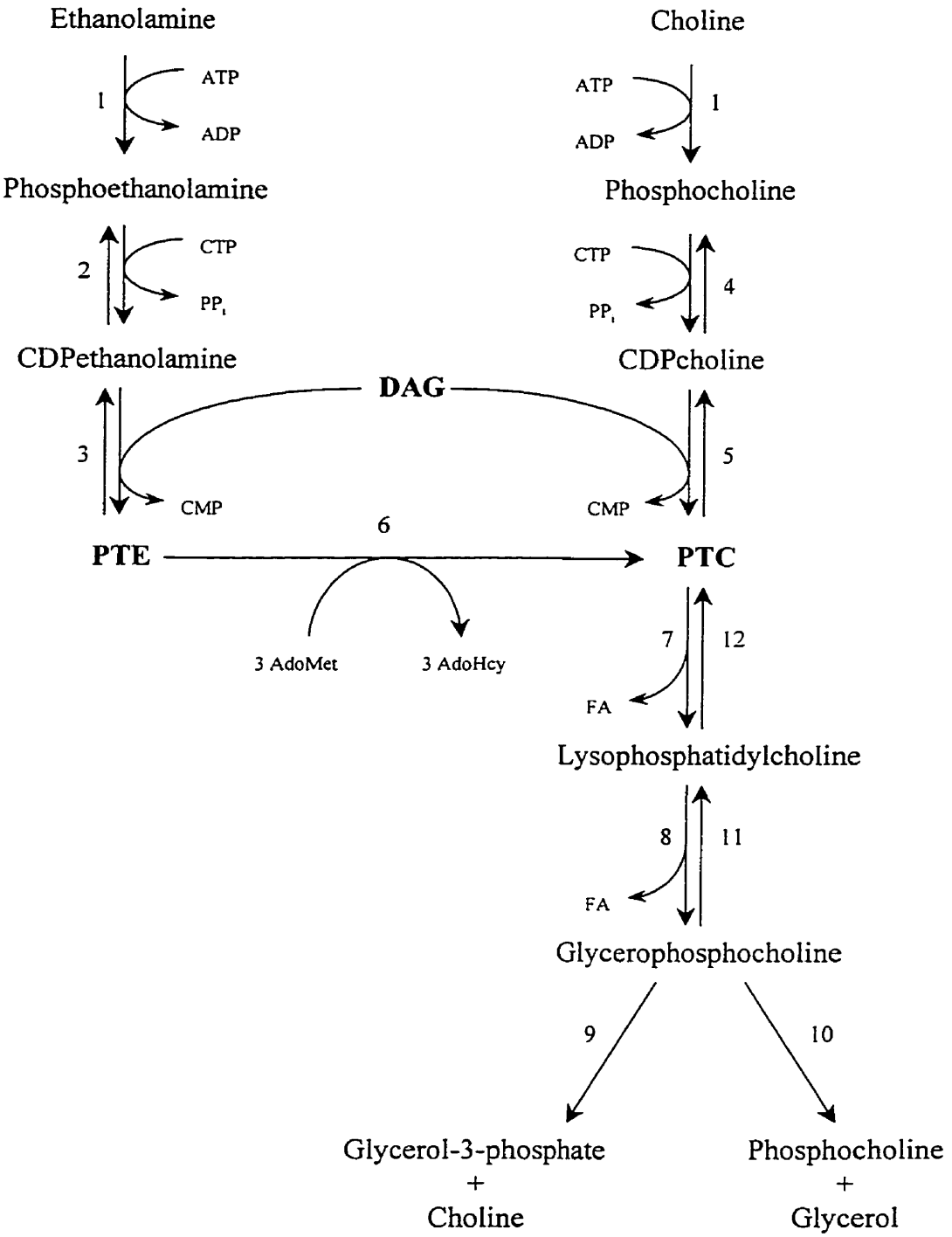
Ethanolamine
Choline
ATP
ADP
1
ATP
ADP
1
Phosphoethanolamine
Phosphocholine
CTP
PPi
2
CTP
PPi
4
CDPethanolamine
CDPcholine
DAG
3
5
CMP
CMP
6
PTE
PTC
3 AdoMet
3 AdoHcy
7
12
FA
Lysophosphatidylcholine
8
11
FA
Glycerophosphocholine
9
10
Glycerol-3-phosphate
+
Choline
Phosphocholine
+
Glycerol

attributed, in part, to the inhibition of CDPcholine:1,2 DAG choline phosphotransferase (Fig. 19, [5]), an enzyme with a pH optimum of 8.0-8.5 (Pelech and Vance, 1984).

Another pathway by which PTC can be synthesized is the PTE methyltransferase pathway (Vance and Ridgeway, 1988; Vance, 1991). In this series of steps, catalyzed by PTE methyltransferase (PEMT) (Fig. 19, [6]), three methyl groups are added to PTE by sequential methylation reactions (Vance, 1991). The optimum pH for PEMT activity is 10.2 (Vance, 1991), and *in vitro* experiments with rat liver microsomes showed nearly a 15-fold increase in PEMT specific activity when the pH is raised from 8.0 to 9.2 (Vance and Ridgeway, 1988). Therefore, if the intracellular environment in *E. multilocularis*-infected animals is more acidic than its normal physiological pH of 7.2-7.4 (Lee *et al.*, 1988; Durand *et al.*, 1993), the possibility exists that the activities of several enzymes will be drastically altered, and the production of PTC via the cytidine pathway, as well as from methylation of PTE, will decrease.

A decrease in the hepatic pH of mice as a consequence of infection with the cestode *Hymenolepis microstoma* was found by Blackburn *et al.* (1993). The effect was attributed to the acidosis caused by excretion of organic acid waste products by the parasite into host tissues. Similarily, Schoen (1997) linked the parasite-induced acidosis to the decrease in hepatic PTC in *E. multilocularis*-infected jirds. Thus the pH effect also cannot be disregarded with respect to renal cells.

The enzymes of the cytidine pathway are present in kidney cells (Longmuir, 1987), and it seems likely that if extracellular acidosis can affect the reactions in the liver, kidney metabolism might be altered as well. Novak *et al.* (1993) detected increased levels of

succinate, acetate and lactate in kidneys of *E. multilocularis*-infected jirds, and it was speculated that this may have been due to absorption of parasite waste products by the host tissue. Sodium (Na^+)-dependent transport mechanisms for mono-, di- and tricarboxylic acids have been characterized in the plasma membranes of renal proximal tubule cells, and both lactate and acetate are readily metabolized in all types of kidney cells (Gullans and Hebert, 1996). Therefore, excretion of acidic waste products by metacestodes may very well cause a decrease in the intracellular pH of renal cells and a concomitant decrease in the rate of synthesis of PTC via the cytidine pathway. Synthesis of PTC via methylation of PTE is said to occur in all eukaryotic cells (Dowhan, 1997) and PEMT activity has been detected in the rat kidney (Bjønstad and Bremer, 1966). Therefore, it seems reasonable to assume the kidney enzyme would be susceptible to the same pH effect as hepatic PEMT. However, the level of its activity in non-liver tissue is extremely low ($\leq 1\%$) meaning that a decrease in renal PEMT activity due to acidosis would represent a negligible contribution to the changes in PTC concentration observed in the present experiment.

Results also showed a decrease in renal PTE levels in infected jirds which could again be readily explained by the parasite-induced depletion of precursors such as ethanolamine. Similarily, Corbin (1997) reported a decrease in hepatic PTE levels in *T. crassiceps*-infected mice which was thought to be a result of GPL precursor uptake by the cysticerci. On the other hand, Schoen (1997) observed an increase in hepatic PTE levels in jirds infected with *E. multilocularis* which she attributed in part to the inhibition of PEMT activity due to acidosis. Other experiments have shown that a reciprocal

mechanism of regulation exists between the two cytidine pathways leading to PTC and PTE biosynthesis, and that when pH is lowered, PTE formation increases at the expense of PTC (Kuesel *et al.*, 1990). Therefore, an increase in tissue PTE levels is expected under conditions of intracellular acidosis. However, increased acidity within host tissues might not be the sole physiological alteration. In the present experiment the mean weight of *Echinococcus* cysts was 17.76 ± 3.05g, whereas that measured by Schoen (1997) was only 10.64 ● 5.00g. All experimental parameters being the same in both studies, including age and gender of host and the duration of infection, it seems that the larger parasite biomass in the present experiment may account for this discrepancy. While the uptake of PTE precursors by the parasite may not have been severe enough to obscure the intracellular accumulation of PTE due to enzyme modification in Schoen's experiment, this may very well have been the case in the present study, especially when it is considered that renal levels of PEMT are relatively insignificant compared to those seen in hepatocytes, and account for less than 1% of the PTC synthesis within the kidney (Vance and Ridgeway, 1988).

For an additional possible explanation for the depletion of PTE (and indeed, other GPLs), it is necessary to examine other metabolic pathways in the kidney. Crane and Masters (1981) showed that alterations in organ lipid profiles as a result of starvation differ between liver and kidney. In mice starved for four days, renal lipid synthesis decreased and phospholipids, including PTC and PTE, were utilized for the generation of energy - a response not observed in hepatocytes. As a decrease in renal function can be fatal, it was speculated that GPL catabolism in the kidney occurred as a means of

preserving the total protein content in order to conserve all renal physiological functions during starvation (Crane and Masters, 1981). Evidence that the *E. multilocularis*-infected jirds in the present experiment were, in fact, suffering from starvation is apparent when body mass is compared between the infected and uninfected groups. The infected animals lost an average of 6.8% of their body weight, and this result was statistically significant. Thus, the starvation condition of the infected jirds could contribute to the observed decrease in levels of both PTC and PTE in the kidney. The fact that hepatic GPLs are not preferentially utilized for energy generation (Crane and Masters, 1981), coupled with the lesser degree of starvation observed by Schoen (1997) may explain why the concentration of PTE decreased in kidneys of infected animals, but not in the liver.

As a final discussion of renal GPL levels, it is important to mention the role of gluconeogenesis. Not only is the kidney cortex the only non-hepatic tissue capable of the *de novo* synthesis of Glc (Seifter and Englard, 1994), the proximal tubule portion of the nephron actually exhibits a higher rate of gluconeogenesis per gram of tissue than hepatocytes (Gullans and Hebert, 1996). Only a very small fraction of renal Glc is exported under normal physiological conditions, however, as it is the distal tubule portion of the nephron that is the most active consumer of endogenous Glc. Renal cells do not store glycogen (Cahill, 1986), but during prolonged starvation renal gluconeogenesis can supply up to 50% of the body's Glc needs (Kida *et al.*, 1978; Gullans and Hebert, 1996). As in hepatocytes, renal Glc synthesis is increased as a result of starvation, but unlike hepatic gluconeogenesis, the pathway in renal cortical cells is also stimulated by a decrease in cellular pH (Gullans and Hebert, 1996). Glycerol is a preferred substrate for

Glc synthesis in the kidney, so the parasite-induced acidosis discussed above would result in an increase in the uptake of this compound by renal cortical cells and its incorporation into Glc. This means less precursor would be available for GPL synthesis and increased renal gluconeogenesis becomes another possible explanation for the observed decrease in PTC and PTE. But, in order for this reasoning to be acceptable, it is necessary to account for the fact that the levels of TAG did not differ between the control and infected groups. If glycerol is being incorporated into gluconeogenesis instead of lipogenesis, we expect to see a drop in TAG levels as well. The reason there was no difference may have to do with the presence of the perirenal fat pad, an accumulation of adipose tissue containing predominantly TAGs (Ross *et al.*, 1995). Normally, adipocyte TAGs are depleted during starvation when FAs become an important source of energy, but the perirenal fat tends to be conserved at the expense of adipose tissue in other locations in the body (Mayo-Smith *et al.*, 1989; Orphanidou *et al.*, 1997). Although Hegarty and Kim (1981) observed a total depletion of the perirenal fat pad in rodents subjected to a prolonged and complete starvation, the infected animals in the present experiment did have, at the time of dissection, a significant amount of fat around their kidneys that did not differ in appearance from that in control animals. If TAGs in subcutaneous adipose tissue are mobilized before those within the intraperitoneal fat stores, as has been suggested (Mayo-Smith *et al.*, 1989; Orphanidou *et al.*, 1997), then TAG and FA levels in both kidney (present study) and liver (Schoen, 1997) could remain unchanged. Indeed, this is what was observed. Furthermore, the decrease in body weight of infected animals in the present study was likely a result of a depletion in subcutaneous fat only, for there was no

decrease in the mean weight of either of the two organs studied, kidneys or adrenal glands.

An additional change seen in the renal lipid profile of *E. multilocularis*-infected jirds was a decrease in the concentration of AA as compared to controls, along with a decrease in the ratio of this FA relative to total renal FAs. In order to explain why AA levels dropped in infected animals while concentrations of all other FA moieties remained unchanged, it is necessary to consider the special metabolic role played by AA in the mammalian kidney.

As stated above, AA is the sole precursor for the eicosanoids, a large group of biologically active molecules (Figure 20). AA itself is formed within the ER of hepatocytes by the elongation and desaturation of the essential FA linoleic acid. Once synthesized, AA may be incorporated into GPLs and transported out of the liver to other tissues in plasma lipoproteins such as LDL. When delivered to renal cells, the AA-containing GPLs are incorporated into cellular membranes or else stored within the lipid droplets of interstitial cells (Ardaillou *et al.*, 1996; Breyer and Badr, 1996). The synthesis of eicosanoids begins with the liberation of AA from GPLs through the activity of phospholipase enzymes. Phospholipase A_2 (PLA_2) liberates the FA from PTC and PTE while phospholipase C (PLC) in conjunction with DAG lipase cleaves AA from PTI and its derivatives (Belley and Chadee, 1995; Breyer and Badr, 1996). The stimuli for AA release are varied, and include the activity of peptides such as angiotensin II and bradykinin, some of the adrenocortical hormones and less specific effects like mechanical trauma and immunologic responses (Belley and Chadee, 1995). Because eicosanoids play

Figure 20

Pathways of eicosanoid synthesis.

1. Cyclooxygenase pathway (COX): this is the major pathway for AA metabolism in the mammalian kidney. Produces prostaglandins and thromboxanes.

2. Lipoxygenase pathway: produces mono-, di- and trihydroxyeicosatetraenoic acids, leukotrienes and lipoxins.

3. Cytochrome P-450 (epoxygenase) pathway: pathway by which AA is oxidized to produce epoxyeicosatetraenoic acids

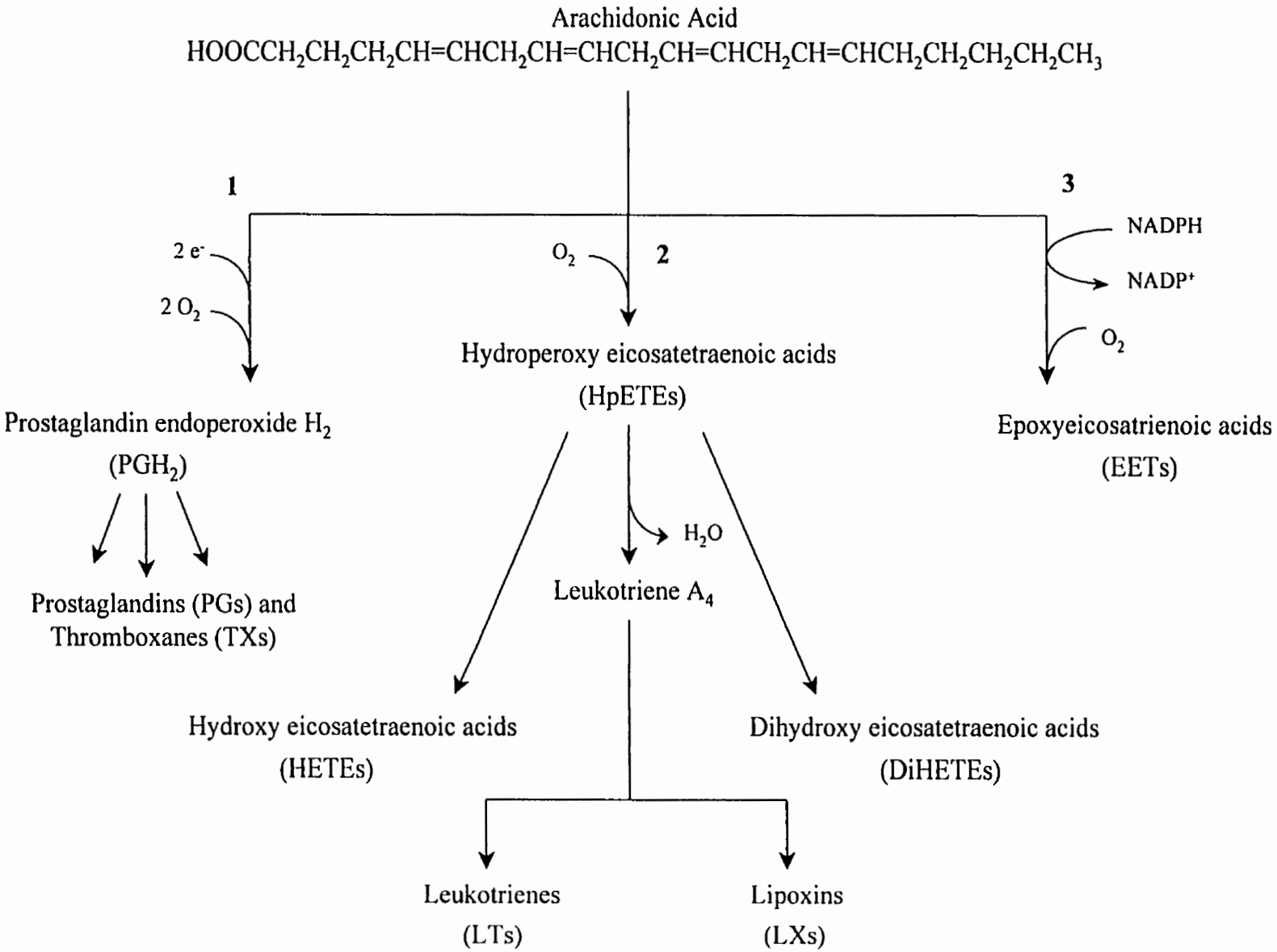
Arachidonic Acid
HOOCCH2CH2CH2CH=CHCH2CH=CHCH2CH=CHCH2CH=CHCH2CH2CH2CH2CH3
1
2
3
2 e-
2 O2
O2
NADPH
NADP+
O2
Prostaglandin endoperoxide H2
(PGH2)
Hydroperoxy eicosatetraenoic acids
(HpETEs)
Epoxyeicosatrienoic acids
(EETs)
H2O
Prostaglandins (PGs) and
Thromboxanes (TXs)
Leukotriene A4
Hydroxy eicosatetraenoic acids
(HETEs)
Dihydroxy eicosatetraenoic acids
(DiHETEs)
Leukotrienes
(LTs)
Lipoxins
(LXs)

a role in the mammalian immune response to disease, and because circulating levels of the aforementioned activators of phospholipase activity are increased in response to stress (Alberts *et al.*, 1994), it seems logical to assume that the release of AA within renal cells will be enhanced in animals infected with *E. multilocularis*. In addition, PLC isozymes isolated from mammalian liver, muscle, brain, platelets and seminal vesicles all exhibit a maximal activity at acidic-neutral pHs of 4.5-7.0 (Waite, 1991). It could be assumed that a renal isozyme of PLC (although not yet characterized) would also have a pH optimum of 7 or lower, and would therefore show increased activity in infected animals due to parasite-induced cellular acidosis.

All three pathways leading to the production of eicosanoids from AA (Figure 20) are present within the mammalian kidney (Morrison, 1986; Breyer and Badr, 1996). The COX pathway gives rise to PGs and TXs, the lipoxygenase pathway produces LTs, LXs and HETEs and the remaining eicosanoids are synthesized by the cytochrome P-450 (epoxygenase) pathway (Smith *et al.*, 1991; Breyer and Badr, 1996). It has been proposed that renal eicosanoids have one, all-encompassing function: cytoprotection (Schlondorff and Ardaillou, 1986). By constantly adjusting renal blood flow, interstitial ion concentration and pH, these compounds serve to protect renal cells from the drastic changes that can occur in their environments. COX products act as both vasodilators and vasoconstrictors, depending on the specific type and circumstance. They also stimulate the release of renin, an enzyme that in turn stimulates an increase in arterial blood pressure (Breyer and Badr, 1996; Guyton and Hall, 1996), and are thought to have a role in the control of urine concentration, sodium excretion and blood flow through the kidney

(Venuto and Ferris, 1982). All of these effects are achieved through the mediation or modulation of hormone action. LTs are potent vasoconstrictors and leukocyte activating agents, while LXs seem to act as vasodilators. HETEs are vasoactive as well, and seem to have an effect on sodium transport (Breyer and Badr, 1996).

It is known that PGs play a role in controlling renal hemodynamics and physiology in humans with advanced liver disease (Epstein, 1986), so it is logical to assume that they do so with any illness with systemic effects. In the immune response to injury or the presence of a pathogen, once an inflammatory response has been triggered, eicosanoid production in surrounding cells increases and they contribute to the defence by promoting tissue swelling, triggering pain impulses and attracting platelets and leukocytes (Alberts, *et al.*, 1994). Eicosanoids are extremely short-lived (Schlondorff and Ardaillou, 1986; Smith *et al.*, 1991). Once synthesized, they are released to act on the tissues in which they were produced before being broken down by oxidative pathways, and they are never stored within cells (Morrison, 1986; Smith *et al.*, 1991; Lehninger *et al.*, 1993). While eicosanoids possess methylene protons that will contribute to the AA resonance that was integrated in this study, the products of their oxidative breakdown will not (Smith *et al.*, 1991). Therefore, if eicosanoids are being produced within, and released from, renal cells faster than AA can be quantitatively replaced, infected animals will have a lower intrarenal concentration of AA than controls.

Interestingly, many species of obligate parasites are also able to synthesize eicosanoids (Belley and Chadee, 1995). Therefore, the possibility may exist that metacestodes of *E. multilocularis* are selectively absorbing AA from the host and

utilizing it for their own eicosanoid production. Two cestode species, *Taenia taeniaeformis* and *Spirometra erinacei*, will both metabolize exogenous AA and release PGs (Leid and McConnell, 1983; Belley and Chadee, 1995). It is thought that these compounds of parasite origin act to suppress the host immune response by inhibiting leukocyte function, and allow the parasites to persist within host tissues for prolonged periods. *E. multilocularis* metacestodes are able to overcome the immune response of their host and proliferate (Gottstein *et al.*, 1993), and it is possible that they are able to do so by the synthesis and release of eicosanoids. Schoen (1997) detected AA within metacestode tissue that must have been obtained from the host as cestodes are incapable of synthesizing polyunsaturated FAs *de novo* (Frayha and Smyth, 1983), and this AA may very well have been destined for eicosanoid production. The specific demand for AA by metacestodes could result in a systemic depletion of this FA in host tissues, and as the kidney has a rich store of AA-containing lipids (Tisher and Madsen, 1996), this depletion would be especially pronounced in renal cells. If *E. multilocularis* cysts are secreting eicosanoids into the host, it is unlikely that these compounds would contribute to the renal AA resonance in any significant way. Although both Schoen (1997) and Corbin (1997) reported increases in the ratios of AA to total FAs within the livers of cestode-infected rodents, the ratio in kidney tissue in the present experiment decreased. Eicosanoids released into the abdominal cavity by the parasite would be taken up into host tissues, but the bulk of the compounds would end up in cells of the liver and intestine, two organs that make a much greater contribution to the total weight of abdominal viscera than the kidneys (Altman and Ditmer, 1972). The host kidney would

lose a significant amount of AA to the parasite owing to its relatively large pool of stored AA, but not proportionately more than the liver. However, it would not absorb as much of the eicosanoids of parasite origin owing to its relatively small size and the greater absorptive potential of the liver.

In short, the observed decrease in renal AA concentration in infected animals can be attributed both to the uptake of AA by the parasite and to an increase in eicosanoid synthesis as the kidney launches a defense against the systemic metabolic changes induced by the parasite. Many components of the mammalian immune system can stimulate eicosanoid production, including IL-1 (a cytokine released by macrophages), bradykinin and certain complement proteins (Ardaillou *et al.*, 1996). Macrophages and other white blood cells proliferate in *E. multilocularis* infections in mice (Bresson-Hadni *et al.*, 1990) and humans (Vuitton *et al.*, 1989), and complement proteins have been detected on the surfaces of metacestodes in infected mice (Playford and Kamiya, 1992; Heath, 1995). Therefore, some of the appropriate stimuli were most likely present in this experiment. Acidosis may also affect certain lipase enzymes that release AA from membrane GPLs. Increased synthesis of PG, TX, LT and other eicosanoids (Figure 20) by both host and parasite, and their failure to contribute to the relevant resonances in the NMR spectra would account for the results observed in the present experiment.

The final results left to explain are the decreases observed in both the concentration of the CH_2 component of the FA moiety -CH=CH(CH_2CH=CH)$_n$-, and the ratio of this moiety to total FA in infected animals. These decreases are not surprising as -CH=CH(CH_2CH=CH)$_n$- is contained within the AA acyl chain with n=3 (see below).

AA

$HOOCCH_2CH_2CH_2\mathbf{CH{=}CHCH_2CH{=}CHCH_2CH{=}CHCH_2CH{=}CH}CH_2CH_2CH_2CH_2CH_3$

The unsaturated FA moiety is also a component of DHA where n=5 within the acyl chain, however no change was seen in DHA concentration between the two groups. Therefore, the decrease in $-CH{=}CH(CH_2CH{=}CH)_n-$ levels was likely due to the selective depletion of AA alone, which has already been discussed.

II. Adrenal Lipid Metabolism

Infection with *E. multilocularis* induced a great many more alterations to the lipid profile of the jird adrenal gland than was seen in the kidney. Adrenals from infected animals showed decreases in the concentrations of CTL, PTE, GPL, total FA, TAG and all individual FA moieties measured except AA and DHA. One possible explanation for the majorty of these changes (all except the decreases in PTE and GPL concentrations) involves the unique and vital role played by lipids in the adrenals: the production of the adrenocortical hormones.

The steroid hormones are all produced in the adrenal cortex from a common precursor: CTL (Figure 21). Experiments have shown that the synthesis of many of these hormones by *M. unguiculatus* is stimulated in response to various imposed stresses (Fenske, 1983; 1984; 1985), and it is known that the secretion of glucocorticoids such as cortisol is increased as a result of both infection and trauma (Munck and Náray-Fejes-Tóth, 1995; Guyton and Hall, 1996). Due to the prolonged parasitic infection endured by

Figure 21

Synthesis of the corticosteroids.

The following enzymes are involved:

1. CTL ester hydrolase
2. Cytochrome $P450_{SCC}$ (20-22 desmolase)
3. 3β-hydroxysteroid dehydrogenase
4. 21-hydroxylase
5. 11β-hydroxylase
6. 18-hydroxylase
7. 17α-hydroxylase

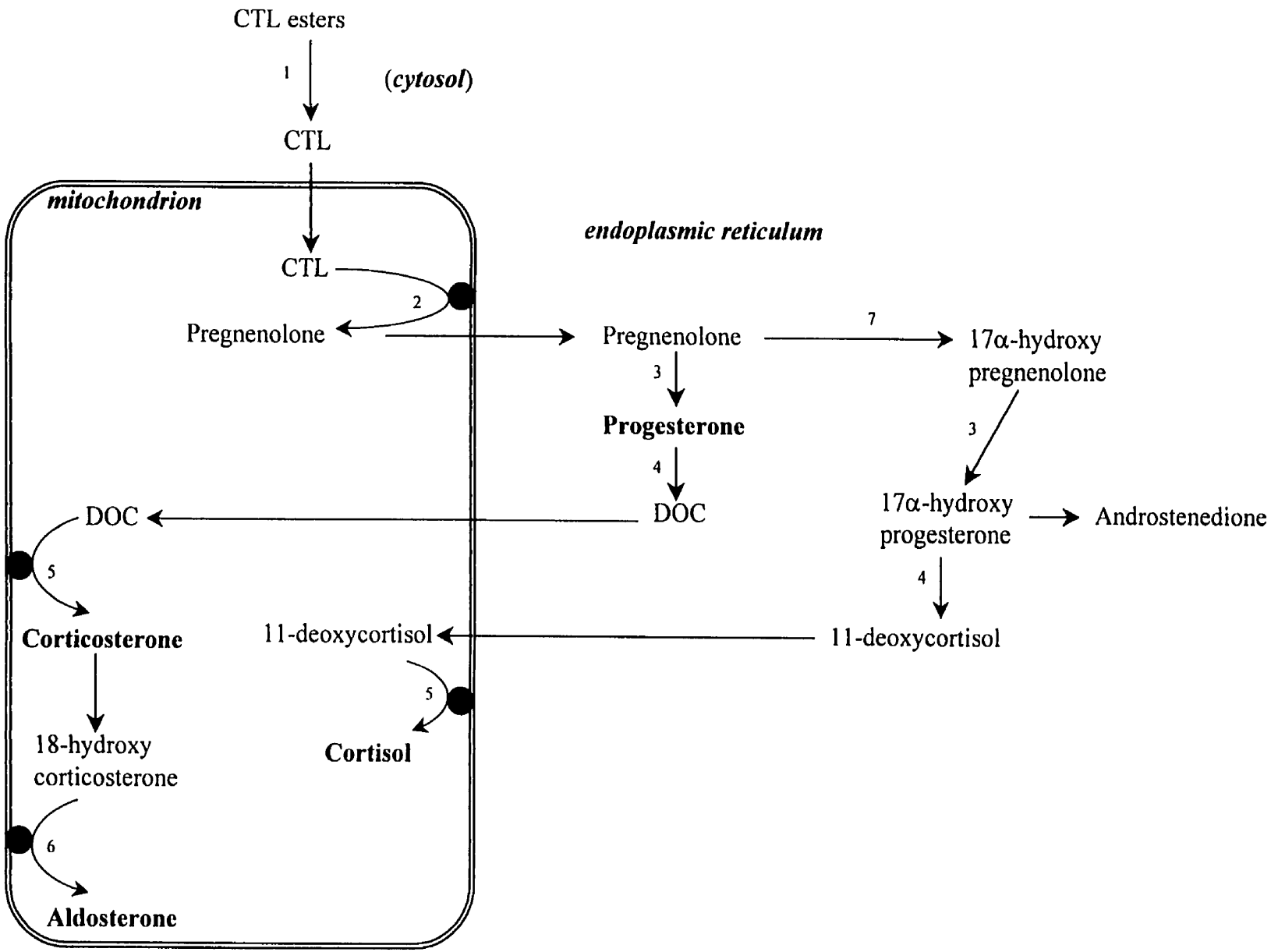
CTL esters
1
(cytosol)
CTL
mitochondrion
endoplasmic reticulum
CTL
2
Pregnenolone
Pregnenolone
7
17α-hydroxy pregnenolone
3
Progesterone
3
4
DOC
DOC
17α-hydroxy progesterone
Androstenedione
5
4
Corticosterone
11-deoxycortisol
11-deoxycortisol
5
18-hydroxy corticosterone
Cortisol
6
Aldosterone

the jirds in this experiment, it can be expected that the production of glucocorticoid hormones was stimulated as a result of both the immune response of the host and the starvation effect exerted by the parasite. The glucocorticoids have many physiological effects, the best-known of which is the stimulation of gluconeogenesis within hepatocytes. This is achieved through the mobilization of amino acids from muscle tissues, and the increase in the hepatic enzymes required to convert the amino acids to Glc (Guyton and Hall, 1996). Therefore, the increase in gluconeogenesis observed in livers of jirds infected with *E. multilocularis* (Schoen, 1997) may very well have been accompanied by an increase in plasma levels of glucocorticoids as the host body attempted to overcome the loss of Glc to the parasite. Another effect of glucocorticoids is the mobilization of FAs from adipose tissue which results in the increase both in plasma levels of free FAs and the utilization of FAs for energy generation (Munck and Náray-Fejes-Tóth, 1995; Guyton and Hall, 1996). The hormones also seem to have the ability to enhance the β-oxidation of FAs within cells, which helps to shift intracellular metabolism away from Glc utilization in times of starvation (Guyton and Hall, 1996). Although this effect is not as powerful as that induced by a decrease in insulin secretion by the pancreas, it is still considered to represent a significant contribution to the long-term conservation of Glc by a starving body. Because *E. multilocularis*-infected jirds are suffering from a systemic starvation, it is very likely that glucocorticoid production within their adrenal glands was enhanced. Finally with respect to this class of steroid hormones, glucocorticoid production is known to increase after the establishment of an immune response against disease or infection (Munck and Náray-Fejes-Tóth, 1995; Guyton and

Hall, 1996). The hormones act to decrease the accumulation of white blood cells at inflammatory sites, an immune reaction known to occur in alveolar hydatidosis (Bresson-Hadni *et al.*, 1990). Therefore, when all the various effects of the glucocorticoids are examined in conjunction with the effects of *E. multilocularis* on host metabolism, it seems very likely that an increase in hormone synthesis would occur in the infected jirds.

Another class of steroid hormones is that of the mineralcorticoids, which too are likely to increase in infected animals in spite of the fact that circulating levels of mineralcorticoids such as aldosterone do not increase in response to applied stresses in the same way as the glucocorticoids (Fenske, 1983; 1985), nor is there any evidence to suggest they are involved in immunity. The primary role of the mineralcorticoids is regulation of electrolyte balances and the conservation of Na^+ by organs like the kidney and large intestine (Fraser, 1992; Mortensen and Williams, 1995; Guyton and Hall, 1996). Aldosterone acts on the distal portion of the nephron to increase the re-absorption of Na^+, and this also serves to regulate fluid volume as renal transport of Na^+ is accompanied by the osmotic absorption of H_2O (Gullans and Hebert, 1996; Guyton and Hall, 1996). A drop in levels of extracellular Na^+ results in a slight increase in aldosterone secretion by the adrenal cortex (Guyton and Hall, 1996), which begs the question of whether or not *E. multilocularis* affects electrolyte levels in the host. Experiments completed by Frayha and Haddad (1980) quantified the concentrations of seven different ions within metacestodes of *E. granulosus*, and it was determined that Na^+ was present in the highest concentrations in both protoscolex tissue and hydatid fluid. Electrolytes have also been detected in metacestodes of *E. multilocularis* (McManus and

Bryant, 1995) where they likely accumulate as a result of simple diffusion from host tissues. The uptake of Na^+ by the parasite could be significant enough to stimulate an increase in aldosterone production since only a 10% reduction in plasma Na^+ levels is required to double mineralcorticoid secretion (Guyton and Hall, 1996). So once again, it seems as though the presence of *E. multilocularis* metacestodes could very well stimulate an increased production of steroid hormones.

An increase in adrenocortical hormone secretion seems to be a logical explanation for the depletion of CTL levels in the adrenals of infected animals because all of these hormones are derived from CTL (Fraser, 1992; Lehninger *et al.*, 1993). Perhaps less obvious, enhanced hormone secretion could also explain the drop seen in concentrations of TAG, total FA, and various FA moieties. An early step in the conversion of CTL to steroid hormones is the formation of pregnenolone catalyzed by the intramitochondrial enzyme 20-22 desmolase (Figure 21). This enzyme, along with all other steroid hydroxylase enzymes, is a cytochrome protein of the P-450 family which is embedded in the inner mitochondrial membrane (Simpson and Waterman, 1995). Activity of cytochrome P-450 enzymes is dependent on an adequate supply of the reducing equivalent NADPH which is supplied by the complete oxidation of organic acids in the TCA cycle and an electron transport chain localized in the mitochondrial matrix. When hormone synthesis is stimulated in cells of the adrenal cortex, the rate of intramitochondrial substrate oxidation will also increase (Simpson and Waterman, 1995). In an animal infected with *E. multilocularis*, there is a systemic depletion of Glc (Novak *et al.*, 1989; 1993) which means the supply of acetyl-CoA for TCA cycle oxidation would

likely be derived primarily from catabolism of FA. Release of glucocorticoids would stimulate the mobilization and oxidation of FA (Munck and Náray-Fejes-Tóth, 1995), the result of which would be the decrease in adrenal concentrations of FA and TAG. This may also account for the decrease in the average fatty acid chain length observed in infected animals. If the rate of FA oxidation were accelerated in adrenals of host jirds, there would have been a higher relative concentration of short-chain FAs in the glands at the time the experiment was terminated as a result of the catabolism of longer chain FAs. In essence, I may have been detecting a larger proportion of FAs in the process of β-oxidation within the infected animals rather than an actual decrease in the relative amount of long-chain FAs.

Although the theory of increased hormone synthesis provides an appealing and succinct explanation for the results of the present experiment, there are some other possibilities as well. For example, the decrease in CTL concentration in infected animals can also be attributed to a diminished supply of the steroid from the liver. The adrenal gland is capable of synthesizing CTL *de novo* from acetyl-CoA, but endogenous production is not the primary source of steroidogenic CTL. Indeed, research has shown that adrenocortical CTL represents only 2-4% of substrate for hormone synthesis, and the bulk of secreted steroids are derived from CTL and CTL esters transported from the liver in the form of lipoproteins (Pederson, 1988; Gwynne and Mahaffee, 1989). The preferred source for steroidogenic CTL is HDL - lipoprotein particles assembled in the liver and intestine that contain free CTL, CTL esters, GPL and TAG (Mims and Morrisette, 1988). Schoen (1997) observed a decrease in hepatic CTL levels in jirds infected with *E.*

multilocularis which was attributed to parasitic uptake of the sterol and the incorporation of HMG-CoA (an intermediate in CTL synthesis) into the reactions of ketogenesis. If there is less hepatic CTL available for transport in HDL, less CTL will arrive at the adrenal gland. Unfortunately, this explanation fails to account for the fact that adrenal CTL ester concentration did not change in the present experiment. If we consider the possibility that CTL was selectively taken up by the parasite, however, the trend in CTL and CTL ester levels can be explained. While in circulation, it is known that lipoprotein-bound CTL can actually diffuse through plasma and enter other lipoprotein species or cells, while CTL esters require a specific transfer protein for transport (Mims and Morrisette, 1988; Gwynne and Mahaffee, 1989; Fielding and Fielding, 1991). The smaller relative size and greater solubility of CTL as opposed to its esters may result in a selective uptake of the free sterol by the parasite. *E. multilocularis* metacestodes can absorb both CTL and CTL esters (McManus and Bryant, 1995), but the lipoprotein-bound esters may be preserved as there is no evidence to suggest that metacestodes can absorb HDL. The selective absorption of free CTL by the parasite could account for the results of the present study. Infected animals would have a depletion in the concentration of free CTL within lipoproteins, but there would be little or no difference in the amount of CTL ester delivered to the adrenal gland.

One rather troublesome aspect of the study of adrenal lipids is the substantial degree of interspecific variation that seems to exist. The magnitude of the CTL ester pool within cortical lipid droplets, the amount of free CTL relative to esterified CTL and the FA composition of the CTL esters are all factors that are highly dependent on the species

under study (Dailey *et al.*, 1960; Chang and Sweeley, 1963; Pederson, 1988). In addition, it has been emphasized in the past that the adrenal physiology of *M. unguiculatus* differs from that of other typical experimental animals like rats or dogs (Nickerson, 1971; Fenske, 1983). The Mongolian gerbil is a desert-dwelling rodent, and one must be careful when making assumptions about adrenal physiology based on data generated from non-desert animals. It is possible that the reason a change in CTL ester concentration was not seen between the two groups in the present study is that free CTL may be preferentially utilized in steroidogenesis in jirds. Along the same lines, it is also possible that DHA in the jird adrenal is confined solely to membrane GPL. If this is the case, and DHA is not a significant component of TAG or CTL esters, then we would not expect to see a decrease in its concentration as membrane GPL is preserved to a much greater extent than other lipid species in organs such as the liver (Groener and Van Golde, 1977; Moir and Zammit, 1992). There is no evidence to suggest that the preservation of membrane integrity is any less important in the adrenal gland, and the theory of the exclusive presence of DHA in membrane GPL would also account for the increase in its relative concentration. If all other FA chains are being used for energy generation due to their presence in TAG, then their levels relative to total FA will fall, while that of DHA will increase. Indeed, this is what happened in the present study. The observation that the ratio of CH_2 in $-CH=CH(CH_2CH=CH)_n-$: total FA did not change between infected and uninfected animals may be explained by the fact that while the net concentration of the moiety within the adrenal cells did decrease in infected animals, the decrease was not as substantial as the decreases of other FA moieties. In the adrenals of many animals, an

FA known as adrenoic acid is localized primarily in the CTL ester pool of lipids as opposed to GPLs (Vahouny *et al.*, 1979). Adrenoic acid is a 22 carbon FA in which n of the $-CH=CH(CH_2CH=CH)_n-$ moiety is repeated three times (Chang and Sweeley, 1963). In a ^1H NMR spectrum, this FA would contribute to the resonance integrated for the group, in addition to both DHA and AA. However, as concentrations of both DHA and AA did not decrease, the observed change is most likley due to adrenoic acid alone. Because the bulk of these FA chains are found esterified to CTL, it is possible that significantly fewer chains were oxidized relative to other FA species. There was no observed drop in CTL ester levels in infected animals, but TAG levels did significantly decrease. Therefore, the presumed decrease in net concentration of adrenoic acid may be due to the catabolism of those chains that were a part of TAG molecules, while the lack of change in its relative concentration may indicate that, when compared to other FA species, more adrenoic acid was conserved as part of CTL esters.

A change that is seemingly unrelated to the steroidogenic role of the adrenal gland is the decrease in the concentration of total GPL and PTE in infected animals. The drop in the tissue level of total GPL must be due to the decrease in PTE since no changes were observed in the levels of the other phospholipids measured. This is an unexpected result owing to the degree of interrelation that exists amongst the GPL biosynthetic pathways. The theories offered for the decrease in PTE concentration seen in kidneys of infected jirds do not apply here as there was no change in PTC concentration between the two groups. For this same reason, the uptake of PTE precursors by the parasite is not an adequate explanation because the results of the present experiment and those obtained by

Schoen (1997), in which GPLs other than PTE also decreased in concentration, do not support the idea that *E. multilocularis* has a preference for PTE precursors over those of other GPLs. For suggestions about why the parasite had the effect on adrenal GPLs that it did, we must look to biochemical pathways that are not linked to reactions of PTC metabolism, as both the CDPethanolamine and PEMT reactions are (see Figure 19, p. 111). As with PTC, there is more than one route to the biosynthesis of PTE, and one of these routes that has not yet been discussed is the decarboxylation of PTS (Ansell and Spanner, 1982; Vance, 1991). In the mammalian liver this reaction is a very minor source of PTE, but few studies have been done on the relative contributions of the various pathways in non-hepatic tissues, and it is possible that PTS is an important source of PTE in the adrenal gland. Unfortunately, there is very little known about the enzyme responsible for this reaction and how it is regulated (Vance, 1991), but the fact that the only measured GPL to drop in concentration in adrenal tissue in infected animals was PTE suggests that this pathway might hold the explanation. PTS is not present at high enough levels in mammalian liver, kidney or adrenal gland to be quantified by ^{1}H NMR spectroscopy (Schoen, 1997; present study), and so it is not known what effect alveolar hydatidosis has on tissue levels of this lipid. It has, however, been detected in cestode tissues by other analytical means (Frayha *et al.*, 1980; Mills *et al.*, 1981) which indicates that cestode parasites do remove PTS precursors from host tissues. Therefore, if the decarboxylation of PTS is the major source of PTE in the jird adrenal gland, uptake of PTS precursors by metacestodes could very well result in the observed decrease in PTE concentration in infected animals.

The final change left to explain is the decrease in the degree of unsaturation that was observed in the adrenals of the infected animals. Mandon *et al.* (1986) reported an inhibition of the activity of certain desaturase enzymes in the adrenal glands of rats in response to the hormone epinephrine. It is known that epinephrine is released by cells of the adrenal medulla in response to decreased plasma Glc levels (Guyton and Hall, 1996), so elevated epinephrine levels in the tissues of infected jirds are likely. This would result in a drop in the rate of desaturation of various FA chains (Mandon *et al.*, 1986), so an increase in epinephrine levels in infected animals could provide for the drop in the degree of unsaturation observed in this study.

All theories aside, it is obvious from the results of the present experiment that considerably more research into the lipid content and physiology of *M. unguiculatus* is required if we are to fully understand the changes that occurred.

III. Hepatic Carbohydrate Metabolism

The results of this experiment clearly demonstrate that alveolar hydatidosis has a profound effect on the partitioning of substrates within the hepatic biochemical pathways of the host. Before these results can be interpreted however, it is necessary to have an understanding of the fate of the ^{13}C label that was introduced into the liver as it passes through the reactions of the TCA cycle. To begin, the flow of the ^{13}C atoms of [1,2-$^{13}C_2$]acetate through this pathway is illustrated in Figure 22. In order to be metabolized in mammalian hepatocytes, acetate must first be converted to acetyl-CoA in a reaction catalyzed by acetyl-CoA synthetase (Fig. 22, [1]). This enzyme is found in both the

cytosol and mitochondria of liver cells, and as acetate can freely diffuse across any plasma membrane (Poole and Halestrap, 1993), acetyl-CoA is readily produced when exogenous acetate is supplied to either isolated hepatocytes (Crabtree *et al.*, 1990) or perfused, whole rat liver (Snoswell *et al.*, 1982; Baranyai and Blum, 1989). In the present experiment, the acetyl-CoA synthesized in the liver from the exogenous acetate is labeled with ^{13}C at carbons 1 and 2 (C1 and C2), and enters the TCA cycle through a condensation reaction with unlabeled OAA. The product of this citrate synthase-catalyzed reaction is a molecule of citrate labeled as shown in Figure 22, for even though citrate has a symmetrical structure, the stereospecific nature of the enzyme attack ensures that scrambling of the label does not occur at this point (Cohen and Bergman, 1994; Voet and Voet, 1995). The label passes through C4 and C5 of isocitrate to end up at C4 and C5 of α-ketoglutarate (α-KG), and at this stage of the cycle, the label reaches a branch point. The α-KG generated from isocitrate by isocitrate dehydrogenase has one of two fates: conversion either to the amino acid Glu, or to succinate and the continuation of the TCA cycle (Voet and Voet, 1995). Within the mitochondrion, labeled α-KG can be converted to Glu by the action of Glu dehydrogenase, a readily reversible enzyme that catalyzes the addition of a molecule of ammonia (NH_4^+) to the α-keto acid. The ^{13}C label derived from [1,2-$^{13}C_2$]acetate will appear at C4 and C5 of Glu, thus adding a second isotopomer (in addition to the unlabeled isotopomer already present) to the intracellular Glu pool. Alternatively, α-KG labeled at C4 and C5 can be decarboxylated by α-KG dehydrogenase to form succinyl-CoA. Because C1 of α-KG is lost as CO_2 in this reaction, ^{13}C labeling of succinyl-CoA will appear at C3 and C4 (Cohen and Bergman,

Figure 22

Entry of [1,2-$^{13}C_2$]acetate into the TCA cycle, and dispersal of the ^{13}C label.

This figure illustrates the flow of ^{13}C label derived from [1,2-$^{13}C_2$]acetate through the reactions of the TCA cycle. The initial labeling of [1,2-$^{13}C_2$]acetate is indicated by the filled circles (●), as is the position of the label in TCA cycle substrates throughout the first turn of the cycle. Note that this figure indicates all possible positions of label, therefore starting with malate, only two carbon atoms in each molecule will actually be labeled. The triangles (▲) represent the position of the label during the second turn of the cycle. Once again, all possible isotopomers are represented, and label will actually be present at only two of the carbons indicated by ▲ per molecule.

The following enzymes are involved:

1. Acetyl-CoA synthetase
2. Acetyl-CoA hydroxylase
3. Citrate synthase
4. Aconitase
5. Isocitrate dehydrogenase
6. α-ketoglutarate dehydrogenase and succinyl-CoA synthetase
7. Succinate dehydrogenase
8. Fumarase
9. Malate dehydrogenase
10. Glutamate dehydrogenase

The following abbreviations are used:

CIT: citrate
ICT: isocitrate
α-KG: α-ketoglutarate
SUC: succinate
FUM: fumarate
MAL: malate
OAA: oxaloacetate
GLU: glutamate

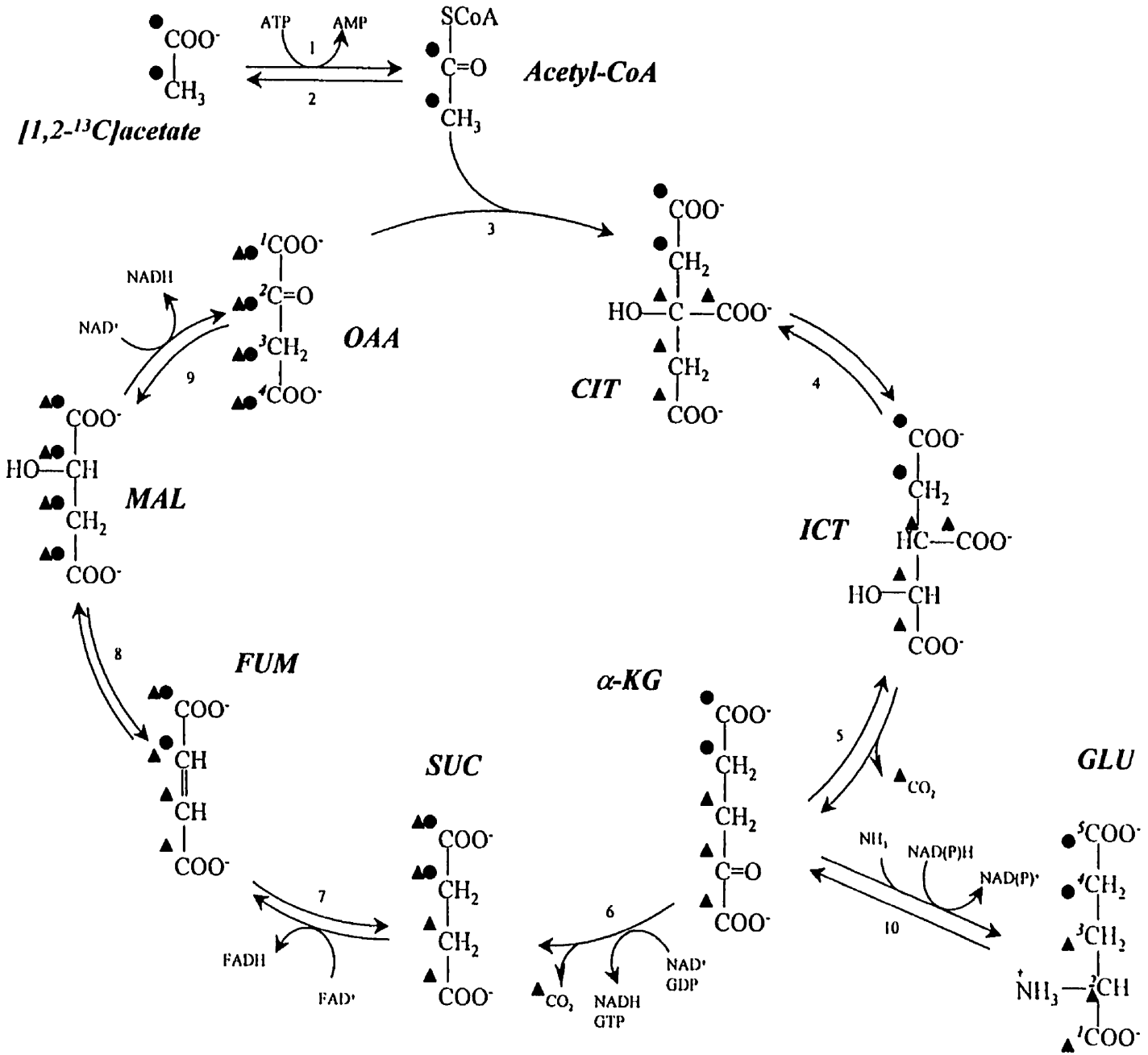
[1,2-13C]acetate
ATP
AMP
1
2
SCoA
C=O
CH3
Acetyl-CoA
3
COO-
CH2
HO—C—COO-
CH2
COO-
CIT
4
COO-
CH2
HC—COO-
HO—CH
COO-
ICT
5
CO2
α-KG
COO-
CH2
CH2
C=O
COO-
6
CO2
NADH
GTP
NAD+
GDP
7
FADH
FAD+
SUC
COO-
CH2
CH2
COO-
8
FUM
COO-
CH
CH
COO-
9
NADH
NAD+
OAA
1COO-
2C=O
3CH2
4COO-
MAL
COO-
HO—CH
CH2
COO-
10
NH3
NAD(P)H
NAD(P)+
GLU
5COO-
4CH2
3CH2
+NH3—2CH
1COO-

1994), and the labeled carbons then pass through the intermediates succinate, fumarate and malate to appear in OAA. Owing to the symmetry of the succinate and fumarate molecules, scrambling of the label occurs within the mitochondrial pool of malate as fumarase can add the hydroxyl group to either a labeled or an unlabeled carbon. This results in the production of two possible isotopomers of OAA at the end of the first turn of the cycle. Half of the OAA will be labeled at C1 and C2 while the other half will be labeled at C3 and C4 (Voet and Voet, 1995).

At the start of the second turn of the cycle, each of the three possible isotopomers of OAA, including unlabeled OAA, will condense with one of the two possible isotopomers of acetyl-CoA, and the resultant Glu molecules will exhibit a variety of labeling patterns. For example, if [1,2-$^{13}C_2$]OAA condenses with [1,2-$^{13}C_2$]acetyl-CoA, the α-KG produced after a quarter turn of the TCA cycle will be labeled at C3, C4 and C5. The same pattern of ^{13}C incorporation would be seen in the Glu that may be derived from this isotopomer of α-KG. [3,4-$^{13}C_2$]OAA reacting with unlabeled acetyl-CoA could only result in Glu labeled at C1 and C2, whereas reaction of [1,2-$^{13}C_2$]OAA with unlabeled acetyl-CoA would result in a Glu molecule labeled at C3 only, because the carbon atom derived from C1 of OAA is lost as CO_2 in the isocitrate dehydrogenase reaction. Condensation of [3,4-$^{13}C_2$]OAA with [1,2-$^{13}C_2$]acetyl-CoA could produce [1,2,4,5-$^{13}C_4$]Glu, and so after only two turns of the TCA cycle, six different Glu isotopomers can possibly be formed from the exogenous ^{13}C introduced into the cells (see below).

unlabeled OAA + unlabeled acetyl-CoA ---- unlabeled Glu

unlabeled OAA + [1,2-^{13}C]acetyl-CoA ---- [4,5-$^{13}C_2$]Glu

[1,2-^{13}C]OAA + unlabeled acetyl-CoA ---- [3-^{13}C]Glu

[1,2-^{13}C]OAA + [1,2-^{13}C]acetyl-CoA ---- [3,4,5-$^{13}C_3$]Glu

[3,4-^{13}C]OAA + unlabeled acetyl-CoA ---- [1,2-$^{13}C_2$]Glu

[3,4-^{13}C]OAA + [1,2-^{13}C]acetyl-CoA ---- [1,2,4,5-$^{13}C_4$]Glu

Further turns of the cycle will generate additional isotopomers of Glu due to the continued incorporation of ^{13}C from [1,2-$^{13}C_2$]acetate into TCA cycle intermediates, and the situation becomes even more complex when the contribution of ^{13}C from [3-^{13}C]lactate is considered.

Figure 23 illustrates the flow of ^{13}C label from [3-^{13}C]lactate through the primary and anaplerotic reactions of the TCA cycle. In order for the carbon atoms of lactate to contribute to any other hepatic metabolites, the lactate must first be converted to pyruvate by the action of lactate dehydrogenase (LDH), a cytosolic enzyme that is dependent on NAD^+ (Rehbinder, 1971; Voet and Voet, 1995). Although this reaction is reversible, LDH is regulated by the intracellular ratio of pyruvate/lactate (Morand *et al.*, 1993), so under the conditions of the present experiment where lactate is in excess, pyruvate production will be favored. The pyruvate formed from [3-^{13}C]lactate will also be labeled at C3, and is transported into mitochondria by a specific carrier that exchanges pyruvate for either OH^- or acetoacetate (Kummel, 1987). Once located within the mitochondrial matrix, ^{13}C from labeled pyruvate may enter the TCA cycle by one of two routes

Figure 23

Entry of [3-^{13}C]lactate into the TCA cycle, and dispersal of the ^{13}C label.

This figure illustrates the flow of ^{13}C label derived from [3-^{13}C]lactate through the reactions of the TCA cycle. The initial labeling of [3-^{13}C]lactate is indicated by the filled circle (●), as is the position of the label in pyruvate. The labeling of OAA that results from the PCx reaction is indicated by the open circle (○), while that of the acetyl-CoA produced by the PDC is shown as a ring (⦿). Throughout the first turn of the cycle, each intermediate may have either one or two ^{13}C atoms. In the second turn, the label derived from [3-^{13}C]lactate incorporated during the first turn is indicated by either an open triangle (△: from labeled OAA in the first turn) or a filled triangle (▲: from labeled acetyl-CoA in the first turn). Once again, note that label scrambling occurs at the point of malate formation.

The following enzymes are involved:

1. Lactate dehydrogenase (LDH)
2. Pyruvate dehydrogenase complex (PDC)
3. Citrate synthase
4. Aconitase
5. Isocitrate dehydrogenase
6. α-ketoglutarate dehydrogenase and succinyl-CoA synthetase
7. Succinate dehydrogenase
8. Fumarase
9. Malate dehydrogenase
10. Glutamate dehydrogenase
11. Pyruvate carboxylase (PCx)

The following abbreviations are used:

PYR: pyruvate
CIT: citrate
ICT: isocitrate
α-KG: α-ketoglutarate
SUC: succinate
FUM: fumarate
MAL: malate
OAA: oxaloacetate
GLU: glutamate

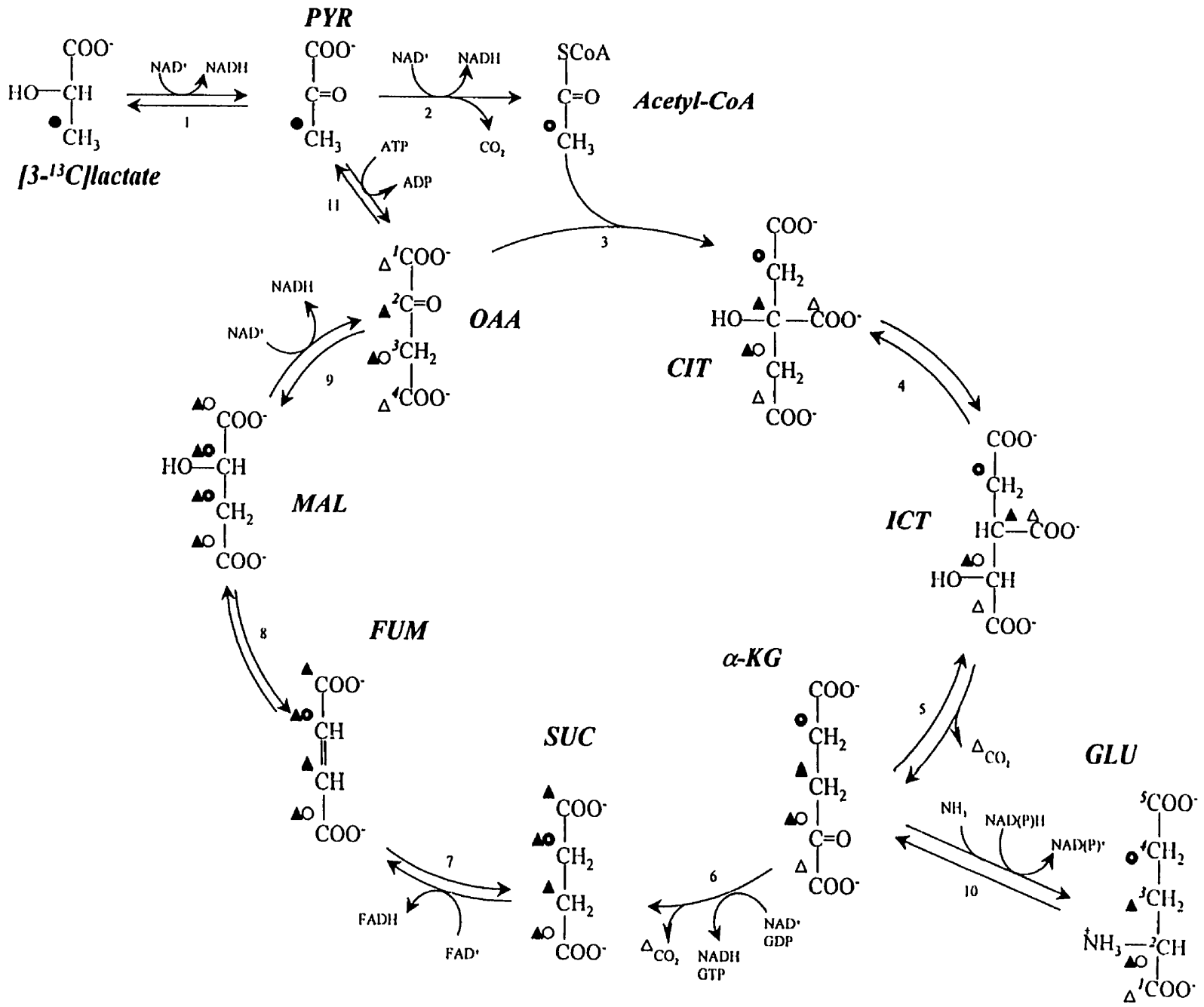
PYR
[3-13C]lactate
NAD+
NADH
1
2
SCoA
Acetyl-CoA
CO2
ATP
ADP
11
3
OAA
CIT
4
ICT
5
CO2
GLU
NH3
NAD(P)H
NAD(P)+
10
α-KG
6
NAD+
GDP
NADH
GTP
CO2
SUC
7
FADH
FAD+
FUM
8
MAL
9
NADH
NAD+

(Lehninger *et al.*, 1993; Voet and Voet, 1995). The pyruvate dehydrogenase complex (PDC), a multienzyme complex comprising three separate enzyme activities, catalyzes the irreversible oxidative decarboxylation of pyruvate to acetyl-CoA in a reaction that produces NADH and CO_2. The acetyl-CoA thus produced from [3-^{13}C]pyruvate will exhibit ^{13}C labeling at C2 and will be available for condensation with OAA via citrate synthase. The enzyme pyruvate carboxylase (PCx) carboxylates pyruvate to form OAA both as an anaplerotic reaction to replenish the mitochondrial pool of OAA, and as an early step in gluconeogenesis (see Figure 6, p. 47). The OAA formed by this enzyme from [3-^{13}C]pyruvate will be labeled at C3, and will either be transported to the cytosol and shunted towards gluconeogenesis, or remain in the mitochondrion and react with acetyl-CoA to form citrate in the first reaction of the TCA cycle. The flow of ^{13}C from exogenous [3-^{13}C]lactate into the hepatic TCA cycle is dependent on the regulation of PCx and PDC. It is known that PDC activity is inhibited if the mitochondrial concentration ratio of acetyl-CoA/CoA is high (Voet and Voet, 1995), which under the conditions of the present experiment is expected to be the case. The large influx of [1,2-$^{13}C_2$]acetate into hepatocytes and the subsequent conversion to [1,2-$^{13}C_2$]acetyl-CoA in a reaction that is known to occur very rapidly in isolated hepatocytes (Crabtree *et al.*, 1990) will dramatically raise the intramitochondrial ratio of acetyl-CoA/CoA. As a consequence, PDC activity will decrease while that of PCx will increase. Therefore, the bulk of labeled pyruvate will undergo conversion to [3-^{13}C]OAA, and enter the TCA cycle in this form. There will likely still be some flux of pyruvate through the PDC, however, so it is expected that limited quantities of [2-^{13}C]acetyl-CoA will be formed.

The production of [1,2-$^{13}C_2$]acetyl-CoA from [1,2-$^{13}C_2$]acetate, and both [2-^{13}C]acetyl-CoA and [3-^{13}C]OAA from [3-^{13}C]lactate means that the potential for the synthesis of a large number of Glu isotopomers exists within the hepatocytes of infected and uninfected animals in the present study. In fact, of the 32 possible Glu, $^{12}C/^{13}C$ isotopomers, 24 may be produced under my experimental conditions (the remaining eight are derived from [1-^{13}C]acetyl-CoA, which cannot be produced from either of the two labeled compounds used) (Malloy *et al.*, 1990a). Of these 24 different isotope isomers, those without ^{13}C label at either C3 or C4 are not relevant to this study since they cannot be detected with the method used. Therefore, I will shift my attention away from pathways of isotopomer synthesis and towards the results of the present experiment.

Both F_{LA} and F_{LL} were larger in *E. multilocularis*-infected jirds than in control animals, while F_U was significantly smaller. As indicated in Table 5 (p. 107), 18% of the acetyl-CoA entering the TCA cycle in livers of uninfected jirds was derived from [3-^{13}C]lactate, 32% was derived from [1,2-$^{13}C_2$]acetate, and the remaining 50% originated in unlabeled, endogenous sources. The comparable values from livers of infected animals were 27%, 38% and 34%, respectively. What these numbers indicate is that more of the exogenous, labeled substrates were incorporated into the reactions of the TCA cycle in infected animals, and that in both groups, [1,2-$^{13}C_2$]acetate was preferred over [3-^{13}C]lactate as a precursor for the acetyl-CoA destined for the citrate synthase reaction. In addition to the changes in F_{LA}, F_{LL} and F_U, the ratio of F_{LA} : F_{LL} was significantly smaller in the infected group, although it was greater than one in both groups. A F_{LA} : F_{LL} ratio of >1 reaffirms that labeled acetate was converted to acetyl-CoA more readily than labeled

lactate, but this substrate preference was significantly less pronounced in livers from infected jirds.

Since the variable F_U is calculated as the difference 1 - (F_{LA} + F_{LL}), its value is dependent on those of both F_{LA} and F_{LL}. Therefore, the observed decrease in F_U in infected animals can be considered in one of two ways: there were fewer endogenous, unlabeled substrates contributing to the pool of acetyl-CoA entering the TCA cycle in infected jirds, or, labeled lactate and acetate together made a greater contribution to the cycle intermediates in this group. Whichever way these values are interpreted, one possible explanation for the change might involve the rate of substrate flux through the TCA cycle. There is substantial evidence from previous research that gluconeogenesis is accelerated in the hepatocytes of *E. multilocularis*-infected jirds as a result of the starvation effect induced by the parasite (Schoen, 1997). This is a pathway that consumes both ATP and NADH (Voet and Voet, 1995), so when gluconeogenesis is increased, the rate of ATP consumption is also increased, and there will be a greater demand placed on energy-generating pathways such as the TCA cycle. Within the livers of the infected animals in the present experiment, gluconeogenesis should be operating at a high rate as well, readily consuming ATP. The ADP produced in the cytosol, as Glc is synthesized, will be transported into the mitochondrion via the ADP-ATP translocator, an antiport system located in the inner mitochondrial membrane. For every molecule of ADP transported into the mitochondrial matrix, a molecule of ATP is transported out, thus replenishing the cytosolic pool of ATP (Voet and Voet, 1995). As mentioned earlier, the enzyme PCx is stimulated when intramitochondrial concentrations of acetyl-CoA are

elevated as they likely were in both groups of animals in the present experiment, and as a result, more OAA is formed from pyruvate. The high levels of mitochondrial OAA in turn affects the enzyme citrate synthase, which is activated by OAA and inhibited by high levels of citrate. The citrate produced does not accumulate when there is a large demand for ATP, however, because isocitrate dehydrogenase, which catalyzes the conversion of isocitrate to α-KG is stimulated by high levels of ADP. Therefore, when gluconeogenesis is accelerated and ATP consumption increases, there will be a rapid production of α-KG, a molecule that is in equilibrium with the mitochondrial pool of Glu (Lehninger *et al.*, 1993; Voet and Voet, 1995). For reasons that are discussed in detail below, it is expected that hepatocytes of *E. multilocularis*-infected jirds will have higher intracellular levels of ^{13}C-labeled acetyl-CoA, OAA and pyruvate, as well as those compounds that are derived from them. Therefore, it is quite plausible that the rate of substrate flux through the feeder reactions of the TCA cycle should be accelerated in infected animals which, in turn, should contribute to the observed increases in F_{LA} and F_{LL}, and the corresponding decrease in F_U.

Although the acceleration of TCA cycle reactions in hepatocytes of *E. multilocularis*-infected jirds is a likely contributor to the observed decrease in F_U, it does not wholly address the question of why ^{13}C-labeled substrates were preferentially utilized. Several research groups have investigated the phenomenon of substrate selection, and there is evidence that a type of "metabolic channeling" may exist within the mitochondrial acetyl-CoA pool. Des Rosiers *et al.* (1991) have presented results from an experiment in which livers from starved rats were perfused with [2-^{13}C]acetate, and it was

found that more label was detected in citrate than in ketone bodies. They theorized that acetyl-CoA produced from acetate or pyruvate may be preferentially used for citrate synthesis, while the acetyl-CoA derived from the β-oxidation of FAs is directed towards ketogenesis (Des Rosiers *et al.*, 1991). Evidence for a similar inhomogeneity in the cytosolic pool of acetyl-CoA was also presented by Zhang *et al.* (1994) who examined the acetylation pattern of various drugs within the liver following the administration of various ^{13}C-labeled substrates. It was found that the mole % enrichment with ^{13}C of acetate, β-HB and the three acetylated drugs varied depending on the identity of the exogenous labeled compound used, be it [2-^{13}C]acetate, [1-^{13}C]octanoate or [1,2,3,4-$^{13}C_4$]docosanoate (the latter two compounds are FAs that are metabolized in mitochondria and peroxisomes, respectively). They concluded that the extra-mitochondrial acetyl-CoA pool was not isotopically homogenous, and that different sub-pools of acetyl-CoA likely exist within the cytosol of hepatocytes. The molecules of the various sub-pools can stream past each other without fully mixing, thus maintaining their individual fates of FA synthesis, CTL synthesis or drug acetylation (Zhang *et al.*, 1994). Therefore, if metabolic channeling is indeed a significant factor in hepatocytes, it could explain why F_U decreased in the infected animals in the present experiment. Normally in hepatocytes of starved mammals, the major source of acetyl-CoA is the β-oxidation of FAs (Hellerstein and Munro, 1994; Seifter and Englard, 1994). This should therefore also be the most important source of unlabeled acetyl-CoA in *E. multilocularis*-infected jirds. However, if the unlabeled acetyl-CoA of FA origin is preferentially directed towards ketogenesis rather than aerobic oxidation, it will not significantly contribute to F_U. Instead, the

labeled acetyl-CoA, derived from [1,2-$^{13}C_2$]acetate, will enter the citrate synthase reaction and F_{LA} will be enhanced. In fed animals, the major source of acetyl-CoA for the TCA cycle is the pyruvate that is generated by glycolysis (Seifter and Englard, 1994). Therefore this pathway would be the most important producer of unlabeled acetyl-CoA detected in control jirds. If the theory of metabolic channeling (Des Rosiers *et al.*, 1991; Zhang *et al.*, 1994) is sound, this unlabeled acetyl-CoA preferentially enters the TCA cycle, and F_U will be larger than that measured in infected animals.

Although Schoen (1997) noted an increase in the rate of ketogenesis in livers of infected jirds when [2-^{13}C]acetate was used as the exogenous substrate, this may not have occurred in the present experiment owing to the presence of labeled lactate. It is known that ketogenesis increases when the mitochondrial concentration of OAA is insufficient to react with elevated levels of acetyl-CoA derived from the breakdown of FAs (Hellerstein and Munro, 1994; Voet and Voet, 1995). In Schoen's experiments, there would have been an excess of acetyl-CoA without a corresponding excess of OAA, whereas in my study, there were likely elevated concentrations of both metabolites. Therefore, while in Schoen's experiment the labeled acetyl-CoA was mostly diverted towards ketogenesis, in the present study, a larger proportion of this labeled compound would have entered the TCA cycle because OAA was more plentiful.

The increase in F_{LA} in hepatocytes of infected animals was likely a result, in part, of the factors I have already discussed. Together, the accelerated rate of substrate flux through the feeder reactions of the TCA cycle and the possibility of metabolic channeling (Des Rosiers *et al.*, 1991) could account for the observed change. However, with respect

to acetate, it is also necessary to examine the other pathways into which it can be incorporated, and how they too may be affected by alveolar hydatidosis. Acetate can freely diffuse across plasma membranes, and once in the cell, acetyl-CoA is readily formed by acetyl-CoA synthetase both in the cytosol and mitochondria (Crabtree *et al.*, 1990; Poole and Halestrap, 1993). Snoswell *et al.* (1982) determined that the rate of uptake of exogenous acetate by perfused rat liver is directly correlated with the concentration of acetate within the perfusion medium. Therefore, it can be assumed that under the conditions of the present experiment, the intracellular concentration of [1,2-$^{13}C_2$]acetate was high. Once converted to acetyl-CoA, there are four fates for the ^{13}C-labeled acetate: i) hydrolysis by acetyl-CoA hydrolase, ii) lipogenesis, iii) ketogenesis and iv) entry into the TCA cycle. The role played by the TCA cycle in the changes observed in this experiment has already been discussed, so I will now turn my attention to the other pathways and their possible effects on the results I obtained.

Acetyl-CoA hydrolase catalyzes the irreversible breakdown of acetyl-CoA, thereby re-forming acetate. The enzyme is located within the cytosol of hepatocytes, and under normal physiological conditions it and acetyl-CoA synthetase function simultaneously and create an intracellular futile cycle that is thought to serve as a means of dissipating excess metabolic energy (Crabtree *et al.*, 1990). The hydrolase enzyme is inhibited when the cytosolic ratio of ADP/ATP is high. As discussed previously, an accelerated rate of gluconeogenesis, due to starvation, will cause this ratio to increase, so in infected animals, acetyl-CoA hydrolase should be operating at a slower rate than in controls. Therefore, less acetyl-CoA will be broken down to acetate, and more of it will enter the

citrate synthase reaction. As the pool of acetyl-CoA serving as substrate for the enzyme includes the [1,2-$^{13}C_2$]acetyl-CoA derived from the exogenous acetate, one effect will be an increase in F_{LA} in the parasitized animals.

Previous research has shown that when labeled acetate was provided to hepatocytes isolated from unstarved animals, the bulk of the label ended up in FAs, CTL and glycerol (Rabkin and Blum, 1985; Baranyai and Blum, 1989). In the present experiment, the animals were also not starved prior to injection of labeled substrates, so it is expected that in livers of uninfected animals, a large proportion of the [1,2-$^{13}C_2$]acetate would have been incorporated into lipids. However, under conditions of starvation lipogenesis is suppressed (Hellerstein and Munro, 1994), therefore utilization of labeled acetyl-CoA for lipid biosynthesis in infected jirds should have been very low. Thus, a decreased rate of lipogenesis might be one of the factors contributing to the observed increase in F_{LA} in the mitochondrial acetyl-CoA pool in infected animals.

Although it could be argued that the excess labeled acetyl-CoA in livers of infected jirds would be incorporated into ketogenesis since this pathway is accelerated during starvation, β-oxidation is also known to increase under this condition. The previously discussed theory of metabolic channeling can therefore be brought forth to account for why the bulk of [1,2-$^{13}C_2$]acetate did not appear to be incorporated into ketone bodies, as may be expected. If the primary substrate for ketogenesis is the unlabeled acetyl-CoA derived from β-oxidation, more of the labeled acetate would be incorporated into TCA cycle reactions in infected jirds.

With respect to [3-^{13}C]lactate, one of the possible explanations for the increase in F_{LL}

observed in infected animals involves the delivery of the substrate to the TCA cycle itself. In order to be incorporated into OAA or acetyl-CoA, the [3-^{13}C]lactate must first pass into the hepatocyte for conversion to pyruvate. The transport of lactate across the plasma membrane of hepatocytes is accomplished with the aid of a monocarboxylate transporter that carries either lactate or pyruvate in conjunction with a proton (Poole and Halestrap, 1993; Jackson and Halestrap, 1996). When the effects of pH on this carrier-mediated transport mechanism were studied, it was determined that the rate of lactate uptake by hepatocytes increased in a linear fashion as the extracellular pH was decreased (Fafournoux *et al.*, 1985). As I discussed earlier, it is assumed that the extracellular environment of the hepatocytes in the *E. multilocularis*-infected jirds was acidic owing to the excretion of acidic waste products by the parasite. Therefore, the transport of labeled lactate into hepatocytes may very well be enhanced in infected animals. Furthermore, Metcalfe *et al.* (1988) examined the effect of starvation on the carrier-mediated transport of lactate into isolated hepatocytes, and it was shown that uptake was enhanced in cells obtained from rats starved for 48 hours. Because *E. multilocularis* exerts a systemic starvation effect within the host (Novak *et al.*, 1989; 1993; 1995), the possibility exists that this effect could also lead to an increased rate of hepatic lactate uptake. That starvation also occurred in the present experiment is evidenced by the significant changes that occurred in body and liver weights. On average, the total body weight of infected jirds was 9.4% less than that of control animals. The livers from infected jirds weighed, on average, 8.3% less than those from controls. Both total body weight and liver weight were also reported to decrease in Syrian hamsters (a species of the same family as *M.*

unguiculatus) that were deprived of food over a period of 4.5 days (Hegarty and Kim, 1981), and in rats after only two days of complete starvation (Goodman and Ruderman, 1980). These studies demonstrate a correlation between body and liver mass and nutrient deprivation, and thus support the view that the infected jirds in my study were indeed suffering from starvation.

As a consequence of both the drop in extracellular pH that is assumed to accompany alveolar hydatidosis, and the systemic starvation of the host, hepatocytes of infected jirds should absorb [3-^{13}C]lactate at a faster rate than those of controls. Along with alterations to the rate of lactate uptake by hepatocytes, it is possible that the rate of lactate utilization was also increased in infected animals. In this regard, it is plausible that the observed increase in the relative amount of ^{13}C-labeled acetyl-CoA within the intramitochondrial acetyl-CoA pool was due to a higher intracellular concentration of labeled lactate which, in turn, resulted in an increase in the concentration of ^{13}C-labeled pyruvate, and therefore, acetyl-CoA. The enzyme LDH is inhibited by high concentrations of pyruvate within the cytosol, but in starving animals this concentration is low, and pyruvate production is expected to increase (Morand *et al.*, 1993). The reason for this is two-fold. First, the rate of hepatic glycolysis is inhibited under conditions of starvation with a concomitant stimulation of gluconeogenesis (Hellerstein and Munro, 1994; Seifter and Englard, 1994). As pyruvate is consumed in gluconeogenesis (see Fig. 6, p. 47), the starvation of *E. multilocularis*-infected jirds should result in a depletion of hepatocellular pyruvate levels. In hepatocytes isolated from rats starved for 24 hours, the rate of lactate utilization was increased when compared to unstarved controls (Morand *et*

al., 1993), and it was theorized that this effect was, in part, due to the depletion of pyruvate in starving animals. Gluconeogenesis is known to be accelerated in livers of animals suffering from cestode infections (Corbin, 1997; Schoen, 1997), and this pathway is a consumer of NADH (Voet and Voet, 1995). In order to maintain the cytosolic redox ratio, the conversion of lactate to pyruvate will be favored in starving animals as this reaction generates the NADH needed for gluconeogenesis. So an increase in lactate utilization in infected animals is not entirely surprising. The second reason why the cytosolic concentration of pyruvate is expected to be lower in infected animals has to do with the synthesis of ketone bodies. Ketogenesis is known to increase in livers of starving mammals (Lehninger *et al.*, 1993; Seifter and Englard, 1994), and one of the ketone bodies, acetoacetate, is transported out of the mitochondrion in exchange for pyruvate (Kummel, 1987; Morand, 1993). Therefore, increased production of ketone bodies coupled with an increased demand for these compounds in extra-hepatic tissues in response to Glc depletion will result in an increase in the rate of export of acetoacetate out of hepatic mitochondria. As a molecule of pyruvate must be imported for every molecule of acetoacetate exported, starvation will result in a depletion of cytosolic concentrations of pyruvate. Evidence for accelerated ketogenesis in *E. multilocularis*-infected jirds was presented by Schoen (1997). Increased levels of hepatic β-HB were found 30 minutes following a portal vein injection of [2-^{13}C]acetate, whereas after 120 minutes, hepatic levels of ^{13}C-labeled β-HB had returned to control levels. It was hypothesized that the initial increase was a result of the host liver attempting to remove the large excess of acetate through an accelerated rate of ketogenesis. Two hours into this

process, most of the ^{13}C-labeled β-HB had been transported out of the liver to supply extra hepatic tissues, with some of it even detected in parasite cysts (Schoen, 1997). The increase in β-HB levels (therefore acetoacetate levels, as β-HB is synthesized from acetoacetate), and the concomitant decrease in the rate of lipogenesis would result in an increase in the rate of utilization of cytosolic pyruvate, which could explain why more ^{13}C label from [3-^{13}C]lactate was incorporated into the TCA cycle in infected jirds.

In both uninfected and infected jirds, the ratio of $F_{LA} : F_{LL}$ was greater than one. A similar observation was made by Malloy *et al.* (1990a) when rat hearts were perfused with a mixture of [1,2-$^{13}C_2$]acetate and [3-^{13}C]lactate. This indicates that labeled acetate makes a greater relative contribution to acetyl-CoA than labeled lactate. The reason why acetate seems to be preferred over lactate as a precursor for acetyl-CoA likely has to do with the fact that lactate is readily converted to OAA, as well as acetyl-CoA (Seifter and Englard, 1994). The conversion of acetate to acetyl-CoA is rapid and occurs in both mitochondria and cytosol of hepatocytes (Crabtree *et al.*, 1990). This conversion, under the present experimental conditions, would result in an almost immediate elevation in cellular levels of acetyl-CoA. Therefore, lactate will be preferentially converted to OAA via pyruvate, and the OAA would then be directed towards gluconeogenesis, as well as the TCA cycle. Even if more [3-^{13}C]lactate was entering the TCA cycle than [1,2-$^{13}C_2$]acetate, it had to be entering primarily as OAA and the analytical method employed in this experiment measures the contribution of substrate to acetyl-CoA only, not OAA. The decrease in the ratio in infected animals is a result of relatively less [1,2-$^{13}C_2$]acetyl-CoA and/or relatively more [2-^{13}C]acetyl-CoA entering the TCA cycle. It seems more

likely that the change in the value of F_{LA} : F_{LL} had more to do with the contribution from F_{LL} than with that from F_{LA} as F_{LA} did not decrease in infected animals, but F_{LL} did increase. Although [1,2-$^{13}C_2$]acetate was still favored over [3-^{13}C]lactate in the infected jirds, much more labeled lactate likely entered the hepatocytes in the infected group thus allowing for an increased synthesis of [2-^{13}C]acetyl-CoA. The larger concentration of [2-^{13}C]acetyl-CoA in infected animals would result in an increase in the F_{LL} denominator of the ratio, and therefore the ratio itself would decrease.

IV. Future Research

Although the present studies answered a few questions about the biochemical nature of the *M. unguiculatus/E. multilocularis* host/parasite relationship, it is obvious that there is a need for future studies. With respect to lipid metabolism, an accurate determination of the extent to which *E. multilocularis* alters the physiological pH of the host would help to confirm, or refute, some of the theories proposed within this study. A quantitative assessment of pH within kidney, adrenal gland, liver and peritoneal cavity of infected and uninfected *M. unguiculatus* would allow for more definite conclusions regarding changes to the activities of enzymes involved in lipid metabolism. Such an analysis would also permit a more concrete understanding of the pH-dependent factors involved in hepatic carbohydrate metabolism, such as the transport of lactate across hepatocyte plasma membranes. Although Blackburn *et al.* (1993) did report alterations to the hepatic pH of mice infected with *H. microstoma*, interspecific variations between

various hosts and various parasites may very well mean that assumptions based on data from one host/parasite model are not valid for another. A study of this nature could be carried out using ^{31}P NMR spectroscopy to measure intracellular pH.

In addition to the question of pH, the lipid metabolism component of this work raised the issue of eicosanoid production by both parasite and host. In order to determine if *E. multilocularis* can synthesize eicosanoids from AA obtained from the host, cyst cells should be cultured *in vitro* with an AA-enriched medium. Then, radioimmunoassays or mass spectroscopy could be employed to quantify the output of AA-derived substances from the parasite. This could also be achieved *in vivo* by injecting exogenous, labeled AA directly into parasite cysts and tracing its fate using either NMR or mass spectroscopy. The concentration of PTS within liver, kidney and adrenal gland of *M. umguiculatus* should also be quantified, and compared between infected and control animals. This would help complete the GPL picture and allow for a more absolute conclusion as to why PTE levels in adrenals in infected jirds dropped while those of PTC and PTI did not. PTS levels would have to be measured using a more sensitive technique than ^{1}H NMR, however. Gas chromatography, either alone or coupled to mass spectroscopy would be adequate for this purpose.

Many questions revealed in these studies, as well as in previous experiments completed in our lab, could be addressed by an examination of the levels of various hormones within the blood or urine of the intermediate host. A simple study using radioimmunoassays could quantify the circulating levels of the adrenocortical hormones such as corticosterone and aldosterone, and measure the degree to which these levels are

affected by alveolar hydatidosis. Hormone levels could even be measured as a function of time in order to establish how the host body responds to infection over the entire course of the disease rather than just a single time point. Hormone assays of this nature could also be compared to studies in which animals were subjected to other forms of stress to determine how a parasitic infection ranks as a metabolic stressor. In addition to the adrenal hormones, circulating levels of insulin, glucagon, epinephrine and norepinephrine should be measured in an effort to obtain further information regarding hepatic metabolism. These hormones all have a role in regulating the processing of metabolic fuel within hepatocytes and should be quantified in order to describe more completely the effect of the parasite on the nutritional processes of the host. A complete hormone profile of infected animals may also serve to highlight other areas or systems within the host body that are affected by alveolar hydatidosis, and open up entire new fields of research.

Further investigations into the partitioning of substrates between various hepatic metabolic pathways using isotopomer analysis is also possible. This could be achieved by administering other labeled compounds to infected and uninfected animals, such as FAs, amino acids or succinate, or by analyzing other resonances within the spectra obtained in the present study. For example, glucose resonances could be examined in order to calculate the amount of exogenous substrate that is incorporated into gluconeogenesis. Other organs, such as cardiac muscle or kidney, could also be perfused with ^{13}C-labeled substrates and isotopomer analyses carried out in order to elucidate additional details of metabolism in these tissues. By using a method other than NMR, it

would also be possible to obtain more information from the same type of samples as were used in this study. By analyzing the samples with HPLC, a researcher could obtain a quantitative measure of exactly how much Glu is produced after the administration of the two labeled compounds. By coupling this information with that obtained in the present study, it would be possible to calculate the actual concentration of all the various Glu isotopomers. From a purely qualitative examination of the ^{13}C spectra acquired in the present study, it seems as though there was more labeled Glu present in the infected samples, and it would be interesting to quantify this apparent difference.

Although not directly related to the study of alveolar hydatidosis, it would be very beneficial to accumulate more information about the mammalian host used in the present model. It has been acknowledged previously that the renal and adrenal physiology of *M. unguiculatus* is very different from those of other commonly-utilized lab rodents owing to the fact that their natural habitat is a desert one. Some simple NMR or chromatographic analyses of organs from desert and non-desert rodents would provide a more solid background for studies of this nature. Some details that should be examined include an analysis of adrenal lipid droplets to determine the FA, CTL and CTL ester profiles of these organelles, and an assay of membrane lipids in order to ascertain the FA composition of the GPLs in jird membranes. A detailed determination of the contents of the various lipoprotein particles found in the circulation of these animals would also be very useful. A better-defined starting point with respect to the tissue composition of *M. unguiculatus* would allow for more concrete conclusions in any research that utilizes this desert-dwelling rodent as an experimental subject.

References

Abbas, A.K., Lichtman, A.H. and Pober, J.S., 1994. Cellular and Molecular Immunology, 2nd ed. W.B. Saunders Co., Philadelphia.

Abra, R.M. and Quinn, P.J., 1976. Some characteristics of *sn*-glycero-3-phosphocholine diesterases from rat brain. Biochim. Biophys. Acta, **164**: 631-639.

Adosraku, R.K., Anderson, M.M., Anderson, G.J., Choi, C., Yardely, V., Phillipson, J.D. and Gibbons, W.A., 1993. Proton NMR lipid profile of *Leishmania donovani* promastigotes. Mol. Biochem. Parasitol., **62**: 251-262.

Adosraku, R.K., Choi, C., Constantinou-Kokotos, V., Anderson, M.M. and Gibbons, W.A., 1994. NMR lipid profiles of cells, tissues and body fluids: proton NMR analysis of human erythrocyte lipids. J. Lipid Res., **35**: 1925-1931.

Akinoglu, A., Demiryurek, H. and Guzel, C., 1991. Alveolar hydatid disease of the liver: a report on thirty-nine surgical cases in Eastern Anatolia, Turkey. Am. J. Trop. Med. Hyg., **45**(2): 182-189.

Alberts, B., Bray, D., Lewis, J., Raff, M., Roberts, K., and Watson, J.D., 1994. Molecular Biology of the Cell, 3rd ed. Garland Publishing Inc., New York.

Ali-Khan, Z., 1978. *Echinococcus multilocularis*: cell-mediated immune response in early and chronic alveolar murine hydatidosis. Exp. Parasitol., **46**: 157-165.

Alkarmi, T. and Behbehani, K., 1989. *Echinococcus multilocularis*: inhibition of murine neutrophil and macrophage chemotaxis. Exp. Parasitol., **69**: 16-22.

Altman, P.L. and Dittmer, D.S., 1972. Biology Data Book, 2nd ed. Federation of American Societies for Experimental Biology. pp. 392-398.

Amman, R. and Eckert, J., 1995. Clinical diagnosis and treatment of echinococcosis in humans. In: *Echinococcus* and Hydatid Disease. Eds: R.C.A. Thompson and A.J. Lymbery. CAB International, Wallingford, UK. pp. 411-463.

Amman, R. and Eckert, J., 1996. Cestodes: *Echinococcus*. Gastroent. Clin. N. Am., **25**(3): 655-689.

Ansell, G.B. and Spanner, S., 1982. Phosphatidylserine, phosphatidylethanolamine and phosphatidylcholine. In: Phospholipids. Eds: J.N. Hawthorne and G.B. Ansell. Elsevier Biomedical Press, Amsterdam. pp. 1-49.

Ardaillou, R., Ronco, P. and Rondeau, E., 1996. Biology of renal cells in culture. In: Brennor and Rector's The Kidney., 5th ed. Ed: B.M. Brennor. W.B. Saunders Co., Philadelphia. pp. 99-192.

Bader-Goffer, R., Bachelard, H.and Morris, P.G., 1990. Cerebral metabolism of acetate and glucose studied by ^{13}C NMR spectroscopy. Biochem. J., **266**: 133-139.

Bader-Goffer, R. and Bachelard, H., 1991. Metabolic studies using ^{13}C nuclear magnetic resonance spectroscopy. Biochem. Essays, **9**: 105-119.

Bain, A.D., Fahie, B.J., Kozluk, T. and Leigh, W.J., 1991. Improvements in the quantitation of NMR spectra by the use of statistical methods. Can. J. Chem., **69**: 1189-1192.

Baldwin, J.J. and Cornatzer, W.E., 1968. Rat kidney glycerophosphorylcholine diesterase. Biochim. Biophys. Acta, **164**: 195-204.

Baranyai, J.M. and Blum, J.J., 1989. Quantitative analysis of intermediary metabolism in rat hepatocytes incubated in the presence and absence of ethanol with a substrate mixture including ketoleucine. Biochem. J., **258**: 121-140.

Belley, A. and Chadee, K., 1995. Eicosanoid production by parasites: from pathogenesis to immunomodulation? Parasitol. Today, **11**(9): 327-334.

Bjørnstad, P. and Bremer, J., 1966. *In vivo* studies on pathways for the biosynthesis of lecithin in the rat. J. Lipid Res., **7**: 38-45.

Blackburn, B.J., Buist, R., Hudspeth, C. and Novak, M., 1993. Phosphorus metabolites of liver from mice infected with *Hymenolepis microstoma*. Int. J. Parasitol., **23**(1): 95-103.

Bresson-Hadni, S., Vuitton, D.A., Lenys, D., Liance, M., Racadot, E. and Miguet, J.P., 1989. Cellular immune responses in *Echinococcus multilocularis* infection in humans. I. Lymphocyte reactivity to *Echinococcus* antigens in patients with alveolar echinococcosis. Clin. Exp. Immunol., **78**: 61-66.

Bresson-Hadni, S., Liance, M., Meyer, J.P., Houin, R., Bresson, J.L. and Vuitton, D.A., 1990. Cellular immunity in experimental *Echinococcus multilocularis* infection. II. Sequential and comparative phenotypic study of periparasitic mononuclear cells in resistant and sensitive mice. Clin. Exp. Immunol., **82**: 378-383.

Breyer, M.D. and Badr, K.F., 1996. Arachidonic acid metabolites and the kidney. In: Brennor and Rector's The Kidney., 5th ed. Ed: B.M. Brennor. W.B. Saunders Co., Philadelphia. pp. 754-788.

Brindley, D.N., 1991. Metabolism of triacylglycerols. In: Biochemistry of Lipids, Lipoproteins and Membranes. Eds: D.E. Vance and J. Vance. Elsevier Science Publishers, Amsterdam. pp. 171-204.

Cahill, G.F., 1986. Physiology of gluconeogenesis. In: Hormonal Control of Gluconeogenesis, Vol.1. Ed.: N. Kraus-Friedmann. CRC Press Inc., Boca Raton. pp. 3-13.

Casu, M., Anderson, G.J., Choi, G. and Gibbons, W.A., 1991. NMR lipid profiles of cells, tissues and body fluids: 1D and 2D proton NMR of lipids from rat liver. Magnet. Reson. Chem., **29**: 594-602.

Chang, T-C.L. and Sweeley, C.C., 1963. Characterization of lipids from canine adrenal glands. Biochem., **2**(3): 592-604.

Choi, G.T.Y., Casu, M. and Gibbons, W.A., 1993. NMR lipid profiles of cells, tissues and body fluids: neutral, non-acidic and acidic phospholipid analysis of Bond-Elut chromatography fractions. Biochem. J., **290**: 717-721.

Cohen, S.M., 1987. ^{13}C NMR study of effects of fasting and diabetes on the metabolism of pyruvate in the tricarboxylic acid cycle and of the utilization of pyruvate and ethanol in lipogenesis in perfused rat liver. Biochem., **26**: 581-589.

Cohen, D.M. and Bergman, R.N., 1994. Prediction of positional isotopomers of the citric acid cycle: the syntactic approach. Am. J. Physiol., **266**(29): E341-E350.

Cook, H.W., 1991. Fatty acid desaturation and chain elongation in eukaryotes. In: Biochemistry of Lipids, Lipoproteins and Membranes. Eds: D.E. Vance and J. Vance. Elsevier Science Publishers, Amsterdam. pp. 141-169.

Corbin, I., 1997. A magnetic resonance study of liver metabolites from mice infected with the larval cestode *Taenia crassiceps*. M.Sc. thesis, University of Manitoba.

Corbin, I., Simcoff, R., Novak, M. and Blackburn, B.J., 1998a. Metabolism of [3-^{13}C]pyruvate by cysticerci of *Taenia crassiceps*. Parasitol. Res., **84**: 516-518.

Corbin, I., Payette, J., Blackburn, B.J. and Novak, M., 1998b. Excretion of citrate by

metacestodes of *Mesocestoides vogae*. Can. J. Zool., In Press.

Crabtree, B., Gordon, M-J. And Christie, S.L., 1990. Measurement of the rates of acetyl-CoA hydrolysis and synthesis from acetate in rat hepatocytes and the role of these fluxes in substrate cycling. Biochem. J., **270**: 219-225.

Crane, D. and Masters, C., 1981. On the turnover of tissue lipids in the mouse during early starvation. Int. J. Biochem., **13**: 117-120.

Dailey, R.E., Swell, L., Field, H. and Treadwell, C.R., 1960. Adrenal cholesterol ester fatty acid composition of different species. PSEBM, **105**: 4-6.

Deckelbaum, R.J., Ramakrishnan, R., Eisenberg, S., Olivecrona, T. And Bengtsson-Olivecrona, G., 1992. Triacylglycerol and phospholipid hydrolysis in human plasma lipoproteins: role of lipoprotein and hepatic lipase. Biochem., **31**: 8544-8551.

Desmet, V.J., 1994. Organizational principles. In: The Liver: Biology and Pathobiology., 3rd ed. Ed: I.M. Arias. Raven Press, New York. pp. 3-14.

Des Rosiers, C., Di Donato, L., Comte, B., Laplante, A., Marcoux, C., David, F., Fernandez, C.A. and Brunengraber, H., 1995. Isotopomer analysis of citric acid cycle and gluconeogenesis in rat liver. J. Biol. Chem., **270**(17): 10027-10036.

Devouge, M. And Ali-Khan, Z., 1983. Intraperitoneal murine alveolar hydatidosis: relationship between the size of the larval cyst mass, immigrant inflammatory cells, splenomegaly and thymus involution. Tropenmed. Parasit., **34**: 15-20.

Dowhan, W., 1997. Molecular basis for membrane phospholipid diversity: why are there so many lipids? Annu. Rev. Biochem., **66**: 199-232.

Durand, T., Gallis, J-L., Masson, S., Cozzone, P.J. and Canioni, P., 1993. pH regulation in perfused rat liver: respective role of Na^+-H^+ exchanger and Na^+-HCO_3^- cotransport. Am. J. Physiol., **265**: G43-G50.

Emery, I., Liance, M., Deriaud, E., Vuitton, D.A., Houin, R. And Leclerc, C., 1996. Characterization of T-cell immune responses of *Echinococcus multilocularis*-infected C57BL/6J mice. Parasite Immunol., **18**(9): 463-472.

Emery, I., Leclerc, C., Sengphommachanh, K., Vuitton, D.A. and Liance, M., 1998. In vivo treatment with recombinant IL-12 protects C57BL/6J mice against secondary alveolar echinococcosis. Parasite Immunol., **20**(2): 81-91.

Epstein, M., 1986. Renal prostaglandins and the control of renal function in liver disease. Am. J. Med., **80**(1A): 46-55.

Fafournoux, P., Deminge, C. and Remesy, C., 1985. Carrier-mediated uptake of lactate in rat hepatocytes. J. Biol. Chem., **260**(1): 292-299.

Fenske, M., 1983. Production of steroids by *in vitro* superfusion from adrenals of the Mongolian gerbil: effect of acute stress. Comp. Biochem. Physiol., **74A**(4): 971-976.

Fenske, M., 1984. Secretion of catecholamines, ascorbic acid, progesterone and corticosterone by *in vitro* superfusion from the adrenal of the Mongolian gerbil: effect of confinement stress. Exp. Clin. Endocrinol., **84**(2): 174-182.

Fenske, M., 1985. Effects of acute stress, (1-24)ACTH administration and changes in superfusion temperature and flow rate on the *in vitro* secretion of glucocorticosteroids and aldosterone from the Mongolian gerbil adrenal gland. Comp. Biochem. Physiol., **82A**(4): 951-958.

Fielding, P.E. and Fielding, C.J., 1991. Dynamics of lipoprotein transport in the circulatory system. In: Biochemistry of Lipids, Lipoproteins and Membranes. Eds: D.E. Vance and J. Vance. Elsevier Science Publishers, Amsterdam. pp. 427-459.

Folch, J., Lees, M. and Sloane-Stanley, G.H., 1957. A simple method for the isolation and purification of total lipides from animal tissues. J. Biol. Chem., **226**: 497-509.

Frayha, G.J. and Smyth, J.D., 1983. Lipid metabolism in parasitic helminths. Adv. Parasitol., **22**: 309-387.

Fraser, R., 1992. Biosynthesis of adrenocortical steroids. In: The Adrenal Gland, 2nd ed. Ed: V.T. James. Raven Press, New York. pp. 117-130.

Fujioka, Y., Aoki, S., Sato, N. and Uchino, J., 1993. Pathology. In: Alveolar Echinococcosis of the Liver. Eds: J. Uchino and N. Sato. Hokkaido University School of Medicine, Sapporo. pp. 51-62.

Goodman, M.N. and Ruderman, N.B., 1980. Starvation in the rat. I. Effect of age and obesity on organ weights, RNA, DNA and protein. Am. J. Physiol., **239**: E269-E276.

Goodridge, A.G., 1991. Fatty acid synthesis in eukaryotes. In: Biochemistry of Lipids,

Lipoproteins and Membranes. Eds: D.E. Vance and J. Vance. Elsevier Science Publishers, Amsterdam. pp. 111-139.

Gottstein, B., Mesarina, B., Tanner, I., Amman, R.W., Wilson, J.F., Eckert, J. and Lanier, A., 1991. Specific cellular and humoral immune responses in patients with different long-term courses of alveolar echinococcosis (infection with *Echinococcus multilocularis*). Am. J. Trop. Med. Hyg., **45**(6): 734-742.

Gottstein, B., 1992. *Echinococcus multilocularis* infection: immunology and immunodiagnosis. Adv. Parasitol., **31**: 321-380.

Gottstein, B., Jacquier, P., Bresson-Hadni, S. and Eckert, J., 1993. Improved primary immunodiagnosis of alveolar echinococcosis in humans by an enzyme-linked immunosorbant assay using the $Em2^{+}$ antigen. J. Clin. Microbiol., **31**(2): 373-376.

Gottstein, B. and Felleisen, R., 1995. Protective immune mechanisms against the metacestode of *Echinococcus multilocularis*. Parasitol. Today, **11**(9): 320-326.

Groener, J.E.M. and Van Golde, L.M.G., 1977. Effect of fasting and feeding a high-sucrose, fat-free diet on the synthesis of hepatic glycerolipids *in vivo* and in isolated hepatocytes. Biochim. Biophys. Acta, **487**: 105-114.

Gullans, S.R. and Hebert, S.C., 1996. Metabolic basis of ion transport. In: Brennor and Rector's The Kidney., 5th ed. Ed: B.M. Brennor. W.B. Saunders Co., Philadelphia. pp. 211-246.

Guyton, A.C. and Hall, J.E., 1996. Textbook of Medical Physiology., 9th ed. W.B. Saunders Co., Philadelphia.

Gwynne, J.T. and Mahaffee, D.D., 1989. Rat adrenal uptake and metabolism of high density lipoprotein cholesteryl ester. J. Biol. Chem., **264**: 8141-8150.

Heath, D.D., 1995. Immunology of *Echinococcus* infections. In: *Echinococcus* and Hydatid Disease. Eds: R.C.A. Thompson and A.J. Lymbery. CAB International, Wallingford, UK. pp. 183-199.

Hegarty, P.V.J. and Kim, K.O., 1981. Effect of starvation on tissues from the young of four species, with emphasis on the number and diameter of skeletal muscle fibers. Pediatr. Res., **15**(2): 128-32.

Hellerstein, M.K. and Munro, H.N., 1994. Interaction of liver, muscle and adipose tissue in the regulation of metabolism in response to nutritional and other factors. In:

The Liver: Biology and Pathobiology., 3rd ed. Ed: I.M. Arias. Raven Press, New York. pp. 1169-1191.

Hers, H-G., 1990. Mechanisms of blood glucose homeostasis. J. Inher. Metab. Dis., **13**: 395-410

Hunt, S.M. and Groff, J.L., 1990. Advanced Nutrtion and Human Metabolism. West Publishing Co., St. Paul.

Jackson, V.N. and Halestrap, A.P., 1996. The kinetics, substrate and inhibitor specificity of the monocarboxylate (lactate) transporter of rat liver cells determined using the fluorescent intracellular pH indicator, 2', 7'-bis(carboxyethyl)-5(6)-carboxyfluorescin. J. Biol. Chem., **271**(2): 861-868.

James, E. and Boyd, W., 1937. *Echinococcus alveolaris* (with the report of a case). Can. Med. Assoc. J., **36**: 354-356.

Jans, A.W.H. and Leibfritz, K-H., 1989. A ^{13}C NMR study on fluxes into the Kreb's cycle of rabbit renal proximal tubular cells. NMR in Biomed., **1**(4): 171-176.

Jans, A.W.H. and Kinne, R.K.H., 1991. ^{13}C NMR spectroscopy as a tool to investigate renal metabolism. Kidney Int., **39**: 430-437.

Jeffrey, F.M.H., Rajagopal, A., Malloy, C.R. amd Sherry, A.D., 1991. ^{13}C-NMR: a simple yet comprehensive method analysis of intermediary metabolism. TIBS, **16**: 5-10.

Jenne, L., Kilwinski, J., Scheffold, W. and Kern, P., 1997. IL-5 expressed by $CD4^-$ lymphocytes from *Echinococcus multilocularis* infected patients. Clin. Exp. Immunol., **109**: 90-97.

Jones, J.G., Sherry, A.D., Jeffrey, F.M.H., Storey, C.J. and Malloy, C.R., 1993. Sources of acetyl-CoA entering the tricarboxylic acid cycle as determined by analysis of succinate ^{13}C isotopomers. Biochem., **32**: 12240-12244.

Kanazawa, T., Asahi, H., Hata, H., Mochida, K., Kagei, N. and Stadecker, M.J., 1993. Arginine-dependent generation of reactive nitrogen intermediates is instrumental in the *in vitro* killing of protoscoleces of *Echinococcus multilocularis* by activated macrophages. Parasite Immunol., **15**(11): 619-623.

Kasai, Y., Koshino, I., Kawanishi, N., Sakamoto, H., Sasaki, E. and Kumagai, M., 1980. Alveolar echinococcosis of the liver: studies on 60 operated cases. Ann. Surg., **191**(2): 145-152.

Kassis, A.I. and Frayha, G.J., 1973. Lipids of the cysticerci of *Taenia hydatigena* (Cestoda). Comp. Biochem. Physiol., **46B**: 435-443.

Kida, K., Nakajo, S., Kamiya, F., Toyama, Y., Nishio, T. and Nakagawa, H., 1978. Renal net glucose release *in vivo* and its contribution to blood glucose in rats. J. Clin. Invest., **62**: 721-726.

Kolářová, L., Pavlásek, I. and Chalupský, J., 1996. *Echinococcus multilocularis* Leuckart, 1863 in the Czech Republic. Helminthologia, **33**(2): 59-65.

Kuby, J., 1994. Immunology, 2nd ed. W.H. Freeman and Co., New York.

Kuesel, A.C., Graschew, G., Hull, W.E., Lorenz, W. and Thielmann, H.W., 1990. ^{31}P NMR studies of cultured human tumor cells. Influence of pH on phospholipid metabolite levels and the detection of cytidine 5'-diphosphate choline. NMR Biomed., **3**(2): 78-89.

Kumagai, M., 1993. Immunodiagnosis. In: Alveolar Echinococcosis of the Liver. Eds: J. Uchino and N. Sato. Hokkaido University School of Medicine, Sapporo. pp. 69-74.

Kummel, L., 1987. Mitochondrial pyruvte carrier - a possible link between gluconeogenesis and ketogenesis in the liver. Biosci. Rep., **7**: 593-597.

Lands, W.E.M., 1991. Biosynthesis of prostaglandins. Annu. Rev. Nutr., **11**: 41-60.

Lazarow, P.B., 1994. Peroxisomes. In: The Liver: Biology and Pathobiology., 3rd ed. Ed: I.M. Arias. Raven Press, New York. pp. 293-307.

Lee, R.G.L., Clause, M.E., and Lanir, A., 1988. Liver adenosine triphosphate and pH in fasted and well-fed mice after infusion of adenine nucleotide precursors. Liver, **8**: 337-343.

Lehninger, A.L., Nelson, D.L. and Cox, M.M., 1993. Principles of Biochemistry., 2nd ed. Worth Publishers Inc., New York.

Leid, R.W. and McConnell, L.A., 1983. PGE_2 generation and release by the larval stage of the cestode *Taenia taeniaeformis*. Prostaglandins Leukot. Med., **11**: 317-323.

Longmuir, K.J., 1987. Biosynthesis and distribution of lipids. Cur. Top. Membr. Transp., **29**: 129-174.

Lubinsky, G., 1960. The maintenence of *Echinococcus multilocularis* without the

definitive host. Can. J. Zool., **38**: 149-151.

Malczewski, A., Rocki, B., Ramisz, A. and Eckert, J., 1995. *Echinococcus multilocularis* (Cestoda), the causitive agent of alveolar echinococcosis in humans: first record in Poland. J. Parasitol., **81**(2): 318-321.

Malloy, C.R., 1990. Nuclear magnetic resonance in clinical medicine: an overview. Sem. Perinat., **14**(3): 193-200.

Malloy, C.R., Sherry, A.D. and Jeffrey, F.M.H., 1990a. Analysis of tricarboxylic acid cycle of the heart using ^{13}C isotope isomers. Am. J. Physiol., **259**: H987-H995.

Malloy, C.R., Thompson, J.R., Jeffrey, F.M.H. and Sherry, A.D., 1990b. Contribution of exogenous substrates to acetyl coenzyme A: measurement by ^{13}C NMR under non-steady-state conditions. Biochem., **29**: 6756-6761.

Mandon, E.C., de Gomez Dumm, I.R.T. and Brenner, R.R., 1986. Effect of epinephrine on the oxidative desaturation of fatty acids in the rat adrenal gland. Lipids, **21**: 401-404.

Mayo-Smith, W., Hayes, C.W., Biller, B.M.K., Klibanski, A., Rosenthal, H. and Rosenthal, D.I., 1989. Body fat distribution measured with CT: correlations in healthy subjects, patients with anorexia nervosa and patients with Cushing syndrome. Radiology, **170**(2): 515-518.

McManus, D.P. and Bryant, C., 1995. Biochemistry, physiology and molecular biology of *Echinococcus*. In: *Echinococcus* and Hydatid Disease. Eds: R.C.A. Thompson and A.J. Lymbery. CAB International, Wallingford, UK. pp. 135-181.

McNicol, A.M., 1992. The human adrenal gland: aspects of structure, function and pathology. In: The Adrenal Gland, 2nd ed. Ed: V.H.T. James. Raven Press, New York. pp. 1-42

Merkle, E.M., Kramme, E., Vogel, J., Kramer, S., Schulte, M., Usadel, S., Kern, P. and Brambs, H-J., 1997. Bone and soft tissue manifestations of alveolar echinococcosis. Skeletal Radiol., **26**(5): 289-292.

Metcalfe, H.K., Monson, J.P., Cohen, R.D. and Padgham, C., 1988. Enhanced carrier-mediated lactate entry into isolated hepatocytes from starved and diabetic rats. J. Biol. Chem., **263**(36): 19505-19509.

Mills, G.L., Taylor, D.C. and Williams, J.F., 1981. Lipid composition of the helminth parasite *Taenia crassiceps*. Comp. Biochem. Physiol., **69B**: 553-557.

Mims, M.P. and Morrissette, J.D., 1988. Role of cholesterol and cholesteryl ester in the structure dynamics and metabolism of plasma lipoproteins. In: Biology of Cholesterol. Ed: P.L. Yeagle. CRC Press Inc., Boca Raton. pp. 71-94.

Modha, A., Novak, M. and Blackburn, B.J., 1997. Treatment of experimental alveolar echinococcosis with albendazole: a ^{1}H NMR spectroscopic study. Can. J. Zool., **75**: 198-204.

Moire, A.M.B. and Zammit, V.A., 1992. Selective labeling of hepatic fatty acids *in vivo*. Biochem. J., **283**: 145-149.

Moore, M., Amberson, J.B., Kazam, E. and Vaughan, E.D., 1989. Anatomy, histology and embryology. In: Adrenal Disorders. Eds: E.D. Vaughan and R.M. Carey. Theme Medical Publishers Inc., New York. pp. 1-11.

Morris, D.L., Dykes, P.W., Marriner, S., Bogan, J., Burrows, F., Skeene-Smith, H. and Clarkson, M.J., 1985. Albendazole - objective evidence of response in human hydatid disease. JAMA, **253**(14): 2053-2057.

Morris, D.L. and Smith, P.G., 1987. Albendazole in hydatid disease - hepatocellular toxicity. Trans. R. Soc. Trop. Med. Hyg., **81**(2): 343-344.

Morrison, A.R., 1986. Biochemistry and pharmacology of renal arachidonic acid metabolism. Am. J. Med., **80**(1A): 3-11.

Mortensen, R.M. and Williams, G.H., 1995. Aldosterone physiology. In: Endocrinology, vol. 2, 3rd ed. Ed.: L.J. DeGroot. W.B. Saunders Co., Philadelphia. pp. 1668-1676.

Munck, A. and Náray-Fejes-Tóth, A., 1995. Glucocorticoid action: physiology. In: Endocrinology, vol. 2, 3rd ed. Ed.: L.J. DeGroot. W.B. Saunders Co., Philadelphia. pp. 1642-1655.

Nickerson, P.A., 1971. Fine structure of the Mongolian gerbil adrenal cortex. Anat. Rec., **171**: 443-456.

Novak, M., Marat, K., Johnson, L. and Blackburn, B.J., 1989. ^{1}H and ^{13}C NMR studies of serum from normal and *Echinococcus multilocularis*-infected jirds. Int. J. Parasitol., **19**(4): 395-400.

Novak, M, Modha, A. and Blackburn, B.J., 1993. Metabolic alterations in organs of *Meriones unguiculatus* infected with *Echinococcus multilocularis*. Comp. Biochem. Physiol., **105B**(3/4): 517-521.

Novak, M., Modha, A., Lee, J., Buist, R. and Blackburn, B.J., 1995. Metabolism of D-[1-^{13}C]glucose in livers of *Meriones unguiculatus* infected with *Echinococcus multilocularis*. Can. J. Zool., **73**: 58-66.

Ochieng-Mitula, P.J., Burt, M.D.B., Tanner, C.E., MacKinnon, B.M., Magambo, J.K., Cowan, F.B.M. and Aterman, K., 1994. The effect of ivermectin on the hydatid cyst of *Echinococcus multilocularis* in gerbils (*Meriones unguiculatus*). Can. J. Zool., **72**: 812-818.

Ogasawara, K., Matsuoka, S., Sato, N., Nakajima, Y. and Uchino, J., 1993. Image diagnosis In: Alveolar Echinococcosis of the Liver. Eds: J. Uchino and N. Sato. Hokkaido University School of Medicine, Sapporo. pp. 97-114.

Ohbayashi, M., 1993. Parasitology. In: Alveolar Echinococcosis of the Liver. Eds: J. Uchino and N. Sato. Hokkaido University School of Medicine, Sapporo. pp. 21-32.

Orphanidou, C.I., McCargar, L.J., Birmingham, C.L. and Belzberg, A.S., 1997. Changes in body composition and fat distribution after short-term weight gain in patients with anorexia nervosa. Am. J. Clin. Nutr., **65**(4): 1034-1041.

Pederson, R.C., 1988. Cholesterol biosynthesis, storage and mobilization in steroidogeneic organs. In: Biology of Cholesterol. Ed: P.L. Yeagle. CRC Press Inc., Boca Raton. pp. 39-69.

Pelech, S.L. and Vance, D.E., 1984. Regulation of phosphatidylcholine biosynthesis. Biochim. Biophys. Acta, **779**: 217-251.

Petavy, A.F., Deblock, S. and Walbaum, S., 1991. Life cycles of *Echinococcus multilocularis* in relation to human infection. J. Parasitol., **77**(1): 133-137.

Persat, F., Vincent, C., Mojon, M. and Petavy, A.F, 1991. Detection of antibodies against glycolipids of *Echinococcus multilocularis* metacestodes in sera of patients with alveolar hydatid disease. Parasite Immunol., **13**: 379-389.

Persat, F., Bouhours, J-F., Mojon, M. and Petavy, A-F., 1992. Glycosphingolipids with Galβ1-6Gal sequences in metacestodes of the parasite *Echinococcus multilocularis*. J. Biol. Chem., **267**(13): 8764-8769.

Persat, F., Vincent, C., Schmitt, D. and Mojon, M., 1996. Inhibition of human peripheral blood mononuclear cell proliferative response by glycosphingolipids from metacestodes of *Echinococcus multilocularis*. Infect. Immunol., **64**(9): 3682-3687.

Playford, M.C. and Kamiya, M., 1992. Immune response to *Echinococcus multilocularis* infection in the mouse model: a review. Jpn. J. Vet. Res., **40**: 113-130.

Poole, R.C. and Halestrap, A.P., 1993. Transport of lactate and other monocarboxylates across mammalian plasma membranes. Am. J. Physiol., **264**: C761-C782.

Rabkin, M. and Blum, J.J., 1985. Quantitative analysis of intermediary metabolism in hepatocytes incubated in the presence and absence of glucagon with a substrate mixture containing glucose, ribose, fructose, alanine and acetate. Biochem. J., **225**: 761-786.

Rakha, N.K., Dixon, J.B., Carter, S.D., Craig, P.S., Jenkins, P. and Folkard, S., 1991. *Echinococcus multilocularis* antigens modify accessory cell function of macrophages. Immunology, **74**:652-656.

Rausch, R.L., Wilson, J.F., Schantz, P.M. and McMahon, B.J., 1987. Spontaneous death of *Echinococcus multilocularis*: cases diagnosed serologically (by Em2 ELISA) and clinical significance. Am. J. Trop. Med. Hyg., **36**(3): 576-585.

Rausch, R.L., 1995. Life cycle patterns and geographic distribution of *Echinococcus* species. In: *Echinococcus* and Hydatid Disease. Eds: R.C.A. Thompson and A.J. Lymbery. CAB International, Wallingford, UK. pp. 89-134.

Rehbinder, D., 1971. Biochemistry. In: Lactic Acid. Eds: C.H. Holten, A. Müller and D. Rehbinder. Verlag Chimie, Weinheim/Bergstr. pp. 412-460.

Richards, K.S., Ilderton, E. and Yardley, H.J., 1987. Lipids in the laminated layer of liver, lung and daughter hydatid cysts of equine *Echinococcus granulosus*. Comp. Biochem. Physiol., **86B**: 209-212.

Roberts, L.S., 1983. Carbohydrate metabolism. In: Biology of the Eucestoda., vol. 2. Eds: C. Arme and P.W. Pappas. Academic Press, London. pp. 343-390.

Ross, M.H., Romrell, L.J. and Kaye, G.I., 1995. Histology, 3rd ed. Williams and Wilkins, Baltimore.

Saimot, A.G., Cremieux, A.C., Hay, J.M., Meulemans, A., Giovanangeli, M.D., Delaitre, B. and Coulaud, J.P., 1983. Albendazole as a potential treatment for human hydatidosis. Lancet II: 652-656.

Sato, N., Aoki, S., Matsushita, M. and Uchino, J., 1993a. Clinical features. In: Alveolar Echinococcosis of the Liver. Eds: J. Uchino and N. Sato. Hokkaido University School of Medicine, Sapporo. pp. 63-68.

Sato, N., Uchino, J. and Suzuki, K., 1993b. Chemotherapy. In: Alveolar Echinococcosis of the Liver. Eds: J. Uchino and N. Sato. Hokkaido University School of Medicine, Sapporo. pp. 151-166.

Schantz, P.M., 1982. Echinococcosis. In: CRC Handbook Series in Zoonoses. Section C, Volume 1. Ed: J.H. Steele. CRC Press Inc., Boca Raton. pp. 231-277.

Schantz, P.M., 1993. *Echinococcus multilocularis* in North America. In: Alveolar Echinococcosis of the Liver. Eds: J. Uchino and N. Sato. Hokkaido University School of Medicine, Sapporo. pp. 11-20.

Schantz, P.M., Chai, J., Craig, P.S., Eckert, J., Jenkins, D.J., MacPherson, C.N.L. and Thakur, A., 1995. Epidemiology and control of hydatid disease. In: *Echinococcus* and Hydatid Disease. Eds: R.C.A. Thompson and A.J. Lymbery. CAB International, Wallingford, UK. pp. 233-331.

Schlondorff, D. and Ardaillou, R., 1986. Prostaglandins and other arachidonic acid metabolites in kidney. Kidney Int., **29**: 108-119.

Schmidt, G.D. and Roberts, L.S., 1989. Foundations of Parasitology, 4th ed. Times Mirror/Mosby College Publishing, St. Louis.

Schoen, J., 1997. A NMR spectroscopic study of hepatic metabolism in *Meriones unguiculatus* infected with *Echinococcus multilocularis*. M.Sc. Thesis, University of Manitoba.

Schulz, H., 1991. Oxidation of fatty acids. In: Biochemistry of Lipids, Lipoproteins and Membranes. Eds: D.E. Vance and J. Vance. Elsevier Science Publishers, Amsterdam. pp. 87-110.

Schumann, W.C., Magnusson, I., Chandramouli, V., Kumaran, K., Wahren, J. and Landau, B.R., 1991. Metabolism of [2-^{14}C]acetate and its use in assessing hepatic Kreb's cycle activity and gluconeogenesis. J. Biol. Chem., **266**(11): 6985-6990.

Seifter, S. and Englard, S., 1994. Energy metabolism. In: The Liver: Biology and Pathobiology., 3rd ed. Ed: I.M. Arias. Raven Press, New York. pp. 323-364.

Shank, R.P., Leo, G.C. and Zielke, H.R., 1993. Cerebral metabolic compartmentation as revealed by nuclear magnetic resonance analysis of D-[1-^{13}C]glucose metabolism. J. Neurochem., **61**: 315-323.

Sherry, A.D., Nunnally, R.L. and Peshock, R.M., 1985. Metabolic studies of pyruvate- and lactate-perfused guinea pig hearts by ^{13}C NMR. J. Biol. Chem., **260**(16):

9272-9279.

Shiau, Y-F., 1987. Lipid digestion and absorption. In: Physiology of the Gastrointestinal Tract, 2nd ed. Ed.: L.R. Johnson. Raven Press, New York. pp. 1527-1556.

Simpson, E.R. and Waterman, M.R., 1995. Steroid hormone biosynthesis and its regulation by adrenocorticotropin. In: Endocrinology, vol. 2, 3rd ed. Ed.: L.J. DeGroot. W.B. Saunders Co., Philadelphia. pp. 1630-1641.

Smith, W.L., Borgeat, P. and Fitzpatrick, F.A., 1991. The eicosanoids: cyclooxygenase, lipoxygenase and epoxygenase pathways. In: Biochemistry of Lipids, Lipoproteins and Membranes. Eds: D.E. Vance and J. Vance. Elsevier Science Publishers, Amsterdam. pp. 297-325.

Smyth, J.D. and McManus, D.P., 1989. The Physiology and Biochemistry of Cestodes. Cambridge University Press, Cambridge.

Snoswell, A.M., Trimble, R.P., Fishlock, R.C., Storer, G.B. and Topping, D.L., 1982. Metabolic effects of acetate in perfused rat liver: studies on ketogenesis, glucose output, lactate uptake and lipogenesis. Biochim. Biophys. Acta, **716**: 290-297.

Sokolov, W., 1966. Water content in the tissues of desert animals. Nature, **211**(1): 545.

Sparling, M.L., Zidovetzki, R., Muller, L. and Chan, S.I., 1989. Analysis of membrane lipids by 500 MHz ^{1}H NMR. Anal. Biochem., **178**: 67-76.

Stehr-Green, J.K., Stehr-Green, P.A., Schantz, P.M., Wilson, J.F. and Lanier, A., 1988. Risk factors for infection with *Echinococcus multilocularis* in Alaska. Am. J. Trop. Med. Hyg., **38**(2): 380-385.

Storandt, S.T. and Kazacos, K.R., 1993. *Echinococcus multilocularis* identified in Indiana, Ohio and East-central Illinois. J. Parasitol., **79**(2): 301-305.

Suzuki, K., Sato, N. and Uchino, J., 1993. Epidemiology. In: Alveolar Echinococcosis of the Liver. Eds: J. Uchino and N. Sato. Hokkaido University School of Medicine, Sapporo. pp. 1-9.

Sze, D.Y. and Jardetzky, O., 1990. Characterization of lipid composition in stimulated human lymphocytes by ^{1}H NMR. Biochim. Biophys. Acta, **1054**: 198-206.

Tanner, C.E., 1987. The immunobiology of hydatid disease. In: Immune Responses in Parasitic Infections: Immunology, Immunopathology and Immunoprophylaxis.

Vol. II. Ed.: E.J.L. Soulsby. CRC Press Inc., Boca Raton. pp. 165-182.

Taylor, D.H. and Morris, D.L., 1988. *In vitro* culture of *Echinococcus multilocularis*: protoscolicidal action of praziquantil and albendazole sulphoxide. Trans. R. Soc. Trop. Med. Hyg., **82**: 265-267.

Taylor, D.H., Morris, D.L., Reffin, D. and Richards, K.S., 1989. Comparison of albendazole, mebendazole and praziquantel chemotherapy of *Echinococcus multilocularis* in a gerbil model. Gut, **30**: 1410-1405.

Thompson, R.C.A., 1995. Biology and systematics of *Echinococcus*. In: Echinococcus and Hydatid Disease. Eds: R.C.A. Thompson and A.J. Lymbery. CAB International, Wallingford, UK. pp. 1-50

Tisher, C.C. and Madsen, K.M., 1996. Anatomy of the kidney. In: Brennor and Rector's The Kidney., 5th ed. Ed: B.M. Brennor. W.B. Saunders Co., Philadelphia. pp. 3-71.

Toback, F.G., 1984. Phosphatidylcholine metabolism during renal growth and regeneration. Am. J. Physiol., **246**: F249-F259.

Tornieporth, N.G. and Disko, R., 1994. Alveolar hydatid disease (*Echinococcus multilocularis*)-review and update. Prog. Clin. Parasitol., **4**: 55-76.

Tso, P., and Fujimoto, K., 1991. The absorption and transport of lipids by the small intestine. Brain Res. Bull., **27**:477-482.

Uchino, J., Sato, N., Nakajima, Y., Matsushita, M., Takahashi, M. and Une, Y., 1993. Treatment. In: Alveolar Echinococcosis of the Liver. Eds: J. Uchino and N. Sato. Hokkaido University School of Medicine, Sapporo. pp. 137-149.

Vahouny, G.V., Hodges, V.A. and Treadwell, C.R., 1979. Essential fatty acid deficiency and adrenal cortical function *in vitro*. J. Lipid Res., **20**: 154-161.

Vance, D.E. and Ridgeway, N.D., 1988. The methylation of phosphatidylethanolamine. Prog. Lipid Res., **27**: 61-79.

Vance, D.E., 1991. Phospholipid metabolism and cell signalling in eukaryotes. In: Biochemistry of Lipids, Lipoproteins and Membranes. Eds: D.E. Vance and J. Vance. Elsevier Science Publishers, Amsterdam. pp. 205-240.

Van den Burghe, G., 1991. The role of the liver in metabolic homeostasis: implications for inborn errors of metabolism. J. Inher. Metab. Dis., **14**: 407-420.

Venuto, R.C. and Ferris, T.F., 1982. Prostaglandins and renal function. In: Prostaglandins: Organ and Tissue Specific Actions. Eds: S. Greenburg, P.J. Kadowitz and T.F. Burks. Marcel Dekker Inc., New York. pp. 131-150.

Vlahcevic, Z.R., Hyleman, P.B. and Chiang, J.Y.L., 1994. Hepatic cholesterol metabolism. In: The Liver: Biology and Pathobiology., 3rd ed. Ed: I.M. Arias. Raven Press, New York. pp. 379-389.

Voet, D. and Voet, J.G., 1995. Biochemistry, 2nd ed. John Wiley and Sons, New York.

Vuitton, D.A., Lasségue, A., Miguet, J.P., Herve, P., Barale, T., Seilles, E. and Capron, A., 1984. Humoral and cellular immunity in patients with hepatic alveolar echinococcosis. A 2 year follow-up with and without flubendazole treatment. Parasite Immunol., **6**:329-340.

Vuitton, D.A., Bresson-Hadni, S., Lenys, D., Flausse, F., Liance, M., Wattre, P., Miguet, J.P. and Capron, A., 1988. IgE-dependent humoral immune response in *Echinococcus multilocularis* infection: circulating and basophil-bound specific IgE against *Echinococcus* antigens in patients with alveolar echinococcosis. Clin. Exp. Immunol., **71**: 247-252.

Vuitton, D.A., Bresson-Hadni, S., Laroche, L., Kaiserlian, D., Guerret-Stocker. S., Bresson, J.L. and Gillet, M., 1989. Cellular immune responses in *Echinococcus multilocularis* infection in humans. II. Natural killer cell activity and cell subpopulations in the blood and in the periparasitic granuloma of patients with alveolar echinococcosis. Clin. Exp. Immunol., **78**: 67-74.

Waite, M., 1991. Phospholipases. In: Biochemistry of Lipids, Lipoproteins and Membranes. Eds: D.E. Vance and J. Vance. Elsevier Science Publishers, Amsterdam. pp. 269-295.

WHO, 1996. Guidelines for the treatment of cystic and alveolar echinococcosis in humans. Bull. World Health Org., **74**(3): 231-242.

Williamson, J.R. and Cooper, R.H., 1980. Regulation of the citric acid cycle in mammalian systems. FEBS Letts., **117**: K73-K85.

Wilson, J.F. and Rausch, R.L., 1980. Alveolar hydatid disease: a review of clinical features of 33 indigenous cases in Alaskan Eskimos. Am. J. Trop. Med. Hyg., **29**(6): 1340-1355.

Wilson, J.F., Rausch, R.L., McMahon, B.J., Schantz, P.M., Trujillo, D.E. and O'Gorman, M.A., 1987. Albendazole therapy in alveolar hydatid disease: a report of

favorable results in two patients after short-term therapy. Am. J. Trop. Med. Hyg., **37**(1): 162-168.

Wilson, J.F., Rausch, R.L., McMahon, B.J. and Schantz, P.M., 1992. Parasiticidal effect of chemotherapy in alveolar hydatid disease: review of experience with mebendazole and albendazole. Clin. Infect. Dis., **15**: 234-249.

Wirthensohn, G. and Guder, W.G., 1983. Phosphatidylcholine biosynthesis in rabbit kidney tubule suspensions: effect of metabolic substrates on precursoe incorporation. Biochim. Biophys. Acta, **750**: 388-396.

Wirthensohn, G., LeFrank, S., Wirthensohn, K. and Guder, W.G., 1984. Phospholipid metabolism in rat kidney cortical tubules. I. Effect of renal substrates. Biochim. Biophys. Acta, **795**: 392-400.

Zhang, Y., Agarwal, K.C., Beylot, M., Soloviev, M., David, F., Reider, M., Anderson, V., Tserng, K-T. and Brunengraber, H., 1994. Nonhomogenous labeling of liver extra-mitochondrial acetyl-CoA. J. Biol. Chem., **269**(15): 11025-11029.